THESIS

EVALUATING THE SPATIAL VARIABILITY OF SNOWPACK PROPERTIES ACROSS A NORTHERN COLORADO BASIN

Submitted by

Graham Andrew Sexstone

Department of Ecosystem Science and Sustainability

In partial fulfillment of the requirements

For the Degree of Master of Science

Colorado State University

Fort Collins, Colorado

Fall 2012

Master's Committee:

Advisor: Steven Fassnacht

Melinda Laituri
Jason Sibold

ABSTRACT

EVALUATING THE SPATIAL VARIABILITY OF SNOWPACK PROPERTIES ACROSS A NORTHERN COLORADO BASIN

Knowledge of seasonal mountain snowpack distribution and estimates of its snow water equivalent (SWE) can provide insight for water resources forecasting and earth system process understanding, thus, it is important to improve our ability to describe the spatial variability of SWE at the basin scale. The objectives of this thesis are to: (1) develop a reliable method of estimating SWE from snow depth for the Cache la Poudre basin, and (2) characterize the spatial variability of SWE at the basin scale within the Cache la Poudre basin. A combination of field and Natural Resource Conservation Service (NRCS) operational-based snow measurements were used in this study. Historic (1936 – 2010) snow course data were obtained for the study area to evaluate snow density. A multiple linear regression model (based on the historical snow course data) for estimating snow density across the study area was developed to estimate SWE directly from snow depth measurements. To investigate the spatial variability and observable patterns of SWE at the basin scale, snow surveys were completed on or about April 1, 2011 and 2012 and combined with NRCS operational measurements. Bivariate relations and multiple linear regression models were developed to understand the relation of SWE with physiographic variables derived using a geographic information system (GIS). SWE was interpolated across the Cache la Poudre basin on a pixel by pixel basis using the model equations and masked to observed SCA (from an 8-day MODIS product).

The independent variables of snow depth, day of year, elevation, and UTM Easting were used in the model to estimate snow density. Calculation of SWE directly from snow depth measurement using the snow density model has strong statistical performance and model verification suggests the model is transferable to independent data within the bounds of the original dataset. This pathway of estimating SWE directly from snow depth measurement is useful when evaluating snowpack properties at the basin scale, where many time consuming measurements of SWE are often not feasible. Bivariate relations of SWE and snow depth measurements (from WY 2011 and WY 2012) with physiographic variables show that elevation and location (UTM Easting and UTM Northing) are most strongly correlated with SWE and snow depth. Multiple linear regression models developed for WY 2011 and WY 2012 include elevation and location as independent variables and also include others (e.g., eastness, slope, solar radiation, curvature, canopy density) depending on the model dataset. The final interpolated SWE surfaces, masked to observed SCA, generally show similar patterns across space despite differences in the 2011 and 2012 snow years and differing estimation of SWE magnitude between the combined dataset of field-based and operational-based measurements ($model_{O+F}$) and the dataset of operational-based measurements only ($model_{O}$). Within each of the model surfaces, interpolated volume of SWE was greatest within Elevation Zone 5 (3,043 – 3,405 m). The percentage of the total interpolated SWE volume for each model was distributed similarly among elevation zones.

ACKNOWLEDMENTS

Partial funding for this research was provided by a NASA grant (NNX11AQ66G) entitled: "Improved Characterization of Snow Depth in Complex Terrain Using Satellite Lidar Altimetry." Additional support was provided by the National Park Service (contract number H2370094000) project entitled: "Understanding Past/Future Effects of Climate Change on Water-Dependent Cultural Resources at Kaloko-Honokōhau National Historical Park (KAHO)." I would like to thank my advisor, Steven Fassnacht, for his guidance and support throughout this study. I would also like to acknowledge my committee members, Melinda Laituri and Jason Sibold, as well as Stephanie Kampf for providing valuable direction and insight. Thanks to members of ECOL592 and WR474/WR574 as well as everyone who volunteered to help with field data collection. Finally, special thanks go to my family and friends for their continuous support and encouragement in my academic pursuits.

TABLE OF CONTENTS

CHAPTER 1: INTRODUCTION

1.1 Introduction

Snow is integral to the earth system, playing a key role in the hydrologic cycle as well as energy exchanges between the land surface and atmosphere. A majority of earth's moving freshwater originates in snow dominated mountainous areas [Viviroli *et al*., 2003], with 60-75% of annual streamflow in the western United States originating from snowmelt [Doesken and Judson, 1996]. A comprehensive understanding of the distribution of the seasonal mountain snowpack and estimation of its snow water equivalent (SWE) is essential for the accurate forecasting of streamflow and water availability, as well as for the availability of input data for regional climate and hydrologic models. Additionally, the recent shift towards earlier snowmelt in regions of the western U.S. [Stewart, 2009; Clow, 2010] necessitates a more accurate accounting for future water resources planning, especially due to the lack of understanding of spatial and temporal variability of snow properties. Mountainous landscapes have complex topography and strong and highly variable climatic gradients yielding spatial and temporal (seasonal and interannual) variability in snowpack properties. Determining the meteorology and related feedbacks that drive hydrologic processes in these areas is challenging in such complex terrain and requires spatial scaling [Bales *et al*., 2006]. Often the resolution of available SWE measurements is much larger than the scale needed to characterize the correlation length of its spatial variability [Blöschl, 1999].

Across the western United States, the Natural Resource Conservation Service (NRCS) SNOwpack TELemetry (SNOTEL) and snow course network provide operational snowpack measurements of snow depth and SWE and thus calculated average density at a daily and monthly time step, respectively. NRCS operational stations were established to measure the snowpack for water supply forecasts, yet, they have been shown to represent SWE only as point locations rather than surrounding areas [Molotch and Bales, 2005]. Nonetheless, SNOTEL and snow course sites are the most widely available and utilized ground based measurements of SWE.

Research on the spatial distribution of snow has emphasized the statistical relation between snow properties and terrain characteristics, the latter as a surrogate for the driving meteorology. These studies have used SNOTEL data to interpolate SWE over large basins [e.g., Fassnacht *et al*., 2003], as well as snowpack field measurements over small catchments [e.g., Elder *et al*., 1991]. However, few studies have described snow's spatial and temporal variability at the basin scale using both operational and field measurements. Operational measurements can provide regional knowledge on the spatial distribution of snow [e.g., Fassnacht *et al*., 2003; Bales *et al*., 2008], yet cannot accurately characterize the spatial variability of the snowpack at the basin scale [Bales *et al*., 2006]. It has been recommended that future research should focus on more accurate estimations of SWE at the basin and regional scale to effectively assess and manage mountain water resources [Viviroli *et al*., 2011]. At the basin scale, an approach to reducing the sampling effort needed for more measurements is to use snow depth as a surrogate for SWE by developing a model for snow density, since manual snow density measurements require more time and effort than snow depth measurements. Recent studies have attempted to characterize the spatiotemporal characteristics of snow density [e.g., Mizukami and Perica, 2008; Fassnacht *et al*., 2010], or to develop reliable methods for modeling snow density and thus estimating SWE from snow depth measurements [e.g., Jonas *et al*., 2009, Sturm *et al*., 2010].

1.2 Scientific Objectives

To address the limitations of estimating the distribution of SWE over large areas from satellite-derived and operational snow data, this research has focused on the 2011 and 2012 water year (WY) using the previously mentioned operational snowpack measurements, additional supporting field measurements, and remotely sensed snow covered area (SCA) to evaluate the spatial variability of snowpack properties at the basin scale. The objectives of this thesis are to address the following research questions:

1) Can a reliable method of estimating SWE be developed from snow depth for the Cache la Poudre basin?
2) Can the spatial variability of SWE within the Cache la Poudre basin be characterized at the basin scale?

1.3 Study Area

The Cache la Poudre basin is a located within northern Colorado and a small portion of southeastern Wyoming (Figure 1.1). The basin has an area of 4867 km^2 and ranges in elevation from 1406 to 4125 m. The upper portion of the basin that contributes to the canyon mouth is gaged by a Colorado Division of Water Resources (CDWR) gaging station (Cache la Poudre River at Canyon Mouth) with an area of 2729 km^2 (Figure 1.1). Since this portion of the basin is responsible for the majority of input to the river system, it will be the focus of this study. Subalpine and montane coniferous forests dominate the basin, with the alpine community located at the highest elevations and the mountain shrub and grassland communities located at the lowest elevations. From the parameter-elevation regressions on independent slopes model (PRISM) [Daly *et al*., 1994], the average annual (1971–2000) precipitation within the basin ranges from

330 mm at the lowest elevations to 1350 mm at the highest elevations, and the average annual (1971-2000) temperature ranges from 9°C to -5°C [Richer, 2009]. Snow is the dominant form of precipitation within the basin, as the hydrograph peak is driven by snowmelt generally occurring in late May to June. Study area maps of elevation and land cover are provided in Appendix A.

1.4 Snowpack Monitoring

1.4.1 NRCS Snow Monitoring Network

The NRCS operational snow monitoring network consists of SNOTEL stations and snow courses. These monitoring sites are located within 12 western U.S. states as well as Alaska and generally positioned in high elevation meadows up to but not above the tree line to minimize blowing snow and sublimation losses [Cayan, 1996; Gillespie, 2011]. The snow course network began in the 1900s and provides manual measurements of snow depth and SWE and thus average snow density averaged across 10 (in some cases 15) measurements using a Federal Sampler. Most snow courses are monitored on or about the first day of the month from January through June. The SNOTEL network was established in 1978 and utilizes meteor burst communication technology to provide automated daily (and now hourly) measurements of SWE, snow depth, precipitation and air temperature, with other measurements such as soil moisture at some sites [Gillespie, 2011].

Within the Cache la Poudre basin there are nine snow courses and five SNOTEL stations. Within a 15 km buffer surrounding the study area, there are additionally eight snow courses and five SNOTEL stations. The operational stations that are located within the study basin as well as within the 15 km buffer around the basin were analyzed for this study (Figure 1.1). This includes SNOTEL stations and snow courses within the Cache la Poudre basin and in the North

Platte, Big Thompson, Upper Laramie and Colorado River basins, yielding a total of 10 SNOTEL stations (Table 1.1) and 17 snow courses (Table 1.2).

Deadman Hill and Joe Wright are the two long-term SNOTEL stations located within the Cache la Poudre basin that have a mean (1980–2012) peak SWE of 538 mm and 690 mm, respectively (Figure 1.2). The lowest snow year was 2002 at Deadman Hill (Figure 1.3a) and 2012 at Joe Wright (Figure 1.3b), while the maximum snow year was 2011 at both SNOTEL stations. Despite the similar elevation of the two stations, Joe Wright has historically shown a greater accumulation of SWE than Deadman Hill.

1.4.2 Field Snow Surveys

Field snowpack measurements, including snow density (ρ_s) and/or snow depth (d_s), were collected within the study area during monthly snow surveys in WY 2011 and WY 2012. Latitude, longitude, and elevation were identified at each sampling location using a Garmin GPSMAP 76 GPS receiver capable of positioning accuracy within 3 meters. At each sampling location, 11 measurement points of snow depth were taken using a snow depth probe to the near cm of depth at a one-meter interval in one of the four cardinal directions and averaged to account for the small scale spatial variability located at a point location [e.g. López-Moreno *et al.*, 2011]. Snow density is a conservative variable that varies less spatially than depth [Logan, 1973; Fassnacht *et al.*, 2010], thus, snow density was measured at a lower spatial density across the study area than snow depth (snow density was not measured at each sampling location). Three methods of measuring snow density were used at each site. A cylindrical metal can with a diameter of 15.3 cm was used to measure snow density if the snowpack was less than 50 cm. A cylindrical snow sampling tube with a diameter of 6.6 cm was used to measure snow density for snowpacks greater than 50 cm and less than 150 cm. Additionally, a Federal Sampler (diameter of 3.77 cm) was used to measure the snow density for snowpacks greater than 150 cm, but it was also used for some snowpack depths shallower than 150 cm. For all (sampling) methods, the mass and volume of the snowpack sample were measured to calculate snow density by the following relation (Equation 1.1):

$$\rho_s = \frac{m_s}{V_s} \qquad (1.1),$$

where ρ_s is snow density, m_s is the mass of snow, and V_s is the volume of snow.

A transect (along Colorado State Highway 14) of 29 field sampling locations ranging in elevation from 1607 m to 3174 m was sampled on or about the first of each month during the WY 2011 and 2012 snow seasons (Figure 1.4). Sampling locations were monitored monthly to assess temporal variability of snowpack properties and to provide a temporal dataset that could be used for verification of physically based snow evolution models. Additional sampling locations were monitored on and about April 1, 2011 and 2012 to assess the spatial variability of the snowpack across the study area (Figure 1.4). A total of 42 field sampling locations (14 locations with no snow) were monitored on and about April 1, 2011 and 121 field sampling locations (14 locations with no snow) on and about April 1, 2012 (Table 1.3). Snowpack data collected during WY 2011 and 2012 are presented in Appendix B.

Forest canopy data were collected at each sampling location during the April 1, 2012 snow survey. Categories of canopy cover, community type, and tree mortality were noted for the tree canopy covering each set of measurement points (Table 1.4). Canopy measurements are presented in Appendix B.

Table 1.1: SNOTEL stations within the study area.

Station Name	Station ID	Basin	Latitude [N]	Longitude [W]	Elevation [m]	Period of Record
Black Mountain	05J28S	Cache la Poudre	40°53’	-105°40’	2719	2010 – Present
Deadman Hill	05J06S	Cache la Poudre	40°48’	-105°46’	3115	1978 – Present
Hourglass Lake	05J11S	Cache la Poudre	40°35’	-105°38’	2859	2008 – Present
Joe Wright	05J37S	Cache la Poudre	40°31’	-105°53’	3085	1978 – Present
Lake Irene	05J10S	Colorado	40°25’	-105°49’	3261	1978 – Present
Long Draw Reservoir	05J27S	Cache la Poudre	40°30’	-105°45’	3042	2008 – Present
Never Summer	06J27S	North Platte	40°24’	-105°57’	3133	2002 – Present
Phantom Valley	05J04S	Colorado	40°24’	-105°51’	2752	1979 – Present
Rawah	06J20S	North Platte	40°42’	-106°00’	2749	2002 – Present
Willow Park	05J40S	Big Thompson	40°26’	-105°44’	3261	1979 – Present

Table 1.2: Snow course stations within the study area.

Station Name	Station ID	Basin	Latitude [N]	Longitude [W]	Elevation [m]	Period of Record
Bennett Creek	05J33	Cache la Poudre	40°39'	-105°37'	2804	1966 – Present
Big South	05J03	Cache la Poudre	40°36'	-105°49'	2621	1936 – Present
Cameron Pass	05J01	Cache la Poudre	40°31'	-105°53'	3135	1936 – Present
Chambers Lake	05J02	Cache la Poudre	40°36'	-105°50'	2743	1936 – Present
Deadman Hill	05J06	Cache la Poudre	40°47'	-105°46'	3115	1937 – Present
Deer Ridge	05J17	Big Thompson	40º 24'	-105º 37'	2743	1949 - Present
Hidden Valley	05J13	Big Thompson	40º 24'	-105º 39'	2890	1941 - Present
Hourglass Lake	05J11	Cache la Poudre	40°35'	-105°38'	2853	1938 – Present
Lake Irene	05J10	Colorado	40º 25'	-105º 49'	3261	1938 – Present
Long Draw Reservoir	05J27	Cache la Poudre	40°30'	-105º 45'	3042	1971 – Present
Mc Intyre	05J15	Upper Laramie	40º 46'	-105º 55'	2774	1949 - Present
Milner Pass	05J24	North Platte	40º 24'	-105º 49'	2606	1952 – Present
Phantom Valley	05J04	Colorado	40º 24'	-105º 51'	2752	1936 – 2008 [D]
Pine Creek	05J31	Cache la Poudre	40º 46'	-105º 30'	2408	1961 – 2001 [D]
Red Feather	05J20	Cache la Poudre	40º 48'	-105º 39'	2743	1949 - Present
Two Mile	05J26	Big Thompson	40º 22'	-105º 40'	3200	1952 – 1992 [D]
Willow Park	05J40	Big Thompson	40º 25'	-105º 43'	3261	1978 – 2008 [D]

[D] Station has been discontinued – historical data utilized for study

Table 1.3: Field-based snow sampling summary table

Survey Type	d_s samples	$\overline{d_s}$ [m]	σd_s [m]	SWE samples	$\overline{SWE}$ [mm]	σSWE [mm]
Monthly Surveys	29	N/A	N/A	9	N/A	N/A
April Survey, 2011	28	1.13	0.660	11	360	235
April Survey, 2012	104	0.702	0.309	12	282	56.1

Table 1.4: Forest canopy categorical measurements taken at each sampling location

Canopy Cover	Community Type	Tree Mortality
Closed	Lodgepole Pine	Alive with Green Needles
Partially Closed	Spruce/Fir	Dead with Needles
Open	Alpine	Dead and Gray (no needles)
		No Canopy

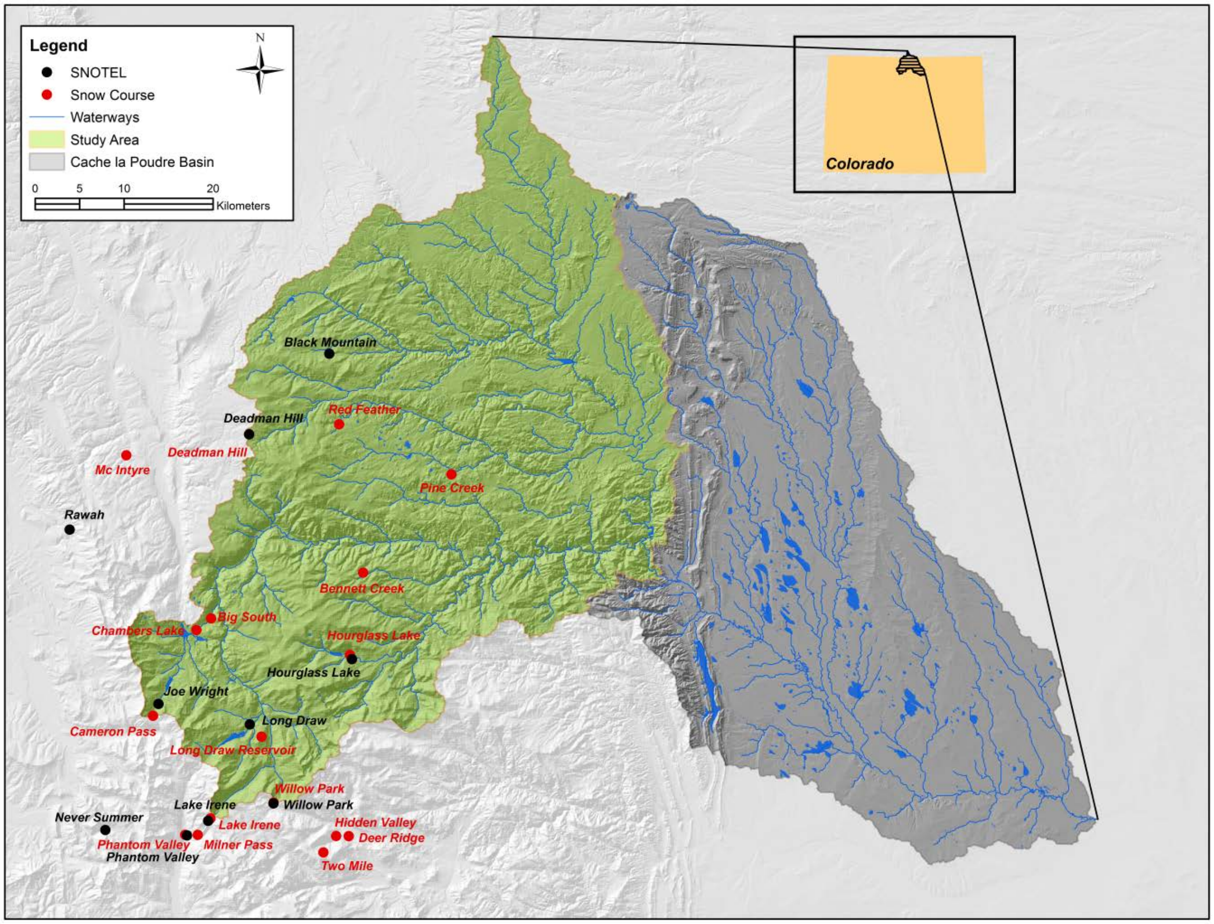

Figure 1.1: Study site map of the Cache la Poudre basin including locations of NRCS operational snowpack measurements within the study area <*http://www.wcc.nrcs.usda.gov/snow/*>.

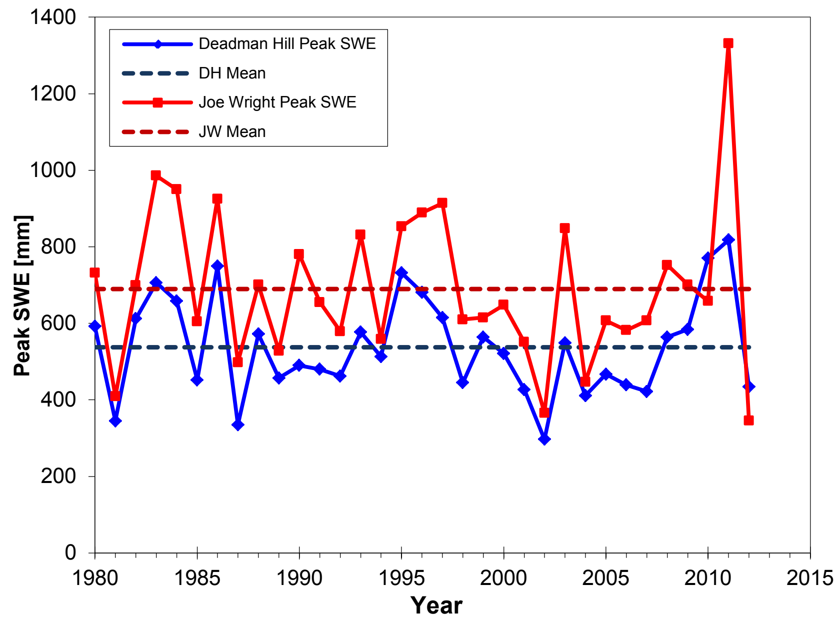

Figure 1.2: Annual peak SWE and mean annual peak SWE (1980-2011) for Deadman Hill and Joe Wright SNOTEL stations.

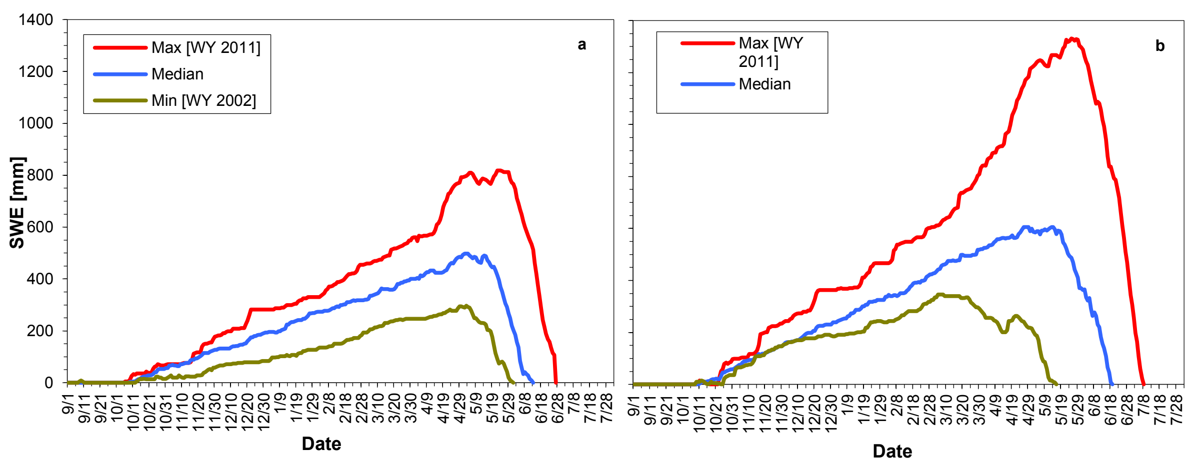

Figure 1.3: Maximum and minimum snow years (1980-2012) and median value for each year at the Deadman Hill [1.3a] and Joe Wright [1.3b] SNOTEL stations.

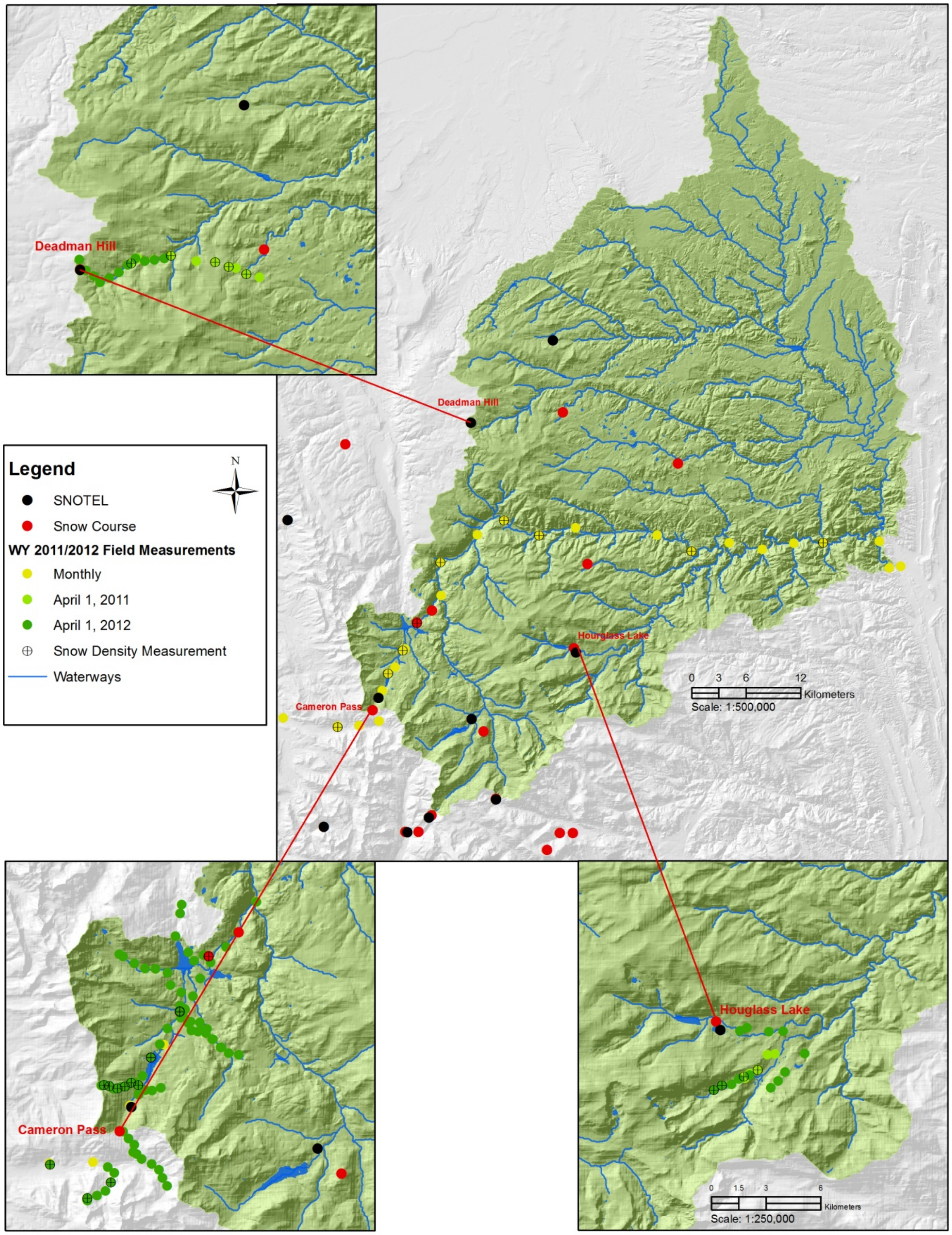

Figure 1.4: Study area field sampling location map including monthly (temporal) and April 1 (spatial) snow suvey sampling locations.

CHAPTER 2: SNOW DENSITY MODEL

2.1 Introduction

Snow water equivalent (SWE) is the most important measure of mountain water resources. The ability to accurately characterize the distribution of SWE across the cryosphere is crucial for modeling and understanding earth system processes and feedbacks [Bales *et al*., 2006] at varying scales [Blöschl, 1999]. Additionally, due to a changing climate, the importance of describing the spatial variability of SWE to effectively describe and manage mountain water resources will continue to increase [Barnett *et al*., 2005].

Currently, SWE measurements can be made directly by either remote sensing or ground-based approaches. Satellite remote sensing estimations of SWE in complex mountainous terrain have proved to be difficult due to the current scale of observation. Global space borne estimations of SWE from the Special Sensor Microwave/Image (SSM/I) and more recently Advanced Microwave Scanning Radiometer – Earth Observing System (AMSR-E) are available at a spatial resolution of 25 km, which can provide accurate SWE estimations over homogenous terrain, but cannot accurately describe the variability of SWE in more complex terrain [e.g., Chang *et al*., 2005; Kelly, 2009]. Although passive microwave estimations of SWE remain unreliable in mountainous terrain, active microwave sensors have shown potential to provide finer resolution SWE estimations for future satellite missions [Cline *et al.*, 2009].

Manual ground-based snowpack measurements have been provided by the snow course network since the mid-1930s. Additionally, since the late 1970s, automated ground-based measurements of SWE from the SNOTEL network are provided across the western United States. These NRCS operational data provide regional knowledge of snow distribution [e.g., Fassnacht *et al*., 2003; Bales *et al*., 2008], but are limited in resolving the spatial variability of the SWE across large areas [Bales *et al*., 2006] due to their low spatial density (approximately 1500 snow courses and 750 SNOTEL sites across the western United States and Alaska [Gillespie, 2011]). Field-campaigns of ground-based measurements [e.g., Elder *et al*., 2009] aimed at measuring SWE are also limited over larger areas due to the time intensive nature of measuring SWE in the field.

Manual ground-based snow depth measurements are a considerably easier to make than SWE measurements, requiring less time and effort. At the basin scale, it has been suggested that an approach to reducing the sampling effort needed for more measurements during intensive field campaigns is to use snow depth as a surrogate for SWE by developing a model for snow density [Viviroli *et al*., 2011]. Recent studies have successfully developed reliable methods for modeling snow density and thus estimating SWE from snow depth measurements at country and continent wide scales [e.g., Jonas *et al*., 2009, Sturm *et al*., 2010]. However, at a much finer scale, such as 1 km^2, the variability of density has been less explainable [Lopéz-Moreno *et al.*, in review]. This study has developed a snow density model at the basin scale, specifically for the Cache la Poudre basin; this is a different domain and scale than used in previous studies.

2.2 Background

SWE, in millimeters, is the product of snow depth (d_s) measured in meters and snow density (ρ_s) in kilograms per cubic meter:

$$SWE = d_s \rho_s \tag{2.1}$$

Therefore, SWE can be computed from measured snow depth by estimating snow density. Snow depth is strongly correlated with SWE (Figure 2.2a), which suggest that this correlation could be used to predict SWE from observed snow depth. Sturm *et al*. [2010] suggested that despite a strong correlation between snow depth and SWE, it is not appropriate to estimate SWE directly from snow depth, as SWE is a complex nonlinear function of snow depth. The range of variability of snow density has been shown to be more conservative than snow depth and SWE [e.g., Logan, 1973; Fassnacht *et al*., 2010]. Historic (1936 – 2010) snow density coefficients of variation (CV) from April 1 at snow course measurements within the study area are considerably lower than those of snow depth and SWE (Figure 2.1). The mean CV of snow density is 0.15 while the mean CV for SWE and snow depth is 0.36 and 0.32, respectively. Due to this conservative range of variability, estimating snow density from snow depth measurements should provide a reasonable pathway for estimating SWE from a snow depth measurement.

2.3 Methods

2.3.1 Data

Historical NRCS snow course data from 17 snow courses (1936 – 2010, n=3637) within the study area were evaluated (Table 1.2). Snow courses within the study area range in elevation from 2408 m to 3261 m and are generally measured on or about the first of the month from January through June each year. Snow density values greater than 600 kg/m^3 and less than 50 kg/m^3 were omitted from the analysis. Additionally, due to the limited precision and possibly the lack of accuracy for snow density measurements in shallow snowpacks, data for snow depth less than 0.13 m (5 inches) and/or SWE less than 50 mm (2 inches) were also omitted. This selection of data resulted in 3,262 data records of snow depth, snow density, and SWE, with 10.3% of the original data removed.

2.3.2 Snow Density Relations

The pairwise relations between snow depth, snow density, and SWE from the historic snow course records are presented in Figure 2.2. A strong correlation exists between snow depth and SWE, which is best fit as a power function (Figure 2.2a). There is considerable scatter about the linear fit for snow density versus snow depth (Figure 2.2b), which suggests that additional variables should be included to describe the variability of snow density. Snowpack relations here are similar to those found in previous studies [e.g., Jonas *et al.*, 2009; Sturm *et al.*, 2010].

The intra-annual variability of snow density is largely dictated by time of year, while inter-annual variability is minimal [Mizukami and Perica, 2008]. Snow density tends to increase gradually throughout the snow season due to crystal metamorphism, settling, and compaction. Therefore, snow density tends to increase with the day of year [Mizukami and Perica, 2008] as well as with increasing snow depth [Pomeroy and Gray, 1995] (Figure 2.3). Elevation and location within the study area were not shown to affect snow density in an obvious way (Figure 2.3). Other variables impact snow densification, such as aspect and canopy cover, as they are surrogates for solar radiation. However, snow courses are often located in flat open areas, limiting the ability of the dataset to represent the variability explained by these variables. For this reason, the following variables were used to develop a multiple linear regression model to estimate snow density: snow depth (d_s), Julian day (DOY), elevation (z), UTM easting (UTM_e), and UTM northing (UTM_n).

2.3.3 Snow Density Trend Analysis

Snow density and SWE were both tested for the presence of significant monotonic long term trends by the Mann-Kendall test and calculated Sen's slope estimate using the MAKESENS 1.0 freeware developed by the Finnish Meteorological Institute [Salmi *et al.*, 2002]. The Mann-Kendall test is a non-parametric test in which the data are not required to exhibit a particular distribution and missing values are allowed [Gilbert, 1987]. In order to test the non-stationarity of the historic snow course data, long term trends were assessed for the entire length of record (1936 – 2010), as well as from 1976 – 2010, which corresponds to the time period of a strong warming trend identified by the Intergovernmental Panel on Climate Change (IPCC) [IPCC, 2007].

2.3.4 Snow Density Model

Multiple linear regression [Kutner *et al.*, 2005], a method used to model the relation between a dependent variable and two or more independent variables, was used to predict snow density based snow depth, Julian day, elevation, UTM Easting, and UTM Northing. Multiple linear regression is expressed by

$$Y_i = \beta_0 X_{i0} + \beta_1 X_{i1} + \beta_2 X_{i2} + \cdots + \beta_{p-1} X_{i,p-1} + \varepsilon_i \qquad (2.2),$$

where β are model parameters, X are known independent variables, and ε is the error term. The statistical software *R* [Ihaka and Gentleman, 1996] was used for all statistical analyses.

The final independent variables included in the multiple linear regression model were selected based on two automated procedures, stepwise regression and all-subsets regression. A stepwise regression procedure was used to determine which combination of variables would provide the lowest resulting Akaike information criterion (AIC) statistic [Akaike, 1974], which is a measure of the relative goodness of fit of the statistical model that introduces a penalty for increasing the number of model parameters. Additionally, an all-subsets regression procedure [Berk, 1978] was performed, which assesses a criterion statistic for every possible combination of independent variables. Mallows' C_p [Mallows, 1973], which assesses the fit of a regression model and increases a penalty term as the number of predictor variables increases, was used as a criterion for the all-subsets regression. Potential models were identified based on favorable results from the automated variable selection procedures. The variance inflation factor (VIF) was used to quantify the severity of multicollinearity between independent variables. A VIF score greater than 4 may suggest multicollinearity between variables [Kutner *et al*., 2005].

The multiple regression model provides an estimate of snow density for each snow depth measurement and their product yields an estimate of SWE. To assess the accuracy of the models identified, and select the final model, several methods of model evaluation were performed. Calibration was performed by comparing modeled snow density as well as calculated SWE with observed values from the original dataset; explained variance as well as the AIC statistic was computed. Verification with two sets of independent data was completed to test model transferability to predict independent data. The two independent datasets included field-based measurements from the 2011 and 2012 snow seasons (n = 84), as well as historic first of the month SNOTEL measurements (n = 121) at sites that are not co-located with a snow course. Additionally, a 10-fold cross verification procedure, which runs 10 iterations of removing a random selection of the dataset and fitting the regression to the remainder of the data, was used to compare modeled values to the observed values removed for each iteration. Performance of the final snow density model was determined from the residuals of both observed snow density as well as calculated SWE through the calculation of the Nash-Sutcliffe Coefficient of Efficiency (NSCE), Mean Absolute Error (MAE), and Root Mean Squared Error (RMSE) performance statistics:

$$NSCE = 1 - \frac{\sum_{i=1}^{n}(O_i - M_i)^2}{\sum_{i=1}^{n}(O_i - \overline{O})^2} \tag{2.3}$$,

$$MAE = \frac{1}{n}\sum_{i=1}^{n}\left|O_i - M_i\right| \tag{2.4}$$,

$$RMSE = \sqrt{\frac{1}{n}\sum_{i=1}^{n}\left(O_i - M_i\right)^2} \tag{2.5}$$,

where n is the number of observations, O is the observed value, $\overline{O}$ is the mean of observed values, and M is the modeled value.

2.4 Results

Historic (1936 – 2010) trends of April 1st SWE and snow density were evaluated for three representative snow courses within the study area. Generally, the entire length of record did not show a strong trend. However, the record from 1976 – 2010 was a period of decreasing SWE and density (Figure 2.4). Specifically, the Deadman Hill and Cameron Pass snow courses showed a significant decrease in SWE and snow density ($p < 0.05$, $p < 0.1$, respectively) from

1976 – 2010, while Hourglass Lake did not show a significant change (Table 2.1). The decrease in SWE was greater than the decrease in density.

The mean snow density from the snow course dataset is 287 kg/m^3 with a standard deviation of 64.8 kg/m^3, and the data appear to be normally distributed (Figure 2.5a). SWE and snow depth have a greater standard deviation (178 mm, 0.46 m, respectively) compared to their mean (275 mm, 0.92 m, respectively) than that of snow density (Figure 2.5b-c). Pairwise scatter plots of all variables used within the regression model are shown in Figure 2.6. Snow density is most highly correlated with Julian day, and also shows a strong positive correlation with snow depth and negative correlation with UTM Easting (Table 2.2).

Seven models were evaluated based on favorable results from the automated variable selection procedures. Table 2.3 shows the independent variables used within each test model and summarizes the model calibration statistics. The performance statistics of model number 1, with independent variables of Julian day, snow depth, elevation, and UTM Easting, were shown to be the best, and was thus selected as the final regression for modeling snow density. The final equation shows the following form:

$$\rho_s = 841 + 1.05DOY + 17.2d_s + 3.53x10^{-2}z - 1.72x10^{-3}UTM_e \qquad (2.6),$$

where ρ_s is snow density, DOY is Julian day, d_s is snow depth, z is elevation, and UTM_e is UTM Easting. The variance inflation factor (VIF) is below 4 for each variable within the final model, suggesting that multicollinearity between independent variables is not observed. The residuals of the regression model are normally distributed and do not violate the underlying assumptions of the regression (normality, linearity, homoscedasticity) [Kutner *et al*., 2005].

The calibrated model underestimated more dense snowpacks and overestimated less dense snowpacks (Figure 2.7ai), while calculated SWE showed generally unbiased residuals that tended to slightly increase with increasing observed SWE (Figure 2.7bi). Performance statistics calculated from the residuals of calibration with the original dataset showed that predicted snow density explained 51% of the total variance in the data with a RMSE of 45.31 kg/m^3, yet, calculated SWE was able to explain 94% of the variance in the data and had a RMSE of 4.4 cm (Table 2.4).

Various methods of model verification were performed to test the utility of the regression model, including cross verification, that all showed similar trends (Figure 2.7) and comparable error estimates (Table 2.4) to model calibration. As expected, a minor increase in error estimation was observed for model verification with independent data, yet the minimal increase in error shows that the regression model should be transferable to independent data within the bounds of the original dataset.

2.5 Discussion

The snow density model developed for the study area performed relatively well in modeling SWE from independent snow depth measurements (Table 2.4). RMSE estimates of predicted SWE ranged from 4.4 cm (calibration data) to 6.6 cm (independent field verification data). Only 0.26% (n=11) of the verification data showed a residual value outside of one standard deviation of SWE from the original dataset (17.8 cm). Additionally, 80% of all residual values (n = 2768) fell within the range ±5 cm. The variance of the model residuals were on average within 12.8% of the observed value. Within site variability of SWE has been conservatively estimated to be 15 – 25% [Jonas *et al.*, 2009], which suggests that the error observed from the model is within the natural range of SWE variability at a site [Fassnacht *et al.*, 2008]. The small range of error suggests that predicting SWE from snow depth measurements though a snow density model works due to the conservative nature of snow density; 52% of snow density data values ranged from 250 kg/m^3 to 350 kg/m^3.

The main weakness of the model is the limitation of the input data. The model is constricted to its spatial domain, range of physiographic inputs, as well as temporal coverage. The model may not be applicable to areas outside of the study area, for elevations that are lower than 2408 m or higher than 3261 m, or for snow depths shallower than 0.20 m or deeper than 2.52 m. The snow course data were collected on or about the 1st of the month from January through June, and thus the model may be less suitable for mid-month days, and may not be useful before January 1st or after June 1st. Finally, the trend analysis of historic snow course data suggests that a significant decrease in snow density has been occurring at some of the operational snow course stations. This non-stationarity of the data illustrating a change in climate should be considered, as historic measurements may not be accurately representing current and future snowpack trends.

Similar snow density models have been developed from historic data for different domains. Jonas *et al.* [2009] developed a set of regression equations driven by snow depth, day of year, elevation, and region for the Swiss Alps to model snow density while Sturm *et al.* [2010] employed a statistical method based on Bayesian analysis, using snow depth, day of year, and climate class to estimate snow density for the United States, Canada, and Switzerland. The principle behind these previous studies as well as our research shows that snow density is a conservative variable that varies spatially much less than snow depth and SWE. The previous studies used spatial domains that are orders of magnitude larger than what has been presented here, yet the current data are at a finer resolution. While there are differences in modeled scale, favorable results have been observed in each approach, suggesting this method is applicable for basin-wide, regional, and global scales.

The strength and utility of the model developed here is its ability to estimate SWE from the most easily measured variable snow depth. This can improve snowpack estimates across varying domains of interest. This method is especially useful for field-based snow surveys at the basin scale, in which many snowpack measurements are required, and the assumption of a constant snow density [Lopéz-Moreno *et al.*, in review] across the study area is not valid. The snow density model is simple to develop and to employ and an effective tool for obtaining estimations of SWE from snow depth measurements across basin scale domains.

2.6 Conclusions

This study has developed a method for modeling snow density across a basin scale study area from historical snow course measurements. Snow density was modeled to develop a reliable method for estimating SWE from snow depth. Historical NRCS snow course data from 17 snow courses within the study area were used as the basis for the analysis. Input data of snow depth, day of year, elevation, and UTM Easting were used within a multiple linear regression model to predict snow density (Equation 2.6). The model explained 51% of the total variance of snow density with a RMSE of 45.31 kg/m^3, and 94% of the variance of calculated SWE with a RMSE of 4.4 cm. Performance statistics from verification procedures illustrates that the model is transferable to independent data within the bounds of the original dataset. The majority of residual values (80%) from estimated SWE fell within the range of ±5 cm, and the variance of model residuals were on average within 12.8% of the observed value, which is similar to the range of variability of SWE expected at a site. The method described here for modeling snow density provides a reasonable pathway for estimating SWE from snow depth measurements, and should be considered when evaluating snowpack properties at the basin scale.

Table 2.1: Sen's slope estimate for historic April 1st SWE and April 1st snow density at snow courses within the study area. [Significance as follows: + = $p < 0.1$, * = $p < 0.05$, ** = $p < 0.01$].

Snow Course	Variable	Record	n	Sen's slope estimate [/100yr]	Significance
Cameron Pass	SWE [mm]	1936 - 2010	75	0	
		1976 - 2010	35	-453	+
	ρ_s [kgm^{-3}]	1936 - 2010	75	-14.7	
		1976 - 2010	35	-149	+
Deadman Hill	SWE [mm]	1937 - 2010	70	-78.7	+
		1976 - 2010	33	-400	*
	ρ_s [kgm^{-3}]	1937 - 2010	70	-42.3	*
		1976 - 2010	33	-155	*
Hourglass Lake	SWE [mm]	1938 - 2010	71	-51.6	
		1976 - 2010	35	-182	
	ρ_s [kgm^{-3}]	1938 - 2010	71	-15.4	
		1976 - 2010	35	-18	

Table 2.2: Correlation pairs (Pearson's r) between snow density, snow depth, Julian day, elevation, UTM Northing, and UTM Easting.

	ρ_s	d_s	DOY	z	UTM_n	UTM_e
ρ_s	---	0.39	0.62	0.24	-0.03	-0.35
d_s		---	0.17	0.64	-0.18	-0.40
DOY			---	0.03	0.03	-0.08
z				---	-0.17	-0.13
UTM_n					---	0.03
UTM_e						---

Table 2.3: Snow density regression model calibration statistics. Variable notes: Julian day (DOY), snow depth (d_s), elevation (z), UTM Easting (UTM_e), UTM Northing (UTM_n).

Model Number	Independent Variables	VIF	AIC	Adjusted R^2
1	DOY, d_s, z, UTM_e	1.04, 2.12, 1.78, 1.22	34132	0.51
2	DOY,d_s,UTM_n,UTM_e	1.03, 1.26, 1.04, 1.19	34184	0.51
3	DOY,z,UTM_n,UTM_e	1.01, 1.05, 1.03, 1.02	34179	0.51
4	DOY,z,UTM_e	1.01, 1.02, 1.02	34177	0.51
5	DOY,d_s,UTM_e	1.03, 1.22, 1.19	34182	0.51
6	DOY,d_s,z	1.04, 1.78, 1.72	34425	0.47
7	DOY,d_s	1.03, 1.03	34440	0.46

Table 2.4: Snow density regression final model performance statistics for snow density and SWE prediction.

Verification Dataset	n	Snow Density Prediction			SWE Prediction		
		NSCE	MAE (kg/m^3)	RMSE (kg/m^3)	NSCE	MAE (mm)	RMSE (mm)
Snow course Calibration	3262	0.51	35.0	45.31	0.94	31.21	43.88
10-Fold Cross Verification	3262	---	---	45.38	---	---	---
Independent Field Data	84	0.58	34.0	43.52	0.92	35.87	66.38
Independent SNOTEL Data	121	0.51	45.31	63.41	0.88	43.41	57.58

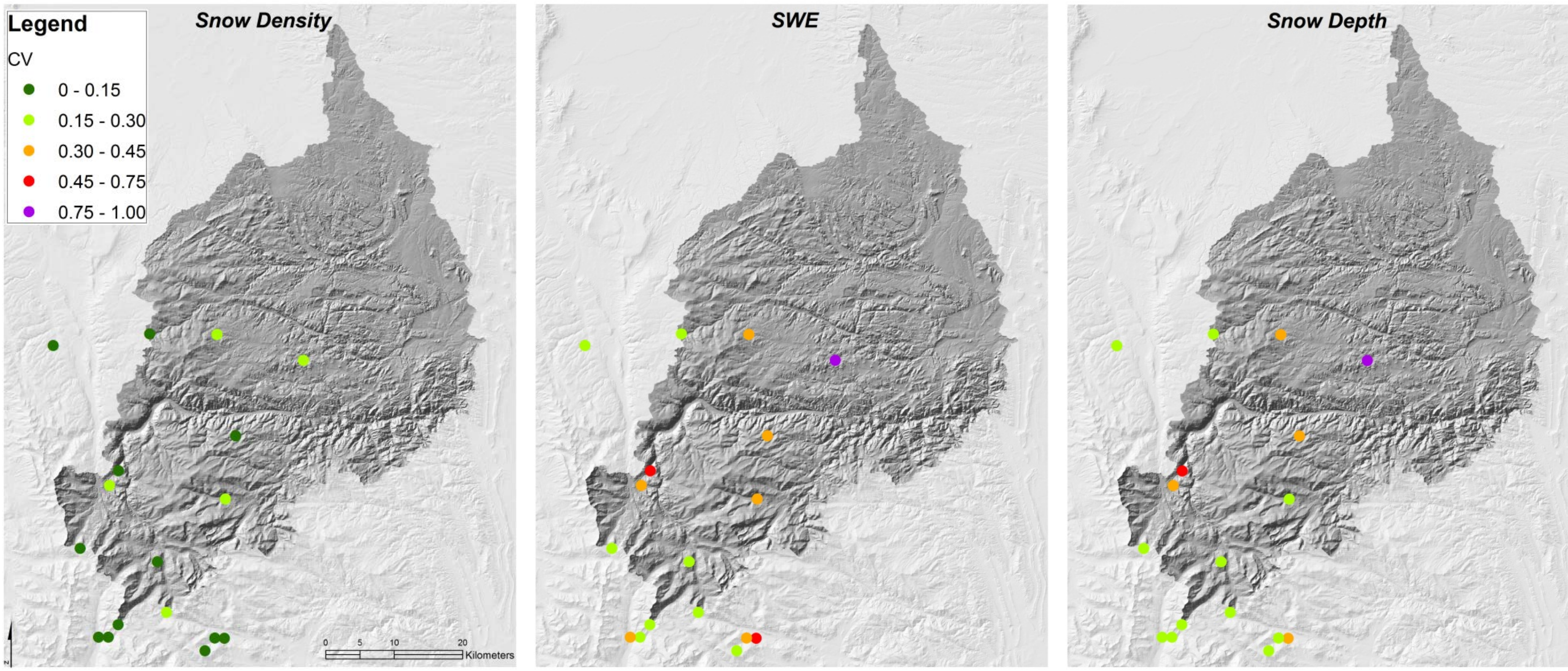

Figure 2.1: Coefficients of variation of snow density, SWE, and snow depth for the beginning of April from historic operational snow course measurements [1936-2010, n=955] within the Cache la Poudre basin study area, Colorado.

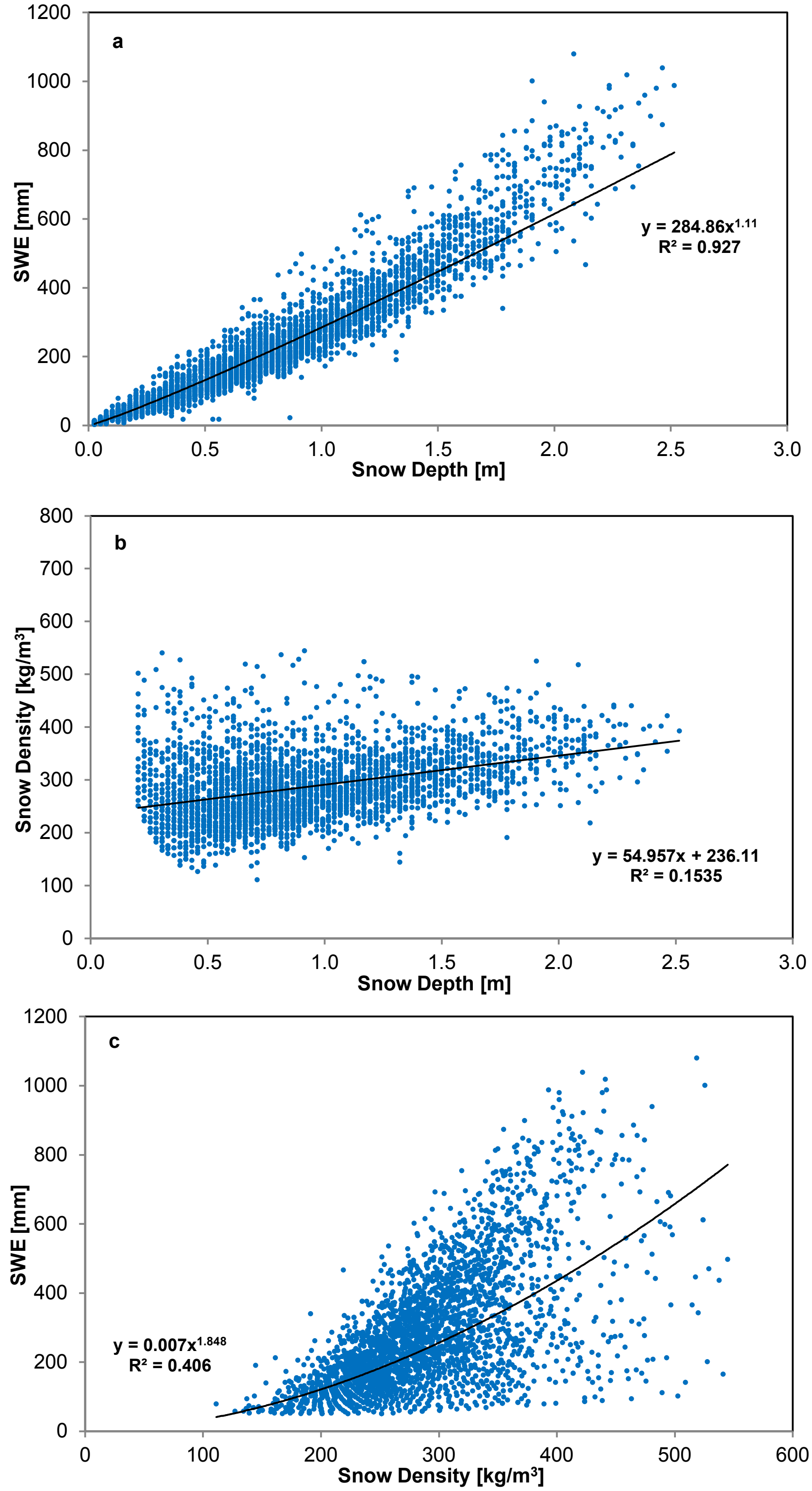

Figure 2.2: Pairwise relations of SWE, snow depth, and snow density from historic snow course measurements [1936-2010, n=955] within the Cache la Poudre basin study area.

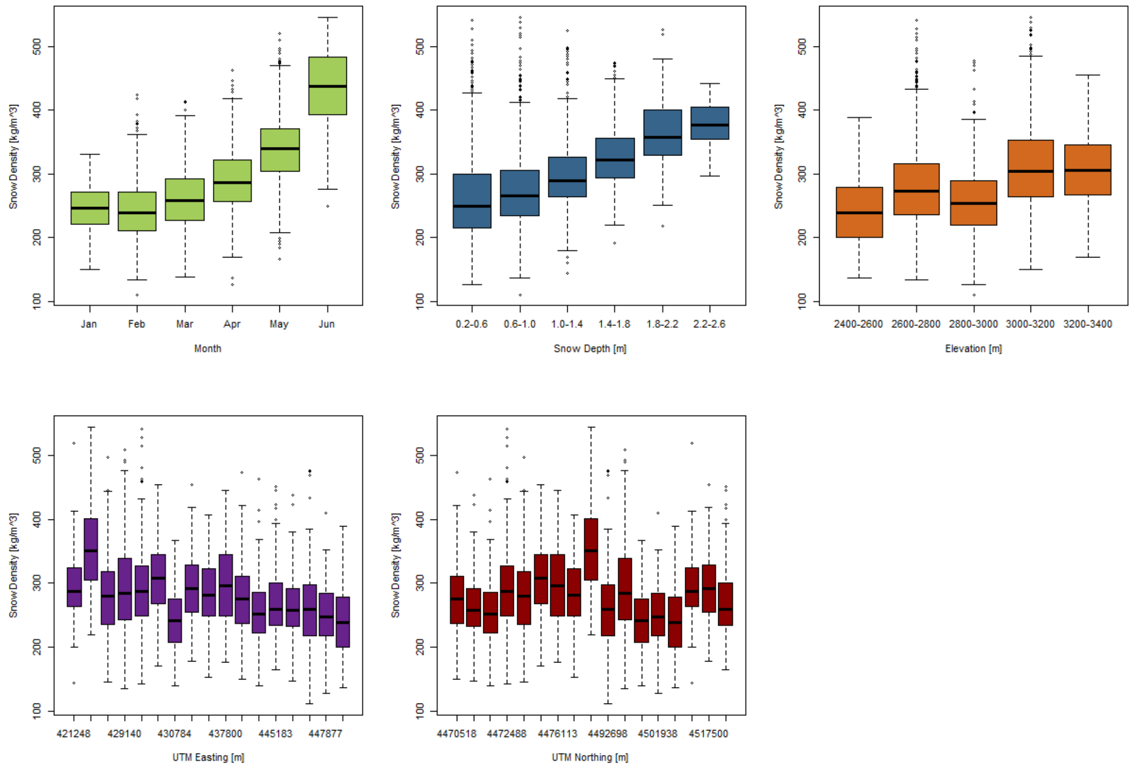

Figure 2.3: Box-and-whisker plots of five physiographic variables in relation to snow density from historic snow course measurements within the Cache la Poudre basin study area, Colorado.

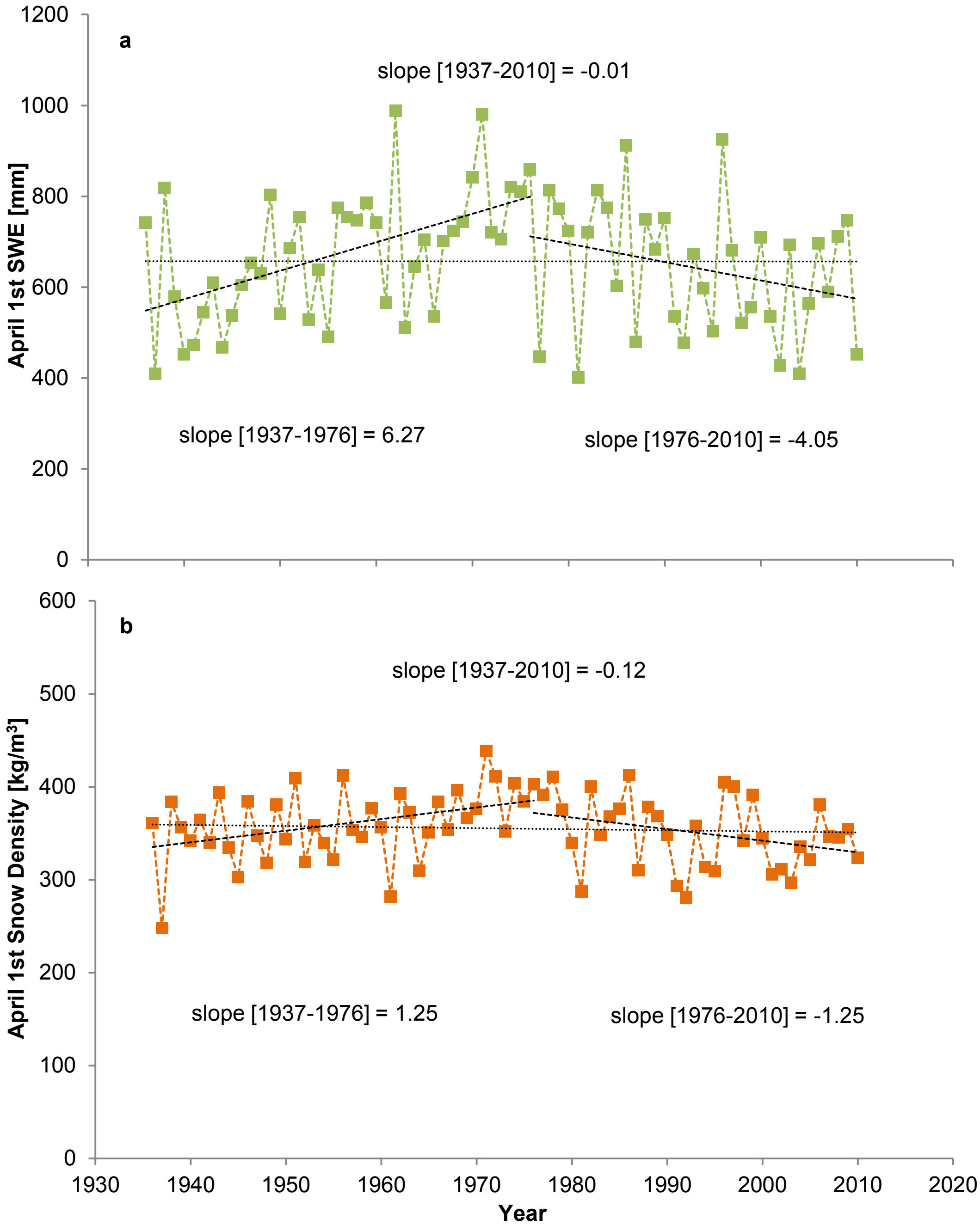

Figure 2.4: Historic trends of April 1st SWE (2.4a) and April 1st snow density (2.4b) at the Cameron Pass snow course, Colorado.

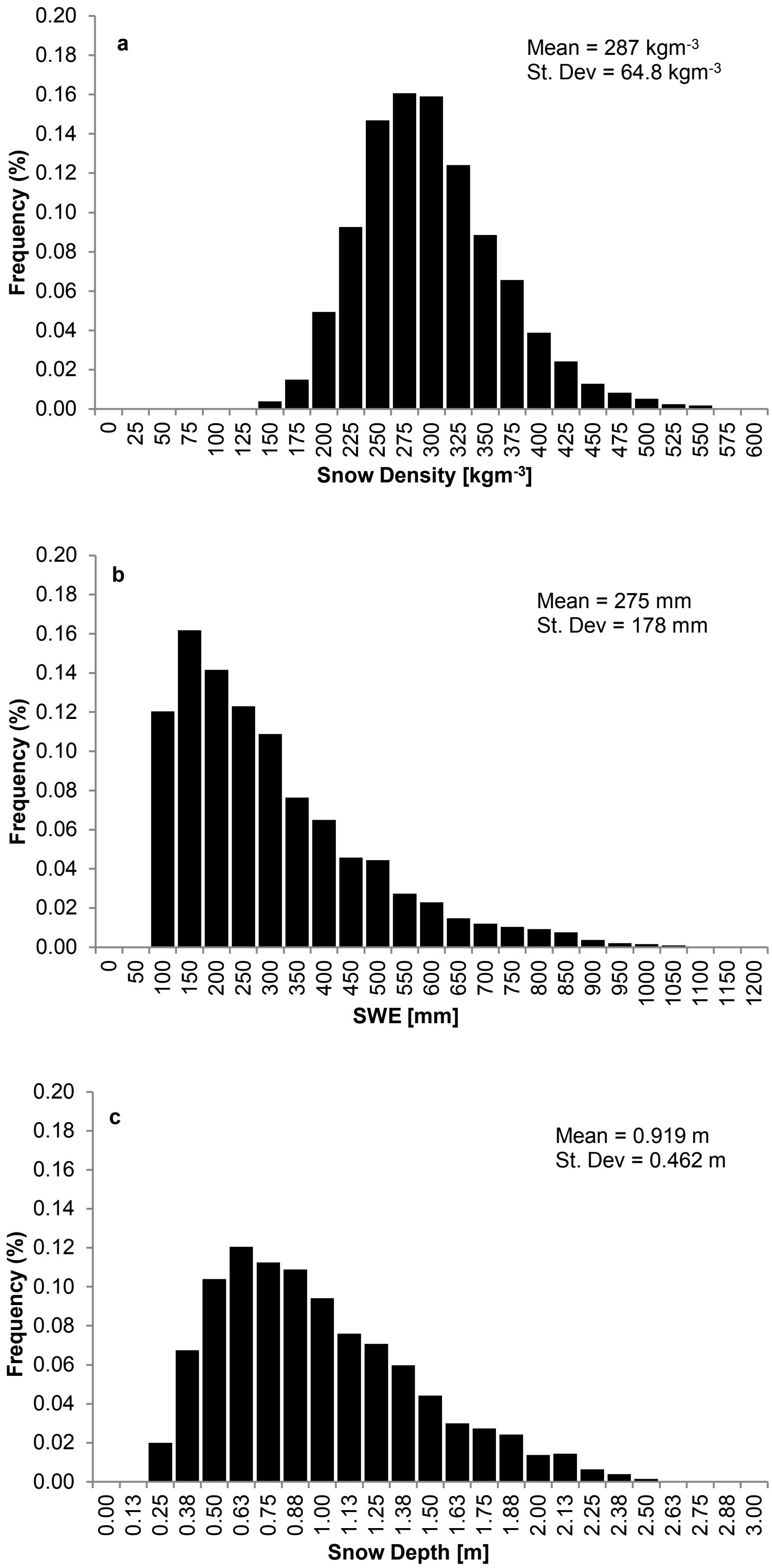

Figure 2.5: Distribution of snow density, SWE, and snow depth from historic operational snow course measurements [1936-2010, n=3262] within the study area.

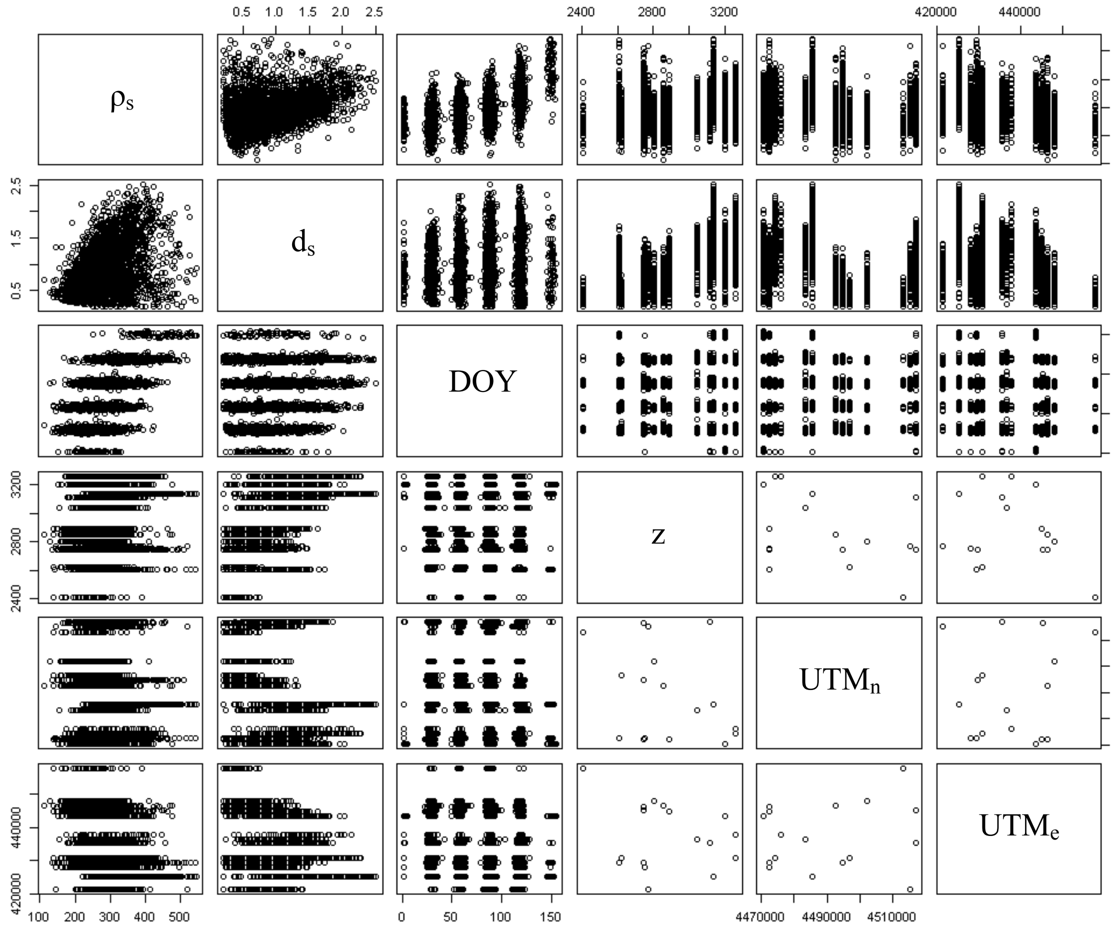

Figure 2.6: Snow course database pairwise scatterplots of snow density (ρ_s), snow depth (d_s), Julian day (DOY), elevation (z), UTM Northing (UTM_n), and UTM Easting (UTM_e).

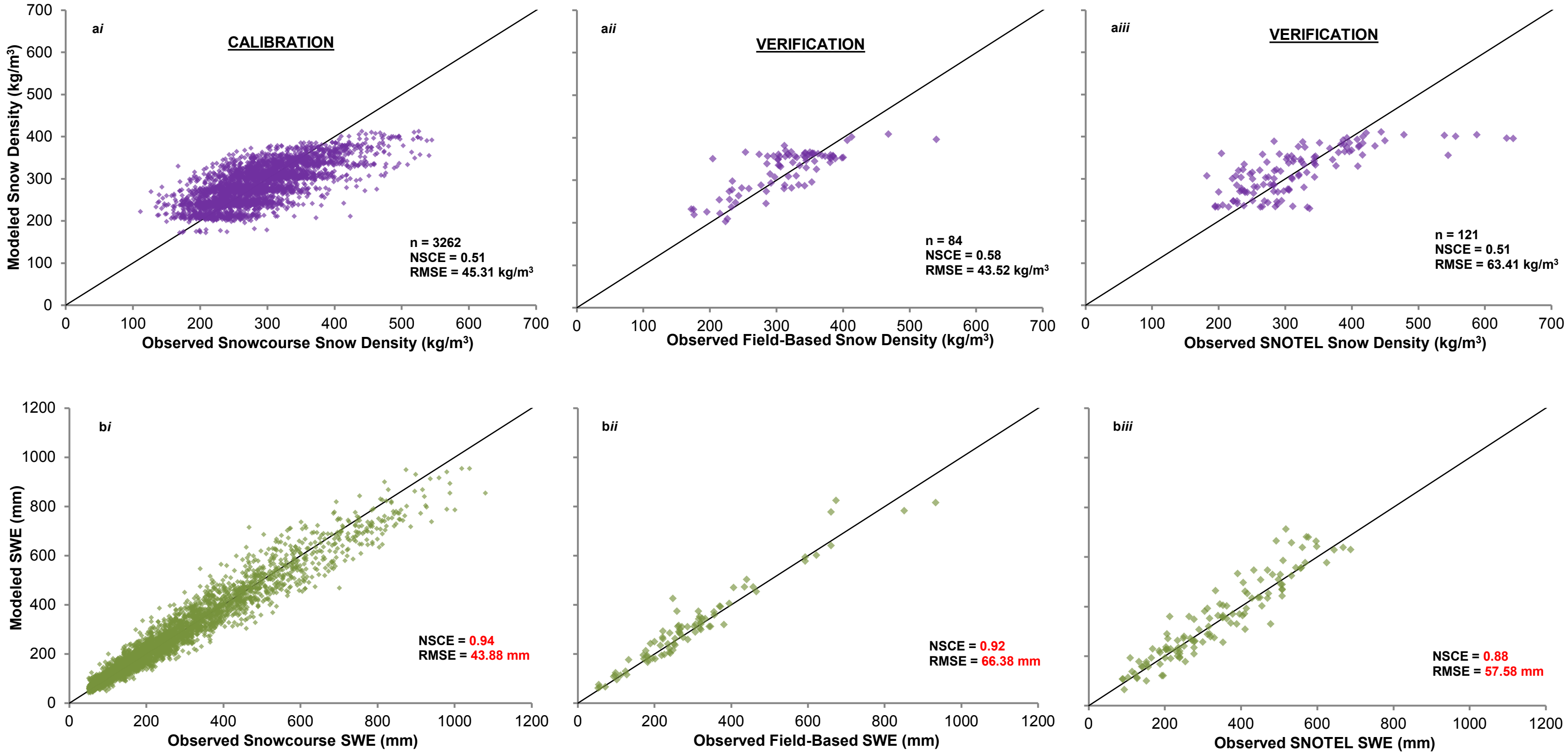

Figure 2.7: Modeled versus observed snow density and SWE calibration and verification data plotted for the snow density multiple regression model.

CHAPTER 3: BASIN SCALE SWE VARIABILITY

3.1 Introduction

Knowledge of the spatial distribution of SWE in mountainous areas of the western United States is crucial for accurate forecasting of water availability and flood potential (through snowmelt runoff), as well as successful management of water resources. Snow influences and intersects hydrologic, atmospheric, and biologic systems, thus the ability to describe the distribution of snow across space is also important for understanding processes that govern these systems (e.g., energy, water, and biogeochemical cycling) [e.g., Deems *et al*., 2008, among others].

The spatial variability of the snowpack in mountainous regions is particularly challenging to characterize due to complex topography that induce strong and highly variable meteorological gradients. Additionally, efforts to assess the variability of the snowpack are constrained by the scale of the available measurements (measurement scale), which is often different than the natural range of variability of the snowpack at a given scale (process scale) [Blöschl, 1999]. Representing the process scale of SWE distribution with field-based snowpack measurements is considerably challenging due to the spatial heterogeneity of the snowpack, time intensive nature of field measurements, as well as inaccessibility due to extensive distances of backcountry travel and avalanche danger.

Despite these challenges, recent studies (e.g., Elder *et al*., 1998; Balk and Elder, 2000; Windstral *et al*., 2002; Fassnacht *et al*., 2003; Molotch and Bales, 2005) analyzing the spatial distribution of the snowpack have shown considerable success through emphasizing the statistical relationship between snow properties and terrain characteristics; however, the majority of studies using field-based measurements have analyzed study watersheds that are less than 100

km^2 in area. There is a need for assessment and evaluation of 1.) how terrain variables may be used to describe the spatial distribution of the snowpack at the basin scale, which is the scale of most interest in terms of water resources management, and 2.) remote sensing observations of the snowpack at this scale. We define the “basin scale” as the size of the 8-digit United States Geological Survey (USGS) hydrologic unit code (huc) basin, which commonly ranges from $500km^2$ to $5,000km^2$. The majority of studies analyzing this scale of interest have only utilized operational snow measurements as input data [e.g., Fassnacht *et al*., 2003; Harshburger *et al.*, 2010], which Bales *et al*. [2006] suggest may not be available at fine enough of resolution to describe the variability at the basin scale. Thus, this study uses a combination of operational SNOTEL and snow course measurements, as suggested by Dressler *et al*. [2006], as well as supporting field-based snowpack measurements to analyze the spatial variability and observable patterns of SWE at the basin scale. Analysis of these snowpack measurements at this scale of interest may provide insight of which processes are most important for driving the variability of the snowpack at the basin scale.

3.2 Methods

3.2.1 Snowpack Measurements

3.2.1.1 Operational Measurements

Operational snowpack measurements of SWE, snow depth, and calculated snow density collected by NRCS personnel at snow courses within the study area as well as automated SNOTEL stations within the study area were used in this study. Tables 1.1 and 1.2 provide a description of the operational measurements located in and near the study area.

3.2.1.2 Field-based Measurements

Field-based snow surveys within the study area were completed on or about April 1st 2011 and 2012 (see Chapter 1 for a detailed explanation of sampling protocol). Each of the field-based surveys included multiple transects, with each transect consisting of a number of snowpack sampling locations at a spacing of approximately 500 meters (Figure 1.4). The location of snow survey transects were selected based on accessibility as well as representation of snow producing regions within the study area. Richer (2009) showed that elevations above 3000 m have the highest probability of snow cover within this study area and that the snow cover depletion within elevation zone from 2680 m to 3042 m may be very important in terms of hydrograph dynamics. Therefore, transects of sampling locations for this study were focused around the elevation range of 2500 – 3500 m. The high elevation areas located around the Colorado State University Pingree Park Campus, Cameron Pass, and Deadman Hill were the regions of focus within the Cache la Poudre basin (Figure 1.4). A total of 42 field sampling locations (14 locations with no snow) were monitored about April 1, 2011 and 121 field sampling locations (14 locations with no snow) on and about April 1, 2012. SWE was estimated at all sampling locations where SWE was not directly measured by using our snow density model (see Chapter 2).

The 2011 field-based snow survey was completed over the span of three days (3/31/11 – 4/2/11), while the 2012 survey was completed over four days (3/29/12 – 4/1/12). No new snowfall was observed at any SNOTEL station within the study area during the 2011 or 2012 survey time period, thus changes to the snowpack during these periods were due to melt, compaction, and/or metamorphism. Changes to snow density over these short periods of time were likely minimal, therefore snow density was not adjusted. However, changes in snow depth were accounted for using daily SNOTEL snow depth measurements to normalize the field-based snow depth measurements to a single date for each survey. The average change in snow depth among SNOTEL stations was added to our field-based snow depth measurements outside of the normalized date to adjust for the change in snow depth over that period (Table 3.1). Snow depth measurements from the 2011 survey were normalized to April 2, while 2012 measurements were normalized to March 31.

3.2.2 Forest Canopy Measurements

Forest canopy data were collected at each field-based sampling location during the April 1, 2012 snow survey. Categories of canopy cover, community type, and tree mortality were noted for the tree canopy covering each set of measurement points (Table 1.4). It should be noted that these categorical measurements taken by the field-worker at each location were considered subjective as a standard numerical measurement for each category was not used. The forest canopy measurements were used to assess how the forest canopy variables may be impacting the distribution of snow depth.

3.2.3 Physiographic and Biological Predictor Variables

Physiographic and biological variables that were thought to potentially drive the spatial distribution of snow at the scale of interest were derived from a 30 m resolution digital elevation model (DEM) of the study area. The DEM was downloaded from the USGS National Elevation Dataset (NED) [<seamless.usgs.gov>]. A value for each of the derived physiographic and biological variables (spatial data grids) was extracted for each sampling location based on its corresponding 30 m DEM pixel. A description of the derivation and importance of each of the spatial data grids is provided below. For simplicity, physiographic and biological variables will be referred to as physiographic variables heron in.

3.2.3.1 Location

Location within the study area is represented by Universal Transverse Mercator (UTM) Zone 13 N Northing and Easting coordinates for each field-based and operational sampling location. A 30 m resolution spatial data grid of UTM Northing and Easting was created for the study area in ArcGIS by assigning the centroid UTM value for each pixel. Spatially continuous coordinates of latitude and longitude can be correlated with the distribution of snow in various ways that depend on site location and scale. Previous studies have used distance to a mountain barrier and distance to ocean or source of moisture [e.g., Fassnacht *et al.*, 2003; López-Moreno and Nogués-Bravo, 2006], which can also be represented by longitude for the study site due to its geographic orientation. Furthermore, given the scale of the study, latitude and longitude represent different regions within the study area that are thought to display different patterns of snow accumulation and ablation due to the variability of meteorology and storm tracks.

3.2.3.2 Elevation

Elevation was extracted for each sampling location directly from the 30 m DEM. Snow accumulation has long been shown to be a function of elevation [e.g., Washichak and McAndrew, 1967; Dingman, 1981] due to orographic precipitation patterns and the effect of air temperature [Doesken and Judson, 1996].

3.2.3.3 Slope

Slope was derived from the 30 m DEM using the Spatial Analyst tools within ArcGIS to provide an output spatial data grid with a value of slope (in degrees) for each pixel. The degree of slope impacts the stability of the snowpack (influencing snow accumulation and redistribution) and input of solar radiation (influencing melt) [Anderton *et al.*, 2004]. Previous studies have successfully used slope angle as an explanatory variable within statistical models describing the distribution of snow [e.g., Erxleben *et al*., 2002; Winstral *et al*., 2002].

3.2.3.4 Northness and Eastness

Aspect (in degrees) was also derived from the 30 m DEM using the Spatial Analyst tools within ArcGIS. Aspect can be problematic as an independent variable due to its continuous range of 0 to 360 degrees, thus normalizing this variable is necessary. Degrees of northness and eastness were calculated to normalize the aspect variable [Fassnacht *et al.*, 2001; Fassnacht *et al*., 2012]. Degree of northness is the product of the cosine of aspect and the sine of slope [Molotch *et al*. 2005], while degree of eastness is the product of the sine of aspect and the sine of slope. Exposure of slope aspect controls solar radiation input, which influences snowpack stability, densification, and ablation [McClung and Schaerer, 2006].

3.2.3.5 Solar Radiation

Solar radiation was derived using the Area Solar Radiation tool in ArcGIS, which calculates incoming solar radiation across a DEM surface for a specified time interval. Given the latitude of the study area, the cumulative clear sky solar radiation (in WH/m^2) from November 15 through March 30 was calculated for each pixel. Cumulative incoming solar radiation is calculated based on solar zenith angle and terrain shading, and does not consider the influence of forest canopy. Previous studies have successfully used solar radiation spatial data grids derived by similar methods within statistical models describing the distribution of snow [e.g., Elder *et al*., 1998; Anderton *et al.*, 2004; Erickson *et al*., 2005].

3.2.3.6 Curvature

Profile curvature was derived from the 30 m DEM using the Spatial Analyst tools within ArcGIS to provide an output spatial data grid with a value of curvature for each pixel. Curvature is defined as the second derivative of the surface (slope of the slope) [Kimerling *et al*., 2011]. This variable represents the local relief of terrain (i.e. concavity or convexity) in the direction of maximum slope, which, in terms of snow accumulation, primarily accounts for wind drifting from high exposure areas with steep slopes to low lying gullies [Blöschl *et al*., 1991a].

Maximum upwind slope [Winstral *et al*., 2002] is a terrain-based variable that has been shown to account for redistribution of snow by wind, which is especially important in alpine areas. However, this variable requires the knowledge of predominant wind direction to account for upwind terrain features, which is not measured across a basin scale, requiring a modeling approach [Liston and Sturm 1998], thus was not used for this study.

3.2.3.7 Canopy Density

Canopy density was obtained from the National Land Cover Database (NLCD 2001) [<http://www.mrlc.gov>]. Canopy density is derived from Landsat Enhanced Thematic Mapper+ (ETM+) circa 2001 satellite data and DEM derivatives [Homer *et al*., 2007]. The canopy density spatial data grid provides an estimated percentage of canopy cover for each pixel at a 30 m resolution. Canopy density can influence how snow is distributed across space as it is directly related to the amount of snow that is intercepted in the tree canopy. Snow sublimation from snow intercepted within the forest canopy is a major component of the overall water balance [Pomeroy and Gray, 1995].

3.2.4 Bivariate Analysis

Pairwise scatterplots of physiographic variables at each measurement location were created to assess the relation of these variables with each other. A correlation matrix was created for the Pearson correlation coefficient amongst all pairs of physiographic variables. The bivariate relations of all field-based and operational snow depth and SWE measurements with associated physiographic variables were then analyzed. Regression analyses of snow depth and SWE with the physiographic variables was performed and the strength of these regressions was evaluated. The strength of each regression was determined by selection of linear or non-linear (exponential, logarithmic, power) equation that provided the strongest coefficient of determination (R^2). Coefficient of determination values that showed explanation of less than 10 percent of the variance in the data were not reported on the scatterplot. Plots showing the mean SWE among ranges (evenly divided among the dataset) of each physiographic variable were also analyzed.

Bivariate relations (analysis of two variables, X, Y) were assessed among subsections of the entire dataset for 2011 and 2012. Regression relations among operational SWE measurements (field-based measurements removed) were analyzed for comparison of observed trends of the combination of field and operational-based data. Also, the 2011 and 2012 datasets were split into groups of stations located in close proximity to the Cameron Pass, Deadman Hill, and Hourglass Lake operational sites to see how relations with physiographic variables may change regionally across the study area.

Summary statistics of the bivariate relations among the forest canopy cover variables and snow depth measurements were also analyzed. Box and whisker plots were used to summarize and compare the mean and variance of snow depth measurements among each forest canopy category.

3.2.5 Multiple Linear Regression

Multiple linear regression (Equation 2.2) was used to model April 2, 2011 and March 31, 2012 SWE based on its relation with independent physiographic variables identified above (see Chapter 2 for a detailed description of multiple linear regression). Multiple linear regression models were developed using both field and operational-based snowpack measurements and also operational measurements only. At the scale of interest, operational data are commonly the only snowpack data available, thus it is useful to compare the results from operational data only those results obtained from using operational data and additional field-based measurements. It is thought that with the inclusion of additional field-based measurements, a more representative dataset of the study area can be provided. The following notation will be used in this study: $model_{O+F}$ will refer to the multiple regression model using both field and operational-based snow measurements and $model_{O}$ will refer to the multiple regression model using operational-based snow measurements only. A total of four regression models will be developed: $model_{O+F11}$ (field and operational data from WY 2011), $model_{O11}$ (operational data from WY 2011), $model_{O+F12}$ (field and operational data from WY 2012), and $model_{O12}$ (operational data from WY 2012). The statistical software *R* [Ihaka and Gentleman, 1996] was used for all statistical analyses.

The independent variables to be included in the multiple linear regression models were selected based on two automated procedures, stepwise regression and all-subsets regression. A stepwise regression procedure was completed to determine which combination of variables would provide the lowest resulting AIC statistic (see Chapter 2) [Akaike, 1974]. Additionally, an all-subsets regression procedure was performed, assessing the Mallows' C_p criterion (see Chapter 2) [Mallows, 1973]. Models were selected based on favorable results from the automated variable selection procedures. The variance inflation factor (VIF) was used to quantify the severity of multicollinearity between independent variables (see Chapter 2). Each of the final regression models were selected based on analysis of lowest multicollinearity, minimum AIC criterion, as well as MAE (Equation 2.4) and RMSE (Equation 2.5) performance statistics calculated during model calibration.

To assess the accuracy of the final multiple linear regression models, a 10-fold cross verification, which runs 10 iterations of removing a random selection of the dataset and fitting the regression to the remainder of the data, was used to compare modeled values to the observed values removed for each iteration. Verification with independent field-based measurements was also completed to test the transferability of $model_{O11}$ and $model_{O12}$ to predict independent data. Performance of model verification was determined from the residuals of modeled SWE by calculation of the RMSE (Equation 2.5) performance statistic.

3.2.6 Basin Scale SWE Interpolation

The linear multiple regression relationships identified from each model were used to interpolate SWE across the study area by calculating the regression equation on a pixel by pixel basis across the study area to create raster surfaces of the distribution of SWE. Snow covered area (SCA), derived from the Moderate Resolution Imaging Spectroradiometer (MODIS)/Terra 8-day 500 m snow cover product, was used to define the extent of snow cover across the study area and mask the interpolation surface to the extent of the snow cover.

Finally, summary statistics of the interpolated SWE surfaces were calculated for the entire study area as well as for each of the elevation zones identified by Richer [2009] (Figure 3.18). Additionally, interpolated SWE Volume was calculated for the study area and each elevation zone by the following:

$$SWEV = \sum \frac{SWE * \alpha}{10^6} \quad (3.1),$$

where SWEV is interpolated SWE Volume in 10^6 m^3, SWE is in m, and 30 m pixel size (α) is 900 m^2.

3.3 Results and Discussion

3.3.1 Snowpack Measurements

A total of 51 and 127 snowpack measurements (both field and operational-based) were analyzed from the April 2, 2011 (WY 2011) and March 31, 2012 (WY 2012) snow surveys, respectively (Figure 3.1). WY 2011 and 2012 snowpack measurement datasets show that mean SWE and snow depth from 2011 were greater than 2012, yet the mean snow density and standard deviation of snow density was shown to be consistent among both years (Table 3.2). The WY 2011 was the maximum snow year on record within the study area, while WY 2012 was one of the minimum years on record (Figure 1.2); thus WY 2011 snowpack measurements were shown to have a higher mean SWE and snow depth, but also had a greater range of variability (Table

3.2a) than that of WY 2012 (Table 3.2b). From the average SWE among SNOTEL stations within the study area, the April 1st snow survey occurred before peak SWE in 2011, however, occurred after peak SWE in 2012 (Figure 3.2). Analysis of the April 1st snowpack from these two water years allows for the comparison between the two extreme snow years (maximum and minimum) as well as between two different stages of the niveograph (during accumulation and melt).

3.3.2 Physiographic Variable Distributions

Physiographic variables derived within GIS at each of the snowpack measurement locations have similar averages when compared to the basin-wide variable average for both 2011 (Table 3.3a) and 2012 (Table 3.3b). Histograms of relative frequency (Figure 3.3) show that the distribution of physiographic variables sampled in 2011 and 2012 is similar to the basin-wide distribution of these variables, suggesting that the snowpack measurement locations sampled during WY 2011 and WY 2012 are representative of the variability of physiography among the entire study area. The range of values of physiographic variables observed at operational stations tended to be smaller than the field-based station ranges (Figure 3.3), which also suggests, the combination of field and operational-based measurements are more representative of the physiography of the basin than the operational-based measurements alone. A formal Kolmogorov-Smirnov test (K-S test) for equality of distributions between a random sample (n = 244) of the continuous physiographic variables within the 50% Snow Cover Index (SCI) [Richer *et al*., in review] of the basin versus the variables associated with the WY 2011 and WY 2012 measurement locations was completed (Table 3.4). The K-S test shows that during both years the difference between the two samples for curvature, eastness, and canopy density is not significant enough (95% significant level) to say they have a different distribution. However, a significant difference between the distributions of elevation, slope, northness, and solar radiation was observed for both years. The difference in elevation is obvious since field data are located more at higher elevations than the entire domain (Figure 3.3a), and the operational data tend to be located in a small elevation zone [Fassnacht *et al*., 2012]. Northness is highly correlated to solar radiation, and both are related to slope so the significance difference for each of these variables may be based on their correlation. For safety purposes manual measurements tend to occur in flatter regions, so steeper slopes can be underrepresented.

3.3.3 Bivariate Analysis

3.3.3.1 Physiographic Variables

Pairwise scatterplots of all physiographic variables and snowpack measurements for each measurement location are shown in Figure 3.4a (WY 2011) and Figure 3.4b (WY 2012). Snowpack variables were shown to have a strong correlation with each other, with SWE and snow depth showing the strongest relation (consistent with the findings of Chapter 2), while also showing to be highly correlated with elevation (Table 3.5). Additionally, northness and solar radiation were strongly correlated with each other (Table 3.5).

Each of the physiographic variables in the bivariate scatterplots from WY 2011 and WY 2012 are similarly related to both SWE (Figure 3.5i) and snow depth (Figure 3.5ii) due to the strong correlation between SWE and snow depth. Given this similarity, the results of SWE, the main hydrologic variable of interest, will subsequently only be reported. The strength of each bivariate regression relation from WY 2011 and WY 2012 was evaluated, and elevation (R^2 = 0.56, R^2 = 0.45, respectively), UTM Northing (R^2 = 0.30, R^2 = 0.01, respectively), and UTM

Easting ($R^2 = 0.48$, $R^2 = 0.15$, respectively) were the only relations that explained greater than ten percent of the variance in SWE. Linear regression showed the strongest R^2 for each of these relations. These bivariate relations suggest elevation and UTM coordinates should be included as independent variables for the multiple linear regression modeling of SWE.

SWE increased with increasing elevation (Figure 3.5ai), with the steepness of this slope being greater in WY 2011 than 2012; mean SWE increased among ranges of elevation that evenly divided each dataset (Figure 3.6a). The strength of the regression relation between SWE and elevation for WY 2011 and WY 2012 suggests that elevation is the most important physiographic variable for driving the distribution of SWE across the study domain, which is consistent with previous findings from studies evaluating SWE at the basin scale [e.g., Fassnacht *et al*., 2003; Jost *et al*., 2007; Harshburger *et al*., 2010]. As UTM Northing increases, SWE decreases in WY 2011 (Figure 3.5bi, Figure 3.6b), suggesting northern regions of the study area receive less snow than southern regions [as suggested by James Meiman, pers. comm., 2010], yet this trend was not apparent in the low snow year of 2012. The apparent greater accumulation of snow in southern regions of the study area could be related to an upwind elevation gradient, with high peaks of Rocky Mountain National Park located in the southern portion of the study area, or due to the possibility of a dominant storm track that preferentially precipitates in southern regions before moving northward. SWE also decreased with increasing UTM Easting (Figure 3.5ci, Figure 3.6c), which corresponds with both the effect of orographic precipitation within the study area (the continental divide is located on the western border of the study area), and also lower elevation regions receiving less snow than higher elevation regions. The other physiographic variables that are known to influence snow accumulation (e.g., forest canopy, aspect, and slope) did not exhibit a strong linear trend based on their bivariate relations with

SWE; however, they may still be important in explaining variability of the datasets once the trends of elevation and UTM coordinates have been removed.

Bivariate relations among operational SWE measurements (field-based measurements removed) show similar trends observed when including field-based data, with a stronger relation between SWE and elevation, and weaker relations between SWE and UTM coordinates (Figure 3.7). Also, the WY 2011 and WY 2012 datasets show that elevation and UTM coordinates generally show stronger trends explaining the variance of SWE when the datasets are split into regional groupings (Figure 3.8). These trends are much more apparent in the WY 2011 dataset (Figure 3.8i), as this maximum snow year showed much greater variation in snow amounts than WY 2012 (Figure 3.8ii).

3.3.3.2 Forest Canopy Cover Variables

Summary statistics of the bivariate relations among the forest canopy cover variables and snow depth measurements from WY 2012 are provided in Table 3.6. Box and whisker plots (showing the median, interquartile range, and entire range) of the forest canopy cover categories show that open forest category showed a greater median snow depth, and a greater range of variability, than the partially closed and closed categories (Figure 3.9). Partially closed canopy had a greater median snow depth than the closed canopy. The alpine community type had a greater median snow depth and also a greater range of variability than the lodgepole pine and spruce-fir forest communities (Figure 3.10). The tree mortality categories show that all categories have a similar range of variability, yet the dead-gray mortality stage had a greater minimum, median, and maximum snow depth than the alive-green and dead-red stages (Figure 3.11).

These results suggest that snow depth tends to be deeper in open areas or disturbed areas in which needles are no longer present on trees compared to closed canopy with needle bearing trees. This difference is likely due to an increase of snow sublimation in closed canopy with needle bearing trees that is promoted by canopy interception of snow [Pomeroy and Gray, 1995], which is consistent with recent research on the impact of forest disturbance on snow distribution [e.g., Pugh and Small, 2011; Boon, 2012]. Given that the forests in northern Colorado are changing drastically due to disturbances from the mountain pine beetle (MPB; *Dendroctonus ponderosae*) and spruce bark beetle (SBB; *Dendroctonus rufipennis*), as well as other forest disturbances, such as wildfires, it should be considered that the canopy density (NLCD, 2001) spatial data grids used within this study may no longer provide current and accurate values of canopy density. Use of a more accurate and up to date forest cover dataset could allow for greater insight into how the changing forest may be influencing the distribution of snow.

3.3.4 Multiple Linear Regression

Multiple linear regression was used to model SWE for April 2, 2011 and March 31, 2012 with the field-based and operational snowpack dataset (model$_{O+F}$) and the operational snowpack dataset only (model$_O$). A total of six combinations of independent variables were tested for each model based on favorable results from the automated variable selection procedures. Table 3.7 and Table 3.8 show the final independent variables used within each model and summarize model calibration statistics for model$_{O+F}$ and model$_O$, respectively. The following notation was used for independent variables within the regression models: UTM Easting (UTM_e in m), UTM Northing (UTM_n in m), eastness (E), slope (S in degrees), elevation (z in m), cumulative solar radiation (SolRad in WHm^{-2}), curvature (C in hm^{-1}), and canopy density (cd in %) Equations for $model_{O+F11}$, $model_{O+F12}$, $model_{O11}$, and $model_{O12}$ are provided below, respectively:

$$SWE_{O+F11} = 1.98x10^4 - 1.34x10^{-2}UTM_e - 3.47x10^{-3}UTM_n + 181E - 4.48S + 0.743z \quad (3.2),$$

$$SWE_{O+F12} = -7.79x10^3 - 1.88x10^{-3}UTM_e + 1.71x10^{-3}UTM_n - 0.701x10^{-2}SolRad + 0.414z \quad (3.3),$$

$$SWE_{O11} = 1.95x10^3 - 9.11x10^{-3}UTM_e + 0.843z - 100C \quad (3.4),$$

$$SWE_{O12} = -1.12x10^4 + 2.20x10^{-3}UTM_n + 0.638cd + 189E - 2.88S + 0.492z \quad (3.5),$$

where, SWE is in mm. $Model_{O+F11}$ explains 86% of the total variance ($R^2_{adj} = 0.84$) with an RMSE of 10.3 cm and all coefficients are statistically significant at the 95% significance level, whereas 50% of the total variance ($R^2_{adj} = 0.48$) with a RMSE of 7.8 cm was observed for $model_{O+F12}$, with all coefficients being statistically significant at the 95% significance level, except for solar radiation, which is significant at the 90% level. The WY 2011 operational model ($model_{O11}$) explains 89% of the total variance ($R^2_{adj} = 0.87$) with an RMSE of 8.7 cm and all coefficients are statistically significant at the 99% significance level. Lastly, $Model_{O12}$ explains 82% of the total variance ($R^2_{adj} = 0.76$; $p < 0.001$) with a RMSE of 5.6 cm. All coefficients of $model_{O12}$ are statistically significant at the 95% significance level, with the exception of solar radiation, which is significant at the 90% significance level and canopy density which is not statistically significant at the 90% level. The variance inflation factor (VIF) is below 4 for each variable within all four of the multiple regression models, suggesting that multicollinearity between independent variables is not observed. Also, the residuals of each regression model do not violate the underlying assumptions of the regression (normality, linearity, homoscedasticity) [Kutner *et al.*, 2005].

A comparison of the error estimation between WY 2011 and WY 2012 models shows that the $model_{O+F11}$ has a greater typical magnitude of error (RMSE) than $model_{O+F12}$, yet describes more of the variance in the data (R^2) (Table 3.7). Similarly, $model_{O11}$ has a greater RMSE and lower R^2 value than $model_{O12,}$ but the difference between these two models is less (Table 3.8). The difference among these performance statistics can partially be explained by the nature of each snow year (WY2011 was the maximum snow year and WY2012 was amongst the lowest) and sampling scheme. WY 2011 showed much more variation in snow amounts WY 2012, which could explain the difference in the RMSE. Additionally, the greater number of measurement locations (n = 127) in WY 2012 compared to WY 2011 (n = 51) could further explain the difference in R^2 between $model_{O+F11}$ and $model_{O+F12}$. Given this difference in field-based sampling locations, a reduced $model_{O+F}$ for WY 2012 was developed including only WY 2012 field-based measurement locations that were co-located with WY 2011 measurement locations (n = 42). The reduced model included UTM Easting, UTM Northing, elevation, eastness, and northness as independent variables and explained 66% of the total variance with an RMSE of 6.6 cm (Figure 3.12b). These results show an improvement from the full model ($model_{O+F12}$), suggesting that fewer data points may be increasing the model's ability to describe the variance of the data. Also, the reduced model showed a lower R^2 value than $model_{O+F11}$ which suggests that the model performs better for the 2011 snow year due to the greater range of observed variability in the data.

Despite WY 2011 being a maximum snow year and WY 2012 being a minimum snow year, the variables driving each SWE regression were similar; including elevation, location within the basin (UTM Easting and/or UTM Northing), and a variable related to slope, aspect, and/or curvature. The inclusion of elevation, latitude, and longitude within each regression as well as the bivariate relations of these variables with SWE suggests that these variables may be consistent drivers of the spatial variability of SWE at the basin scale. However, given that various studies [e.g., Erickson *et al*., 2005; Fassnacht *et al.*, 2012] have shown the spatial variability of snow accumulation to be described by different physiographic variables from year to year, additional years of data collection at the basin scale are needed for evaluation.

Comparison of the error estimation between model_{O+F} and model_{O} for WY 2011 and WY 2012 shows that model_{O} has superior performance statistics for both years. Model_{O11} and model_{O12} showed a similar strong performance to previous research using operational data at a comparable scale (e.g., Harshburger *et al.*, 2010). This strong performance of the operational-based regression model, however, may not be representing the study area, as SNOTEL measurements have been shown to represent point location rather than surrounding areas [Molotch and Bales, 2005] often having more snow [Daly *et al.*, 2000], and tend to be located in areas with similar physiographic features (flat and open canopy areas located near tree line).

Ten-fold cross verification for model_{O+F11} and model $_{O+F12}$ both of the field-based multiple regression models had similar trends in estimation and comparable error estimates to model calibration (Table 3.9). A minor increase in error estimation was observed for cross verification procedures, suggesting each model holds consistent error performance when applied to independent data. Cross verification also had similar trends in estimation and comparable error estimates to model calibration with a slight increase in error estimation for model_{O11} and

$model_{O12}$ (Table 3.10). However, when model verification was completed with independent field-based measurements, the RMSE was considerably worse for $model_{O11}$, while slightly worse for $model_{O12}$ (Table 3.10). This suggests that the strong performance statistics of $model_{O11}$ and $model_{O12}$ do not hold true when applied to independent data. The $model_{O}$ verification with independent field data shows considerable worse error estimates for WY 2011 when compared to the $model_{O+F11}$ cross verification results, however, WY 2012 still shows a slight improvement over the $model_{O+F12}$ cross verification results.

3.3.5 Basin Scale SWE Interpolation

The multiple regression $model_{O+F11}$ and $model_{O+F12}$ (corresponding with April 2, 2011 and March 31, 2012, respectively) were used to interpolate SWE across the entire study domain on a pixel by pixel basis (Figure 3.14a and Figure 3.14b, respectively). The distribution of snow cover derived from the regression surfaces compared to the MODIS derived SCA (Figure 3.14) shows large errors of the presence/absence of snow. $Model_{O+F11}$ displays large omission errors (estimation of no snow where snow was observed) of snow cover, while $model_{O+F12}$ shows errors of commission (prediction of snow where snow was not observed). The MODIS derived SCA was used to mask the regression surfaces of SWE to only locations where SCA was observed (Figure 3.15). However, the omission errors from April 2, 2011 for the model persist. Although the two estimated surfaces differ greatly in magnitude and variability, they show similar patterns across space, due to the physiographic variables used in each regression; these are largely driven by topography.

$Model_{O11}$ and $model_{O12}$ were also used to interpolate SWE across the study domain for comparison with $model_{O+F11}$ and $model_{O+F12}$ (Figure 3.16). $Model_{O}$ for both years show similar errors of omission and commission when comparing the distribution of snow cover calculated by the regression surfaces to the MODIS derived SCA (Figure 3.16a and Figure 3.16b, respectively). The $model_O$ regression surfaces were masked to observed MODIS derived SCA (Figure 3.17) and showed similar patterns across space to the $model_{O+F}$ surfaces.

MODIS SCA shows that snow was present across 53% (1,444 km^2) of the Cache la Poudre basin study area on April 2, 2011, while covering only 31% (852 km^2) of the study area on March 31, 2012 (Table 3.11). Mean interpolated SWE across the study area for $model_{O+F}$ and $model_O$ was greater than the mean SWE among measurement locations (Table 3.2) during WY 2011 and WY 2012. The mean April 2, 2011 $model_{O+F}$ and $model_O$ interpolated SWE across the entire study area was 448 mm and 463 mm, respectively, while the interpolated volume of SWE across the study area was 445 million cubic meters and 531 million cubic meters, respectively (Table 3.11a). The mean March 31, 2012 $model_{O+F}$ and $model_O$ interpolated SWE was 255 mm and 253 mm, and the interpolated volume of SWE was 215 million cubic meters and 211 million cubic meters, respectively (Table 3.11b). The large difference in WY 2011 interpolated SWE between the two models suggests that the operational-based models may tend to over predict the distribution of SWE in above average or maximum snow years.

The elevation zones that were identified by Richer [2009] (Table 3.11; Figure 3.18) were used to analyze how the interpolated SWE surfaces compared across elevation zones within the study area. The mean SWE for all four of the SWE surfaces increased with each increasing elevation zone (Figure 3.19). Interpolated SWE volume was also greatest in Elevation Zone 5 (3,043 – 3,405 m) despite only encompassing 14% of the study area, suggesting this elevation zone is the most hydrologically significant zone in terms of a persistent snowpack within the study area (Figure 3.20). Interestingly, despite the differences of interpolated SWE volume observed among the four regression models between years (due to the nature of the maximum and minimum snow years) as well between model$_{O+F11}$ and model$_{O11}$, the percentage of the total interpolated SWE volume for each model was distributed similarly among elevation zones (Figure 3.21). The percentage of interpolated SWE volume from Elevation Zone 5 was 52% for all models except for the WY 2011 operational-based model in which the percentage was 47%, which again suggests a hydrologic significance of this elevation zone.

Richer [2009] found that Elevation Zone 4, likely representing a snow transition zone, exhibited the strongest correlation between snow cover depletion and hydrograph rise within the Cache la Poudre study area. The results discussed here suggest similar findings, as the depletion of snow cover within the transitional Elevation Zone 4, which accounts for on average 28% of the interpolated SWE volume, likely coincides with an isothermal snowpack following the onset of snowmelt within the persistent Elevation Zone 5, from which the hydrograph peak is likely derived.

3.3.6 Limitations

The range of uncertainty of the multiple regression functions (95% confidence limits) that stems from the range of variables observed at measurement locations is one of the main limitations of this study. These limitations exist due to the need for additional sampling across the basin in regions that are inaccessible to travel. Extrapolation of the regression equations outside of the range of independent variables can yield the greatest uncertainty, e.g., interpolating SWE for elevations of 3387 – 4125 m during WY 2011 and elevations of 3448 – 4125 m during WY 2012. Another limitation of the study is the omission errors in snow cover from the WY 2011 regression surfaces that were discussed previously. However, these errors are likely minimal considering they are mainly located Elevation Zone 3, which has little persistent snow cover throughout the snow season, yielding minimal SWE volume. Finally, the most prominent limitation of this study is attempting to generalize the observed patterns of snow accumulation that are dictated by complex atmospheric forcing conditions as well as interactions with vegetation and topography. Jost *et al*. [2007] suggested that relations derived from studies similar to this are better suited to be tested within physically based models that involve the processes mentioned above to see if the spatial variability and patterns of SWE observed within this study can be reproduced. Thus, future work should include using a spatially distributed snowpack evolution modeling system, such as SnowModel [Liston and Elder, 2006a], to analyze the spatial patterns of snow accumulation at the basin scale.

3.4 Conclusion

This study has used a combination of operational SNOTEL and snow course measurements, supporting field-based snowpack measurements, and a snow density model to analyze the spatial variability and observable patterns of SWE within the Cache la Poudre basin. Inspection of the bivariate relations of SWE and snow depth with physiographic variables (thought to influence the distribution of the snowpack across space) shows that elevation and location (UTM Easting and UTM Northing) are most strongly correlated with SWE and snow depth and exhibit linear relations. Multiple linear regression models were developed for WY 2011 and WY 2012 using both a combined dataset of field-based and operational-based measurements ($model_{O+F}$) and a dataset of operational-based measurements only ($model_{O}$). Model calibration shows that WY 2011models showed better performance than WY 2012 and the $model_{O}$ outperformed the $model_{O+F}$ for both years. However, model verification shows a greater error increase for $model_O$. Both $model_{O+F}$ and $model_O$ from April 2, 2011 and March 31, 2012 were used to interpolate SWE across the study domain by calculating SWE on a pixel by pixel basis. The interpolated regression surfaces show errors of omission (WY 2011) and commission (WY 2012) when compared to the MODIS derived SCA. The final interpolated SWE surfaces, masked to observed SCA, generally show similar patterns across space despite different magnitudes between years as well as between input datasets. Within each of the model surfaces, interpolated SWE volume was also shown to be greatest within Elevation Zone 5 (3,043 – 3,405 m) despite only encompassing 14% of the study area. Also, despite the differences of interpolated SWE volume observed among the four regression models, the percentage of the total interpolated SWE volume for each model was shown to be distributed similarly among elevation zones. This study is limited by the approach of attempting to generalize the observed patterns of snow accumulation that are dictated by complex atmospheric forcing conditions as well as interactions with vegetation and topography. Therefore, future work should include using a spatially distributed snowpack evolution modeling system, such as SnowModel [Liston and Elder, 2006a], to analyze the spatial patterns of snow accumulation at the basin scale and compare the patterns observed with the field-based methods of this study.

Table 3.1: Adjustment of field-based snow depth measurements based on mean daily SNOTEL values used to normalize all field-based snow depth measurements to a single date. Adjustments were based on the mean change of SNOTEL snow depth to the normalized date. [$]Difference of snow depth on the observed day (N) from the previous day (N – 1). *2011 [3.1a] snow depth values normalized to 04/02/11. **2012 [3.1b] snow depth values normalized to 03/31/12.

[a.] 2011

Date	Field Measurements (#)	Mean SNOTEL d_s (cm)	Mean d_s (cm) difference of N and N - 1[$]	Adjustment of d_s (cm)*
03/31/11	11	172.7	---	-6.86
04/01/11	0	170.2	2.54	-4.32
04/02/11	17	165.9	4.32	0.0

[b.] 2012

Date	Field Measurements (#)	Mean SNOTEL d_s (cm)	Mean d_s (cm) difference of N and N - 1[$]	Adjustment of d_s (cm)**
03/29/12	28	77.5	---	-6.14
03/30/12	12	74.9	2.54	-3.60
03/31/12	59	71.9	3.60	0.0
04/01/12	8	67.3	4.44	4.44

Table 3.2: Summary statistics [μ = mean, σ = standard deviation] for snowpack properties from 2011 WY [3.2a] and 2012 WY [3.2b] April 1st snow surveys. Statistics calculated separately for manual and operational measurements as well as manual measurements in which SWE was predicted from the snow density model.

[a.] 2011 Data [4/2/11]	**n**	**SWE [mm]**		**Snow Density [kgm^{-3}]**		**Snow Depth [m]**	
		μ	σ	μ	σ	μ	σ
Manual Measurements	*28*	356	259	307	37.0	1.10	0.68
Manual SWE Measurements	*11*	357	242	309	46.7	1.09	0.60
Manual Snow Depth | Predicted SWE	*17*	356	276	305	30.7	1.10	0.74
SNOTEL Measurements	*10*	577	220	342	38.2	1.66	0.55
Snow course Measurements	*13*	410	239	304	24.5	1.31	0.66
Entire Dataset	***51***	**413**	**256**	**313**	**36.9**	**1.26**	**0.68**

[b.] 2012 Data [3/31/12]	**n**	**SWE [mm]**		**Snow Density [kgm^{-3}]**		**Snow Depth [m]**	
		μ	σ	μ	σ	μ	σ
Manual Measurements	*104*	228	106	313	23.9	0.72	0.30
Manual SWE Measurements	*12*	264	69	318	44.7	0.85	0.26
Manual Snow Depth | Predicted SWE	*92*	224	109	312	20.0	0.70	0.31
SNOTEL Measurements	*10*	241	113	324	69.9	0.72	0.33
Snow course Measurements	*13*	152	105	285	50.4	0.52	0.32
Entire Dataset	***127***	**221**	**108**	**311**	**33.8**	**0.70**	**0.31**

Table 3.3: Average value of physiographic variables located at snowpack measurements from 2011 WY [3.3a] and 2012 WY [3.3b] and across the entire study area. All physiographic variables derived at 30 m resolution.

[a.] 2011 Data [4/2/11]	n	Elevation [m]	Curvature	Slope [°]	Solar Radiation [WHm^{-2}]	Eastness	Northness	Canopy Density [%]
Manual Measurements	*28*	2867	-0.130	9.18	14,566	0.040	-0.006	43.1
SNOTEL Measurements	*10*	3002	-0.062	7.28	14,672	-0.012	-0.009	55.8
Snow course Measurements	*13*	2925	0.104	13.2	14,010	0.077	0.010	52.2
All Measurements	*51*	2908	-0.057	9.82	14,445	0.039	-0.003	47.9
Study Area [30m Resolution]	*3,700,092*	2559	-0.095	12.5	13,629	0.012	0.005	39.8

[b.] 2012 Data [3/31/12]	n	Elevation [m]	Curvature	Slope [°]	Solar Radiation [WHm^{-2}]	Eastness	Northness	Canopy Density [%]
Manual Measurements	*104*	2997	-0.022	9.71	14,507	0.027	0.001	60.9
SNOTEL Measurements	*10*	3002	-0.062	7.28	14,672	-0.012	-0.009	55.8
Snow course Measurements	*13*	2925	0.104	13.2	14,010	0.077	0.010	52.2
All Measurements	*127*	2990	-0.012	9.87	14,469	0.029	0.001	59.6
Basin Variables [30 m Resolution]	*3,700,092*	2559	-0.095	12.5	13,629	0.012	0.005	39.8

Table 3.4: Kolmogorov-Smirnov test (k-s test) results for equality of distributions between a random sample [n = 366] of continuous basin variables versus variables associated with WY2011 and WY2012 measurement locations. K-s test statistic (D) is provided for each test with the associated p-value in brackets [Significance as follows: * = p < 0.05, ** = p < 0.01].

	2011	**2012**
	D [p-value]	
Elevation	0.29 [**]	0.33 [**]
Curvature	0.09	0.07
Slope	0.27 [**]	0.22 [**]
Solar Radiation	0.23 [*]	0.20 [**]
Eastness	0.15	0.09
Northness	0.28 [**]	0.25 [**]
Canopy Density	0.14	0.12

Table 3.5: Correlation matrix [Pearson correlation coefficient] among snowpack properties and physiographic variables at sampling locations from 2011 WY [3.5a] and 2012 WY [3.5b] snow surveys.

[a.] 2011 Data	SWE	Snow Depth	Snow Density	Easting	Northing	Canopy Density	Northness	Eastness	Solar Radiation	Slope	DEM Elevation	Curvature
SWE	---	**0.99**	**0.82**	**-0.69**	**-0.55**	0.12	-0.01	-0.13	0.16	-0.04	**0.75**	0.14
Snow Depth		---	**0.76**	**-0.66**	**-0.56**	0.14	0.00	-0.11	0.19	-0.02	**0.77**	0.15
Snow Density			---	**-0.72**	-0.37	0.09	0.08	-0.27	0.06	-0.09	0.46	0.14
Easting				---	0.27	0.01	0.10	0.32	-0.06	0.12	-0.30	-0.12
Northing					---	0.04	-0.01	0.00	0.06	-0.28	-0.43	-0.07
Canopy Density						---	-0.01	-0.09	0.09	0.07	0.22	0.19
Northness							---	-0.20	**-0.78**	-0.32	-0.06	-0.02
Eastness								---	0.16	0.25	-0.12	-0.31
Solar Radiation									---	0.03	0.31	0.11
Slope										---	0.12	-0.02
DEM Elevation											---	0.30
Curvature												---

[b.] 2012 Data	SWE	Snow Depth	Snow Density	Easting	Northing	Canopy Density	Northness	Eastness	Solar Radiation	Slope	DEM Elevation	Curvature
SWE	---	**0.98**	**0.52**	-0.38	-0.12	-0.07	0.06	0.10	0.06	0.09	**0.67**	0.12
Snow Depth		---	0.40	-0.33	-0.10	-0.07	0.08	0.13	0.04	0.11	**0.67**	0.12
Snow Density			---	**-0.50**	-0.02	0.00	-0.13	-0.08	0.18	0.01	0.40	0.02
Easting				---	0.25	0.10	0.03	0.06	-0.03	-0.12	-0.41	-0.12
Northing					---	0.12	-0.13	0.02	0.18	-0.29	-0.34	-0.09
Canopy Density						---	0.02	-0.02	0.03	-0.05	-0.04	-0.13
Northness							---	0.17	**-0.80**	-0.03	-0.04	0.25
Eastness								---	-0.03	0.10	0.05	-0.03
Solar Radiation									---	-0.15	0.20	-0.15
Slope										---	0.22	0.21
DEM Elevation											---	0.18
Curvature												---

Table 3.6: Summary statistics of field-based snow depth measurements gathered during the WY 2012 April 2nd snow survey, based on the information collected for each category of forest canopy cover.

	Canopy Cover			Community Type			Tree Mortality		
	Closed	Open	Partially Closed	Alpine	Lodgepole Pine	Spruce Fir	Alive Green	Dead Gray	Dead Red
n	8.0	32.0	67.0	6.0	37.0	62.0	48.0	20.0	15.0
Min	29.6	0.0	16.5	0.0	9.5	0.0	16.5	29.9	23.7
Quartile 1	6.1	47.1	36.4	22.4	35.0	54.1	32.0	26.5	18.0
Median	12.2	41.4	10.5	94.7	16.2	20.3	12.2	19.5	23.6
Quartile 3	15.4	26.6	12.6	27.9	7.5	17.5	12.9	18.7	8.4
Max	35.3	47.2	49.4	17.3	57.2	60.5	41.4	44.1	22.1

Table 3.7: April 2, 2011 [3.7a] and March 31, 2012 [3.7b] snow water equivalent model$_{O+F}$ calibration statistics. Variables used in final model selection highlighted in gray.

a.] 2011	Independent Variables	VIF	AIC	Adjusted R^2	MAE (mm)	RMSE (mm)
1	Easting, Northing, Eastness, Slope, DEM Elevation	1.28, 1.37, 1.18, 1.19, 1.30	624.93	0.84	75.75	102.85
2	Easting, Northing, Solar Radiation, Eastness, Slope, DEM Elevation	1.29, 1.46, 1.23, 1.25, 1.19, 1.52	626.35	0.84	74.89	103.41
3	Easting, Northing, Northness, Eastness, DEM Elevation	1.29, 1.28, 1.08, 1.21, 1.30	626.86	0.83	79.02	104.81
4	Easting, Northing, Canopy Density, Eastness, Slope, DEM Elevation	1.29, 1.41, 1.10, 1.20, 1.20, 1.39	626.36	0.84	75.03	103.42
5	Easting, Northing, Eastness, DEM Elevation	1.26, 1.28, 1.13, 1.29	628.37	0.83	82.98	107.28
6	Easting, DEM Elevation	1.10, 1.10	635.36	0.79	95.18	116.97

b.] 2012	Independent Variables	VIF	AIC	Adjusted R^2	MAE (mm)	RMSE (mm)
1	Easting, Northing, Solar Radiation, DEM Elevation	1.22, 1.24, 1.12, 1.40	1473.0	0.48	59.43	77.72
2	Easting, Northing, Solar Radiation, Eastness, DEM Elevation	1.23, 1.25, 1.13, 1.01, 1.41	1474.0	0.48	59.06	77.72
3	Northing, Solar Radiation, DEM Elevation	1.22, 1.12, 1.23	1475.3	0.47	60.44	78.73
4	Easting, Northing, Eastness, DEM Elevation	1.23, 1.15, 1.01, 1.30	1475.0	0.47	59.24	78.33
5	Easting, Northing, DEM Elevation	1.22, 1.15, 1.30	1474.2	0.47	59.50	78.38
6	Easting, DEM Elevation	1.20, 1.20	1476.8	0.46	59.57	79.49

Table 3.8: April 2, 2011 and March 31, 2012 snow water equivalent model$_O$ calibration statistics.

	Independent Variables	VIF	AIC	Adjusted R^2	MAE (mm)	RMSE (mm)
2011	Easting, DEM Elevation, Curvature	1.06, 1.15, 1.08	276.5	0.87	67.39	87.41
2012	Northing, Canopy Density, Eastness, Slope, DEM Elevation	1.39, 1.11, 1.19, 1.25, 1.40	257.6	0.76	38.74	56.17

Table 3.9: 10-Fold cross verification performance statistics for April 2, 2011 and March 31, 2012 snow water equivalent model$_{O+F}$.

10-Fold Cross Verification	Sample Size	RMSE (mm)
April 2, 2011	51	103.4
March 31, 2012	127	81.04

Table 3.10: Verification performance statistics for April 2, 2011 and March 31, 2012 operational snow water equivalent model$_{O}$.

Date	10-Fold Cross Verification		Independent Field Measurement Verification	
	Sample Size	RMSE (mm)	Sample Size	RMSE (mm)
April 2, 2011	23	90.5	28	153.5
March 31, 2012	23	63.4	104	77.5

Table 3.11: April 2, 2011 [3.11a] and March 31, 2012 [3.11b] model$_{O+F}$ and model$_{O}$ interpolation statistics.

[a.] 2011	Elevation Range (m)	Area (km^2)	SCA (km^2)	Mean Interpolated SWE (mm)		Interpolated SWE σ (mm)		Interpolated SWE Volume (10^6 m^3)	
				Model$_{O+F11}$	Model$_{O11}$	Model$_{O+F11}$	Model$_{O11}$	Model$_{O+F11}$	Model$_{O11}$
Study Area	1591 – 4125	2729	1444	448	463	264	278	445.2	530.6
Elevation Zone 1	1591 – 1953	196	0	0	0	0	0	0	0
Elevation Zone 2	1954 – 2316	671	6	0	79.4	0	69.2	0	0.018
Elevation Zone 3	2317 – 2679	896	474	54.7	104	57.6	78.7	3.13	19.2
Elevation Zone 4	2680 – 3042	471	469	266	335	154	144	117.5	156.1
Elevation Zone 5	3043 – 3405	384	384	599	655	140	123	230.1	251.4
Elevation Zone 6	3406 – 3768	104	104	834	915	125	130	87.1	95.5
Elevation Zone 7	3769 – 4125	7	7	1000	1153	119	179	7.28	8.40

[b.] 2012	Elevation Range (m)	Area (km^2)	SCA (km^2)	Mean Interpolated SWE (mm)		Interpolated SWE σ (mm)		Interpolated SWE Volume (10^6 m^3)	
				Model$_{O+F12}$	Model$_{O12}$	Model$_{O+F12}$	Model$_{O12}$	Model$_{O+F12}$	Model$_{O12}$
Study Area	1591 – 4125	2729	852	255	253	97.7	102	214.7	210.6
Elevation Zone 1	1591 – 1953	196	0	0	0	0	0	0	0
Elevation Zone 2	1954 – 2316	671	0	0	0	0	0	0	0
Elevation Zone 3	2317 – 2679	896	73	79.4	80.4	41.7	45.5	4.78	4.38
Elevation Zone 4	2680 – 3042	471	316	191	185	46.8	63.6	60.5	58.0
Elevation Zone 5	3043 – 3405	384	372	298	302	42.9	57.3	111.0	112.2
Elevation Zone 6	3406 – 3768	104	87	415	390	44.5	59.6	36.3	34.1
Elevation Zone 7	3769 – 4125	7	4	539	489	36.6	77.8	2.04	1.86

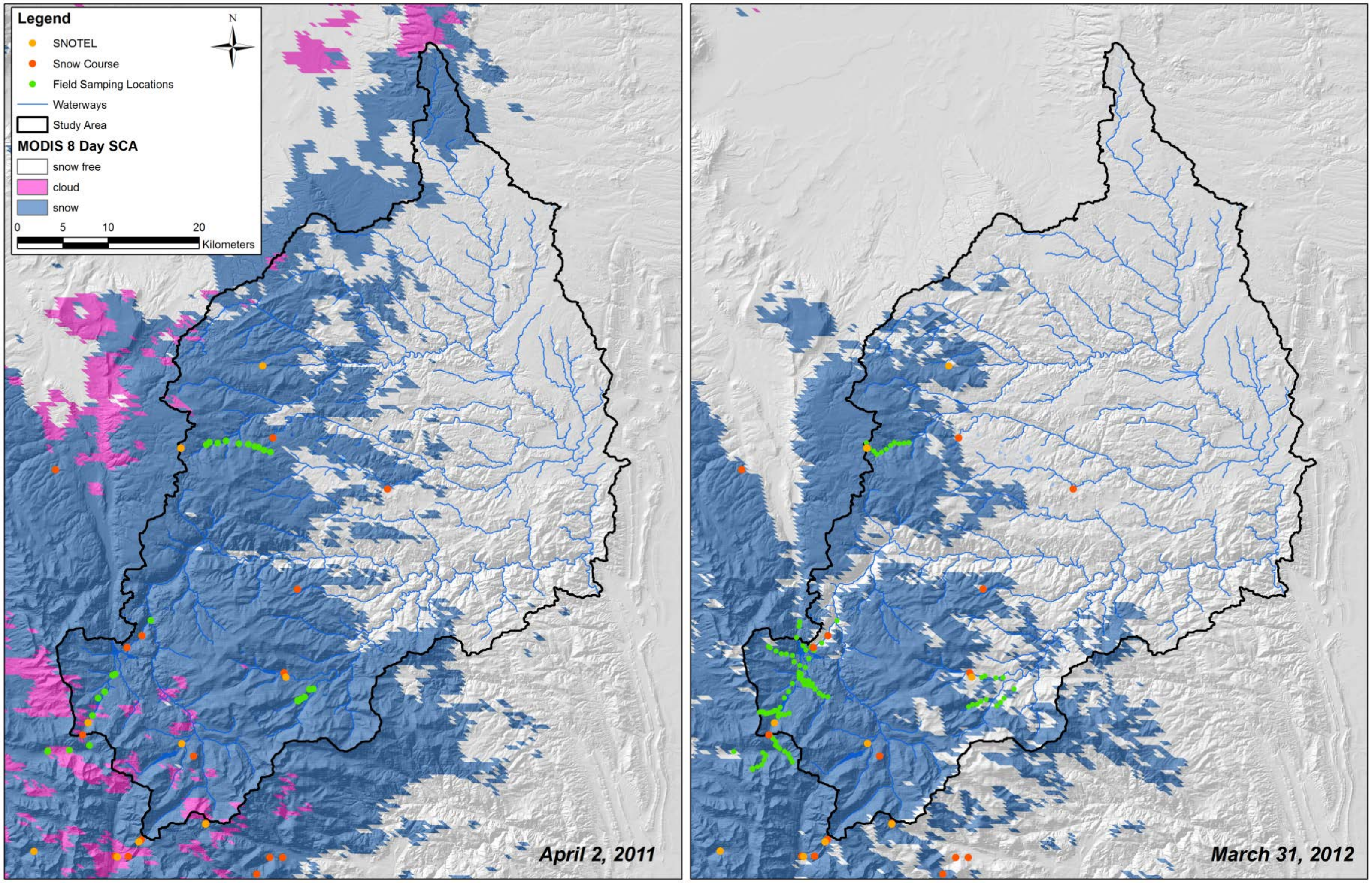

Figure 3.1: Map of Snow Covered Area (SCA) within the study area (shown as blue) for April 2, 2011 [3.1a] and March 31, 2012 [3.1b] with SNOTEL stations shown in orange, snow courses shown in red, and field measurements shown in green. SCA from Moderate Resolution Imaging Spectroradiometer (MODIS)/Terra 8-day 500 m snow-cover products <*http://reverb.echo.nasa.gov*>.

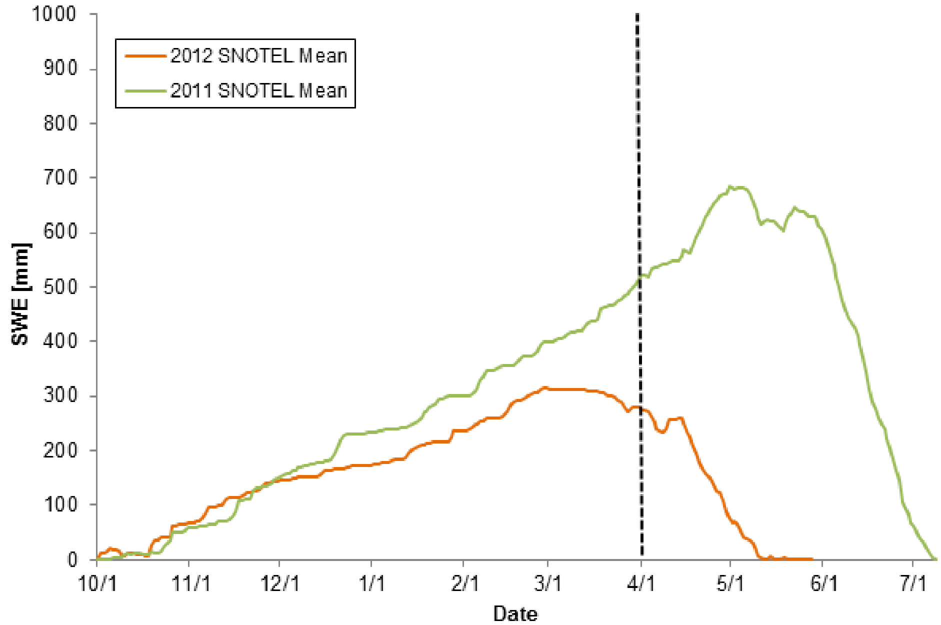

Figure 3.2: Plot of the mean SWE among SNOTEL stations during the 2011 and 2012 snow seasons, exhibiting that the 2011 survey was undertaken before peak SWE and the 2012 survey was completed subsequent to peak SWE.

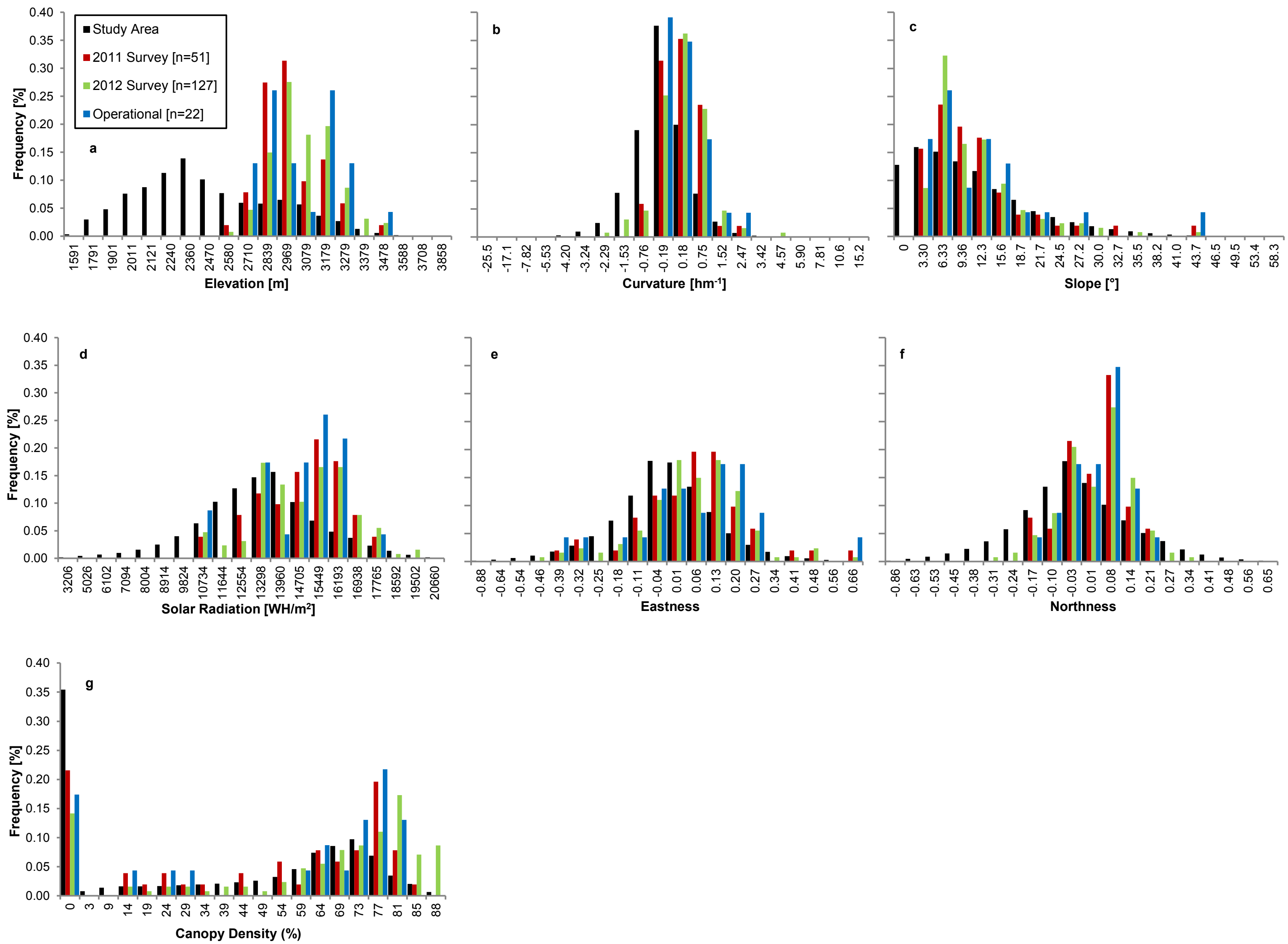

Figure 3.3: Histograms of physiographic variables across the study area comparied to variables found at snow measurement locations.

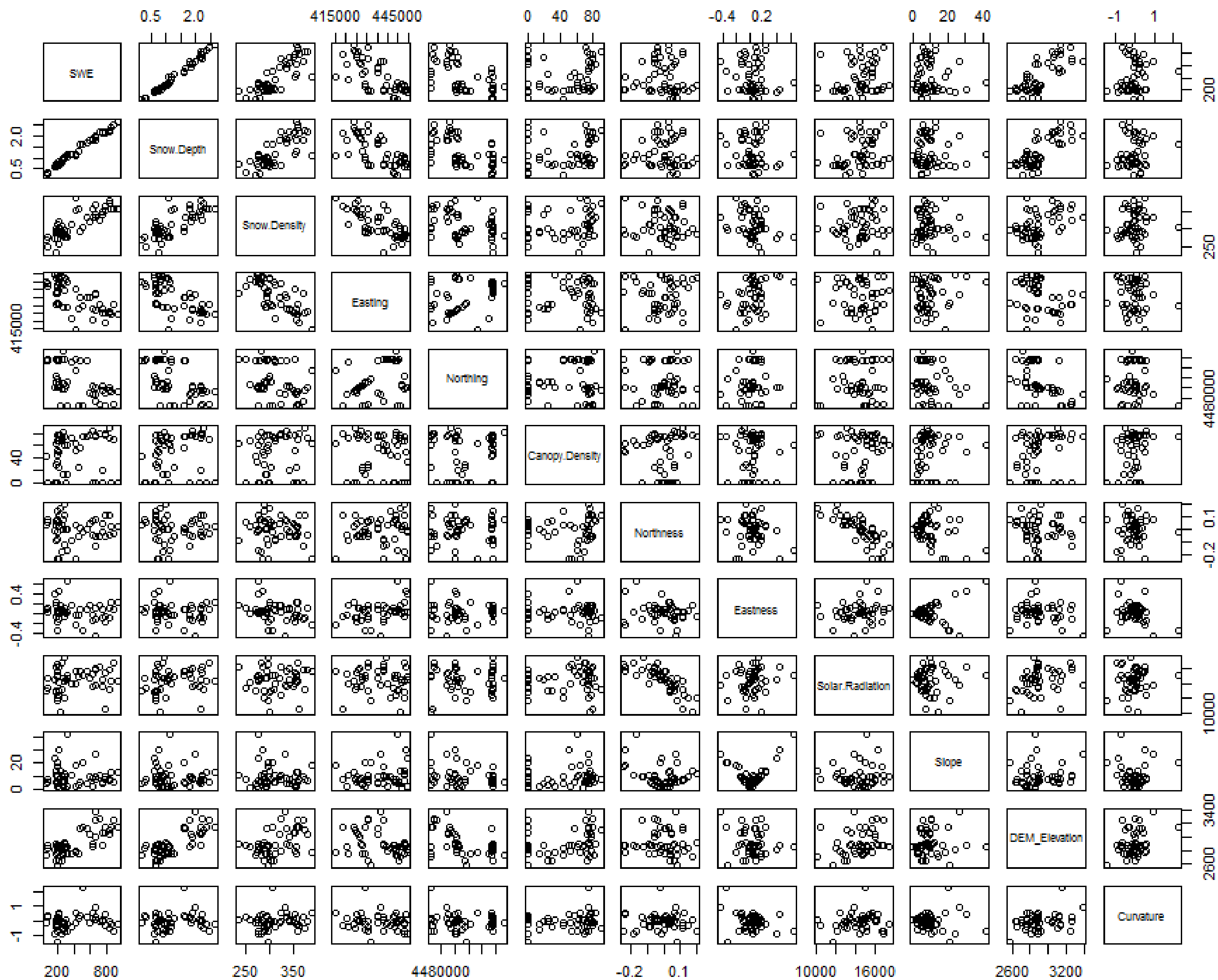

Figure 3.4a: Pairwise scatterplots among snowpack properties and physiographic variables from the 2011WY [4/2/11] snow survey.

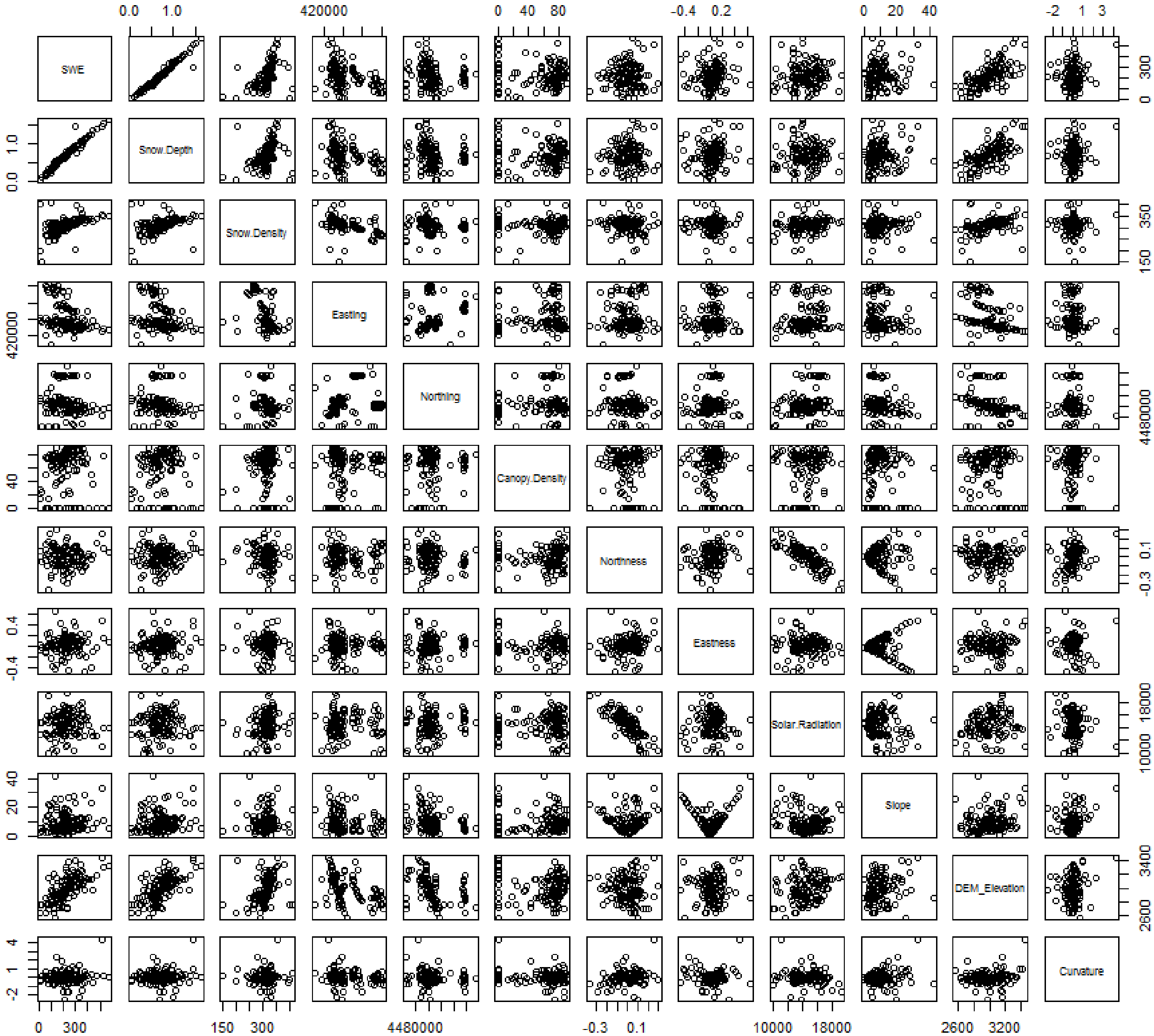

Figure 3.4b: Pairwise scatterplots among snowpack properties and physiographic variables from the 2012WY [3/31/12] snow survey

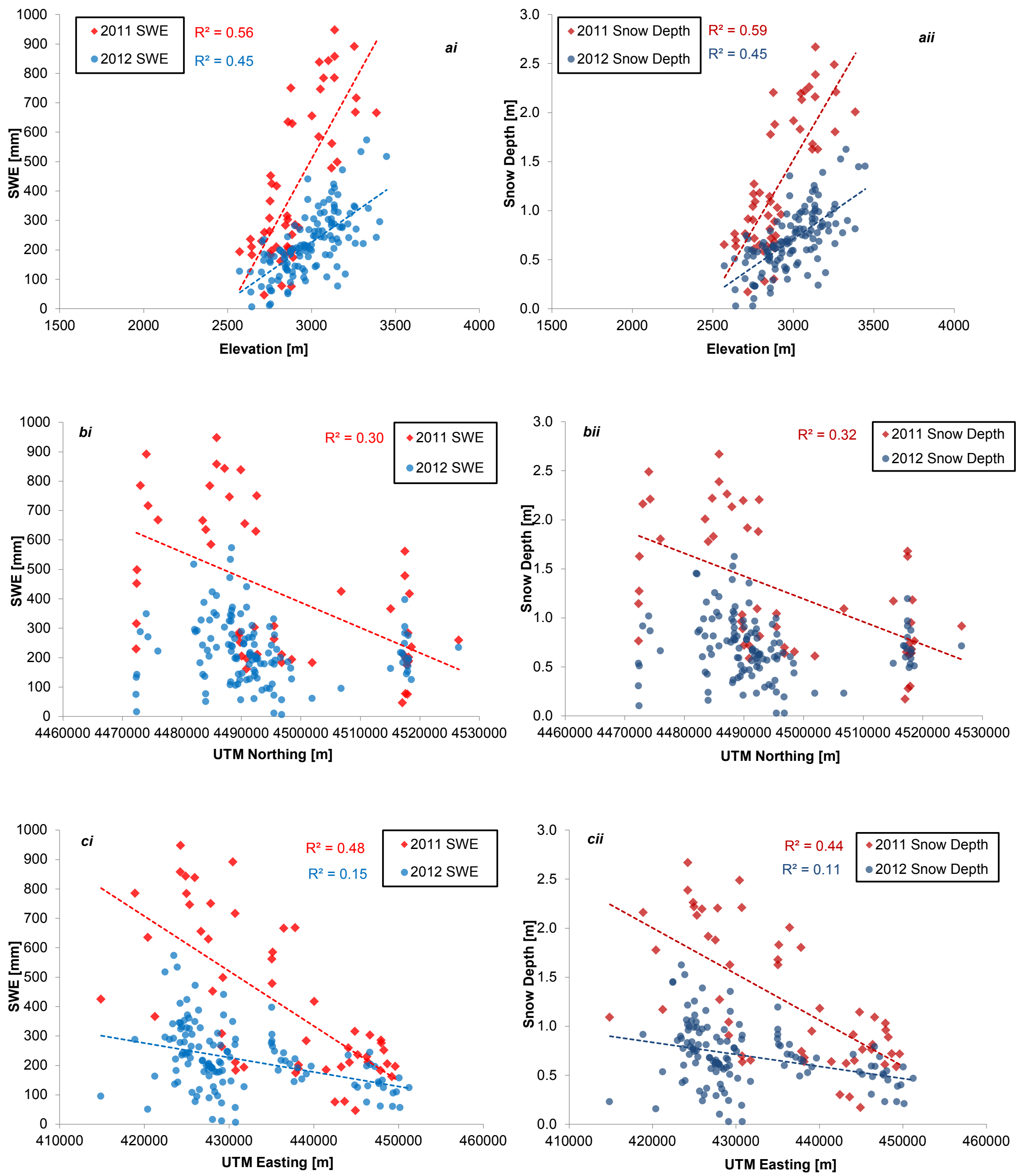

Figure 3.5a: Bivariate scatterplots showing the relation of physiographic and biological variables with SWE [3.5i] and snow depth [3.5ii] field and operational-based measurements.

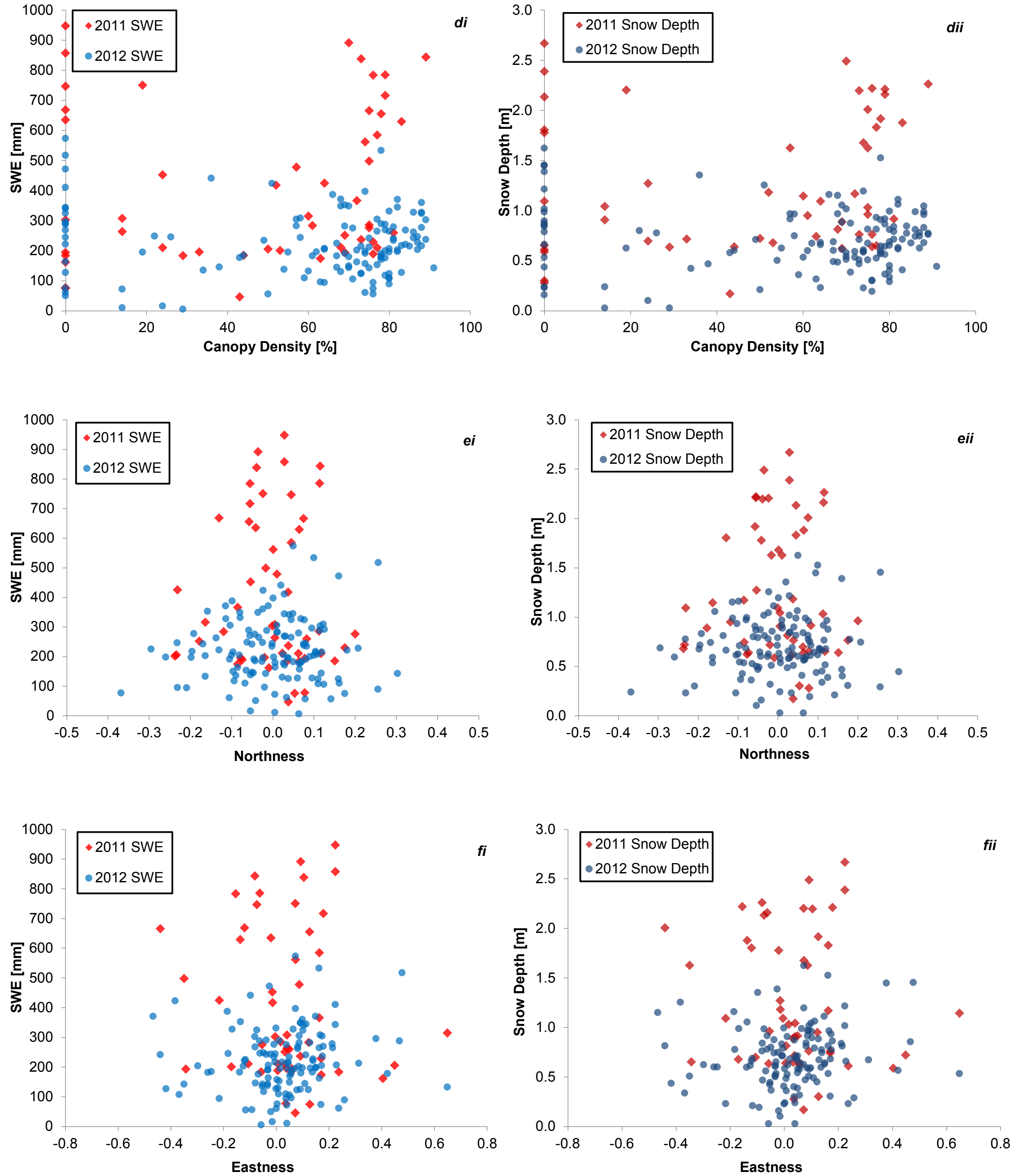

Figure 3.5b: Bivariate scatterplots showing the relation of physiographic and biological variables with SWE [3.5i] and snow depth [3.5ii] field and operational-based measurements.

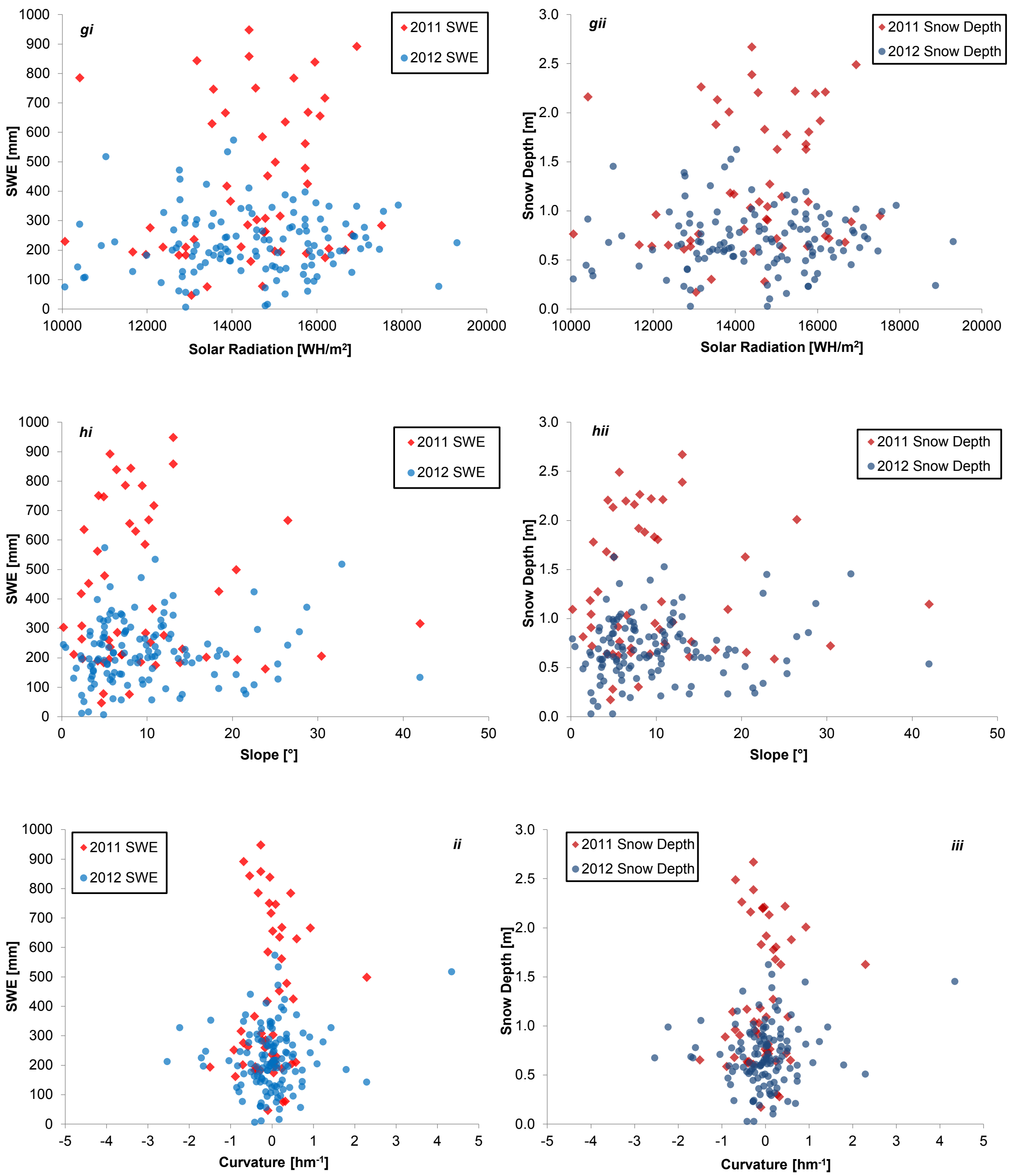

Figure 3.5c: Bivariate scatterplots showing the relation of physiographic and biological variables with SWE [3.5i] and snow depth [3.5ii] field and operational-based measurements.

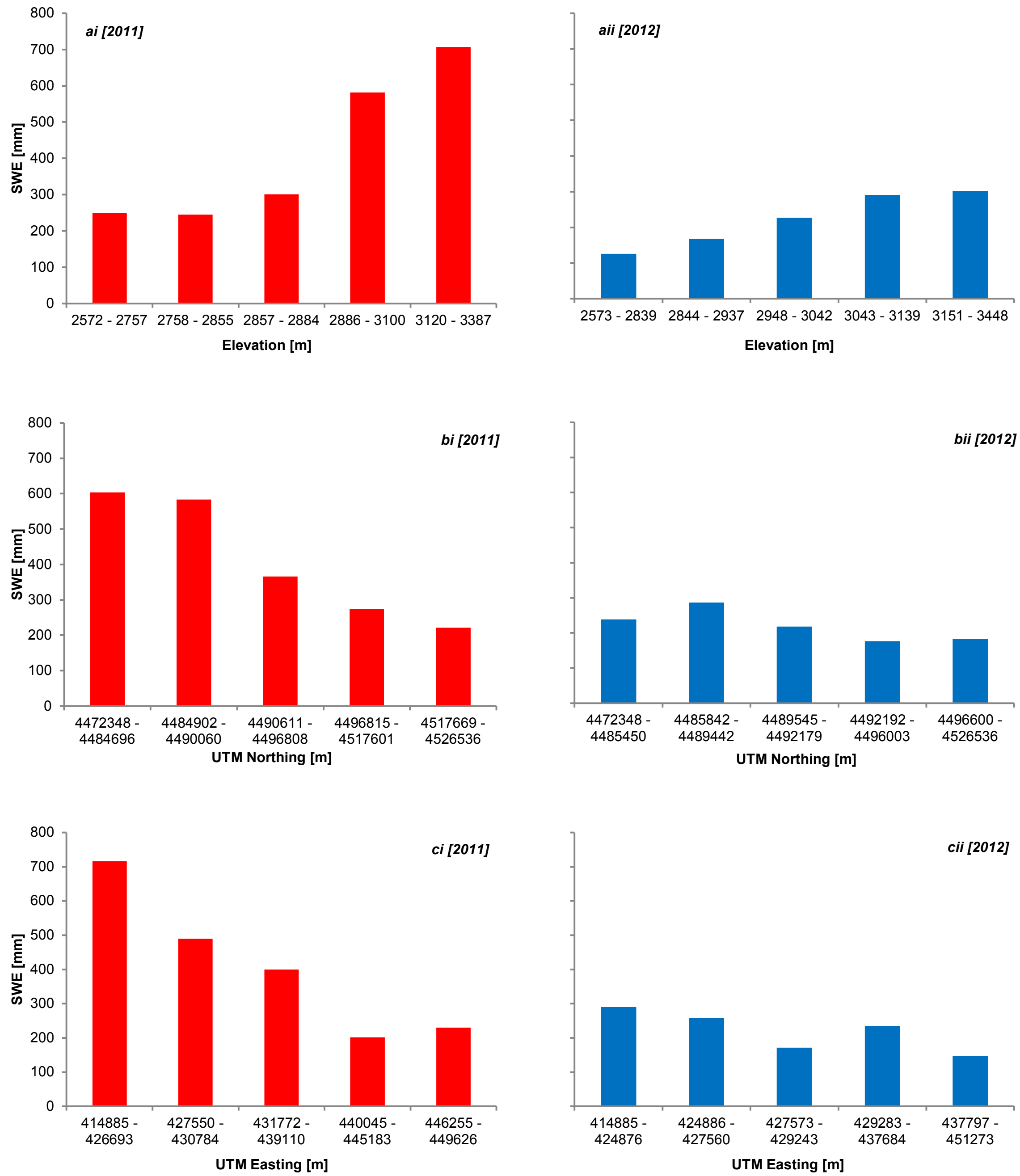

Figure 3.6a: Mean SWE among ranges of physiographic variables for WY 2011 [3.6i] and WY 2012 [3.6ii]. Ranges of physiographic variables were evenly divided among each dataset to produce a large enough sample size of each range.

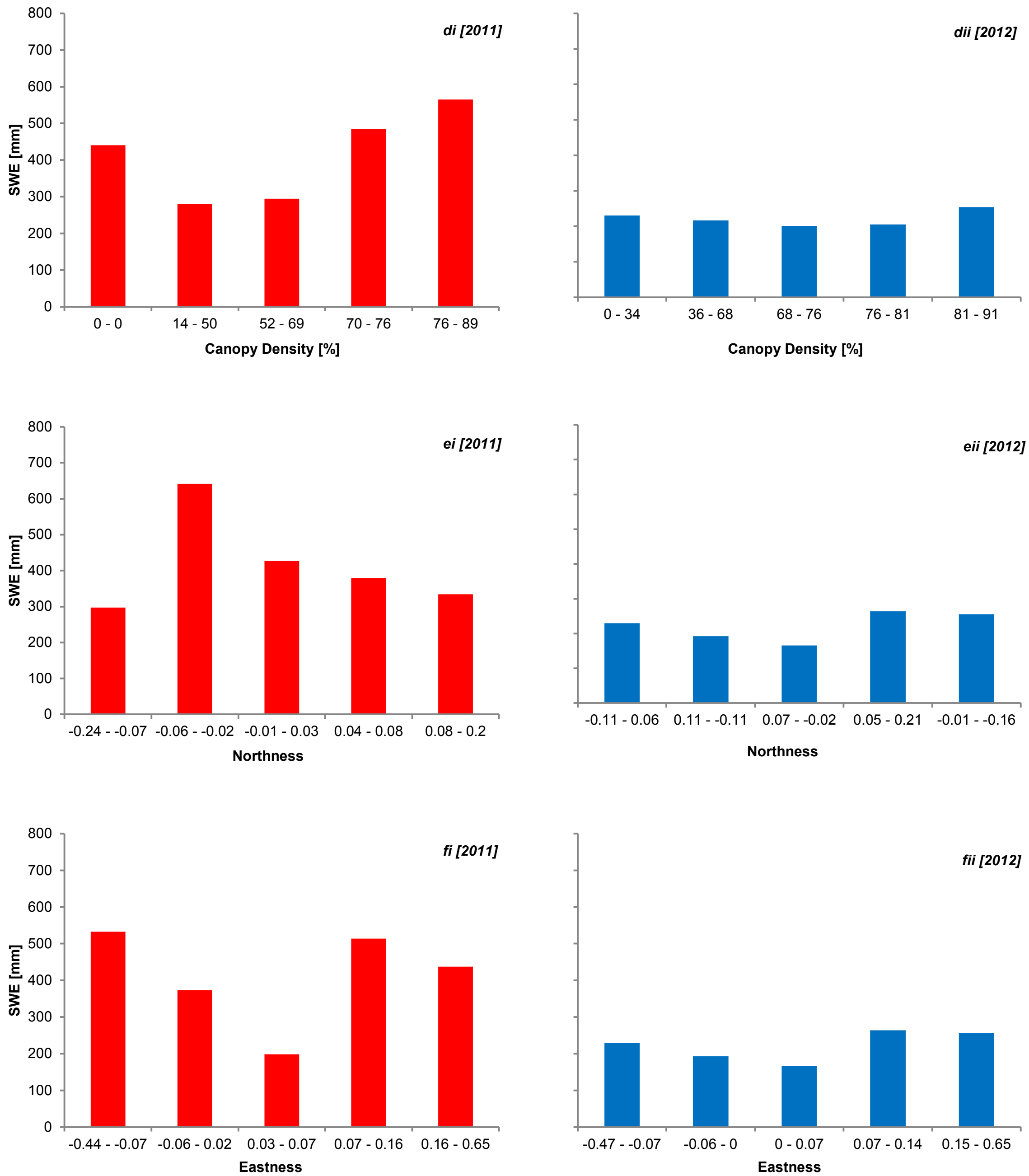

Figure 3.6b: Mean SWE among ranges of physiographic variables for WY 2011 [3.6i] and WY 2012 [3.6ii]. Ranges of physiographic variables were evenly divided among each dataset to produce a large enough sample size of each range.

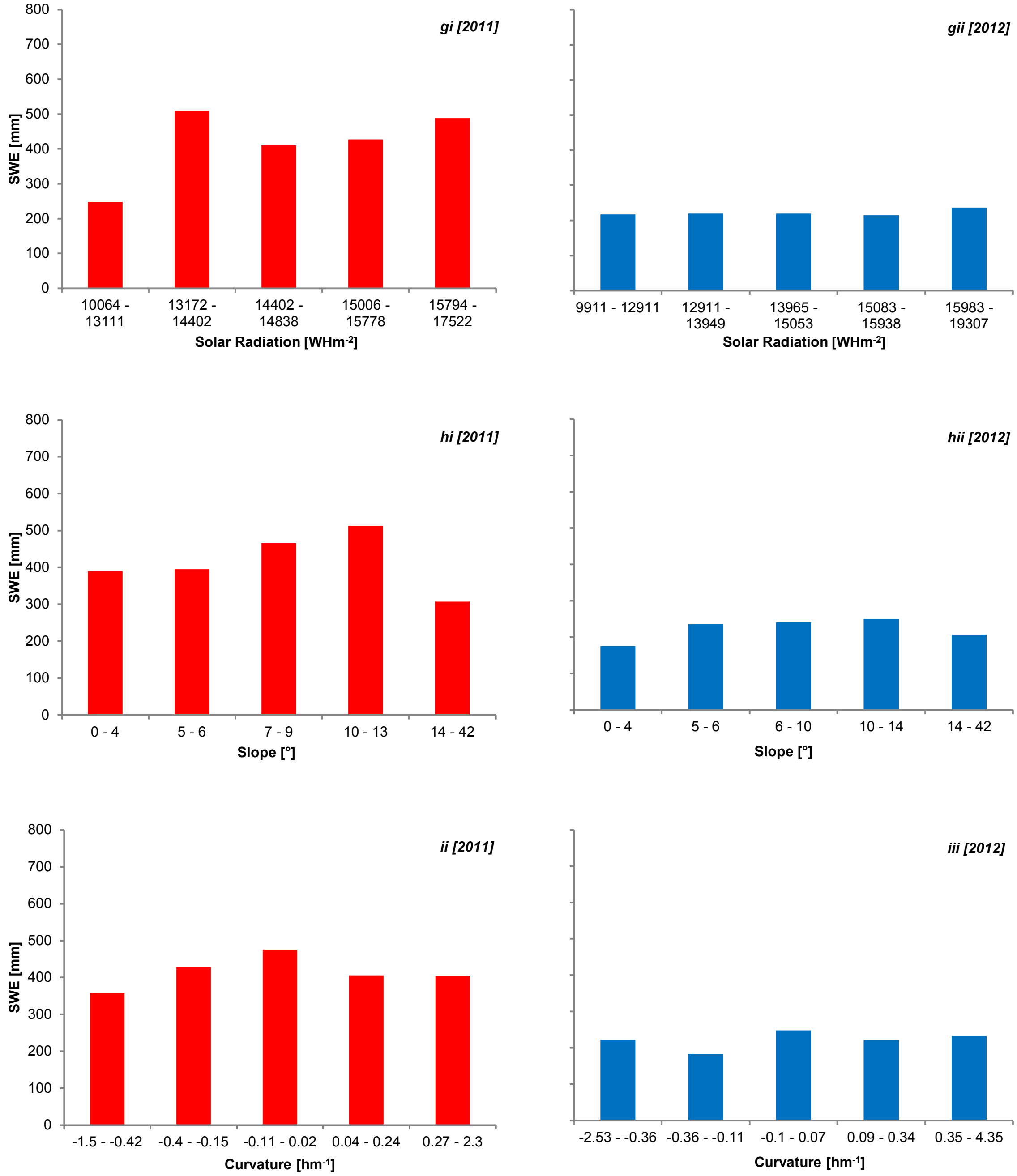

Figure 3.6c: Mean SWE among ranges of physiographic variables for WY 2011 [3.6i] and WY 2012 [3.6ii]. Ranges of physiographic variables were evenly divided among each dataset to produce a large enough sample size of each range.

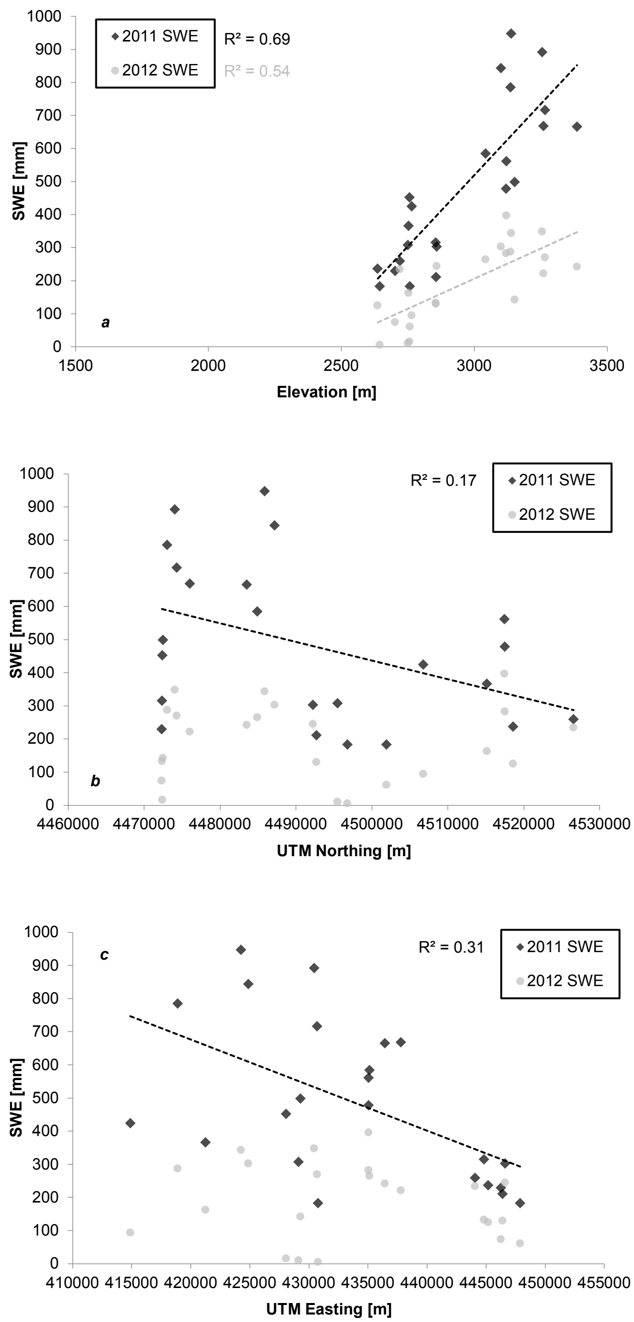

Figure 3.7: Bivariate scatterplots showing the relation of station based variables with operational (SNOTEL and snow course) SWE measurements.

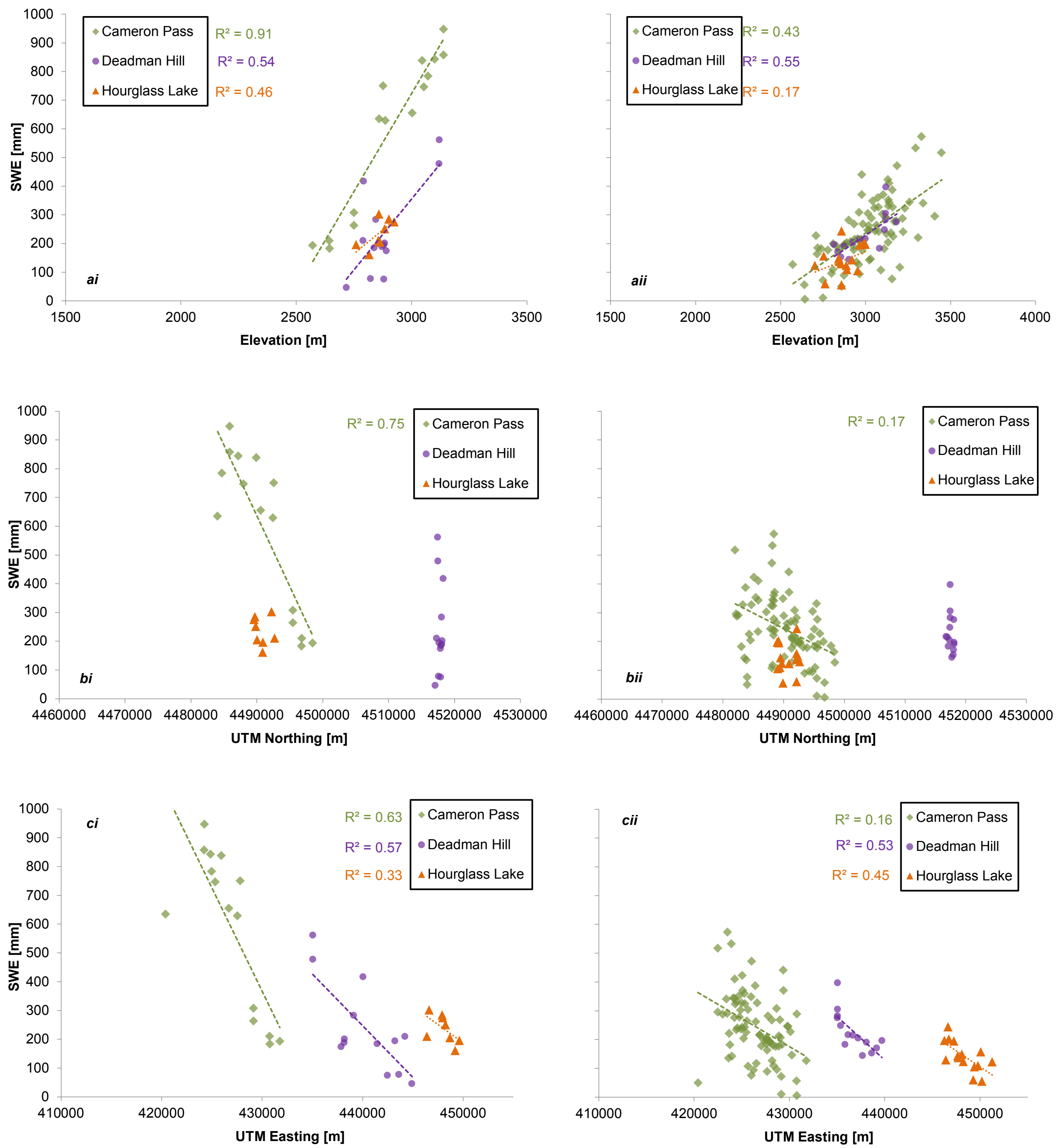

Figure 3.8: Bivariate scatterplots showing the relation of station based variables with regional groupings of field-based and operational SWE measurements from WY 2011[3.8i] and WY 2012 [3.8ii].

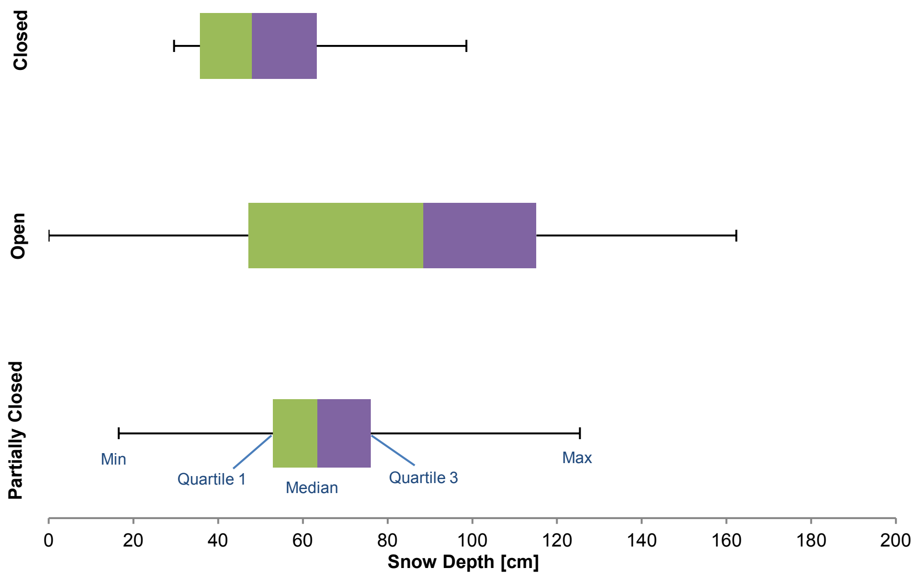

Figure 3.9: Box and whisker plots of WY 2012 field-based snow depth measurements for each of the forest canopy cover categories. A box width indicates the interquartile range, and whisker width represents the entire range.

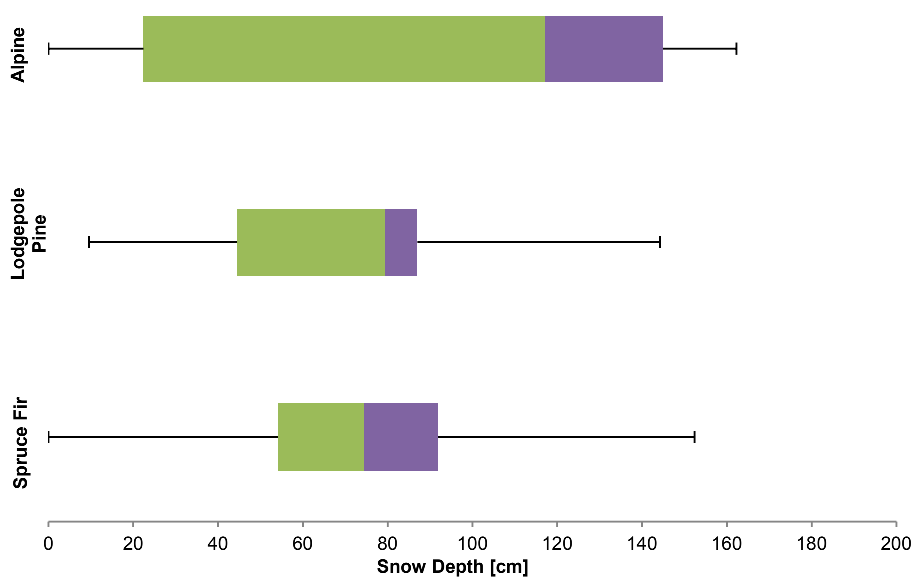

Figure 3.10: Box and whisker plots of WY 2012 field-based snow depth measurements for each of the forest community type categories. A box width indicates the interquartile range, and whisker width represents the entire range.

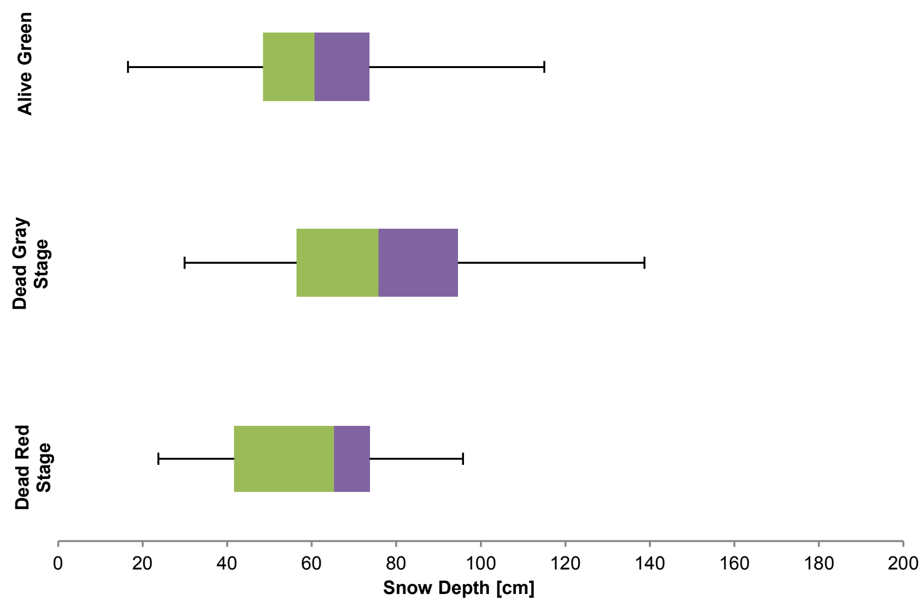

Figure 3.11: Box and whisker plots of WY 2012 field-based snow depth measurements for each of the tree mortality condition categories. A box width indicates the interquartile range, and whisker width represents the entire range.

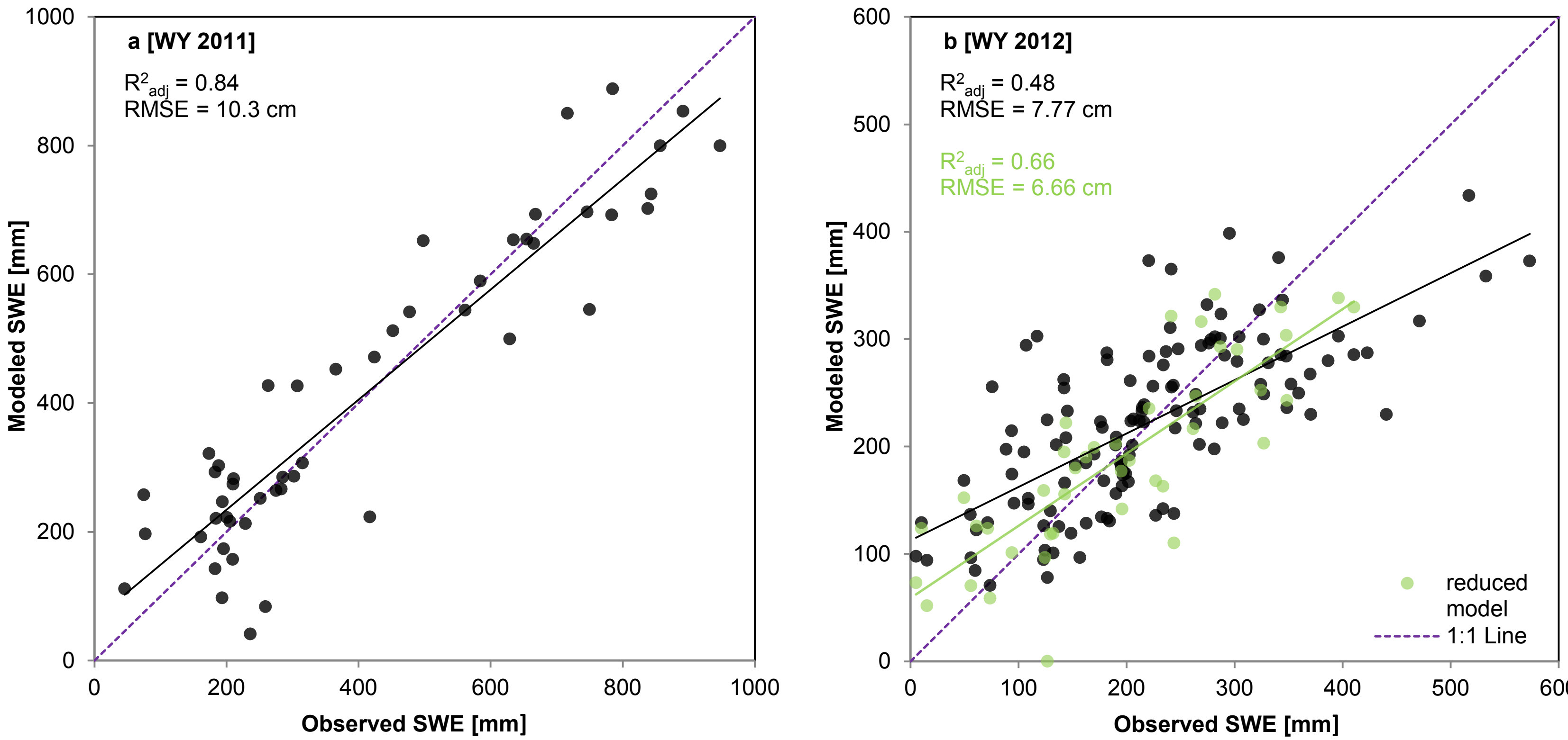

Figure 3.12: Scatterplots showing observed versus modeled SWE from the WY 2011 [3.12a] and WY 2012[3.12b] model$_{O+F}$ multiple regressions. Results from a reduced WY 2012 model$_{O+F}$ including only field-based measurement locations also sampled during WY 2011 are shown in green [Figure 3.12b].

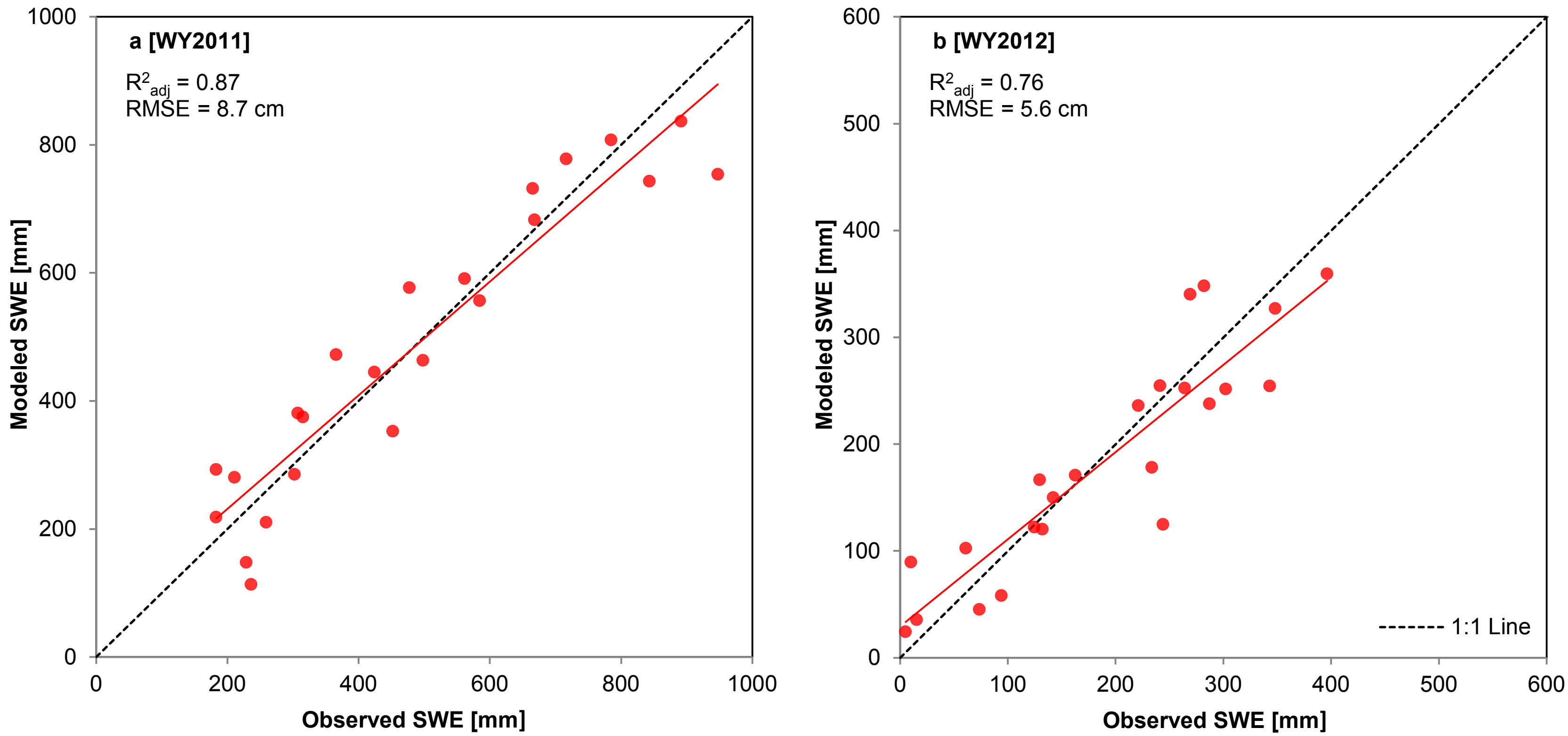

Figure 3.13: Scatterplots showing observed versus modeled SWE from the WY 2011 [3.13a] and WY 2012[3.13b] model$_O$ multiple regressions.

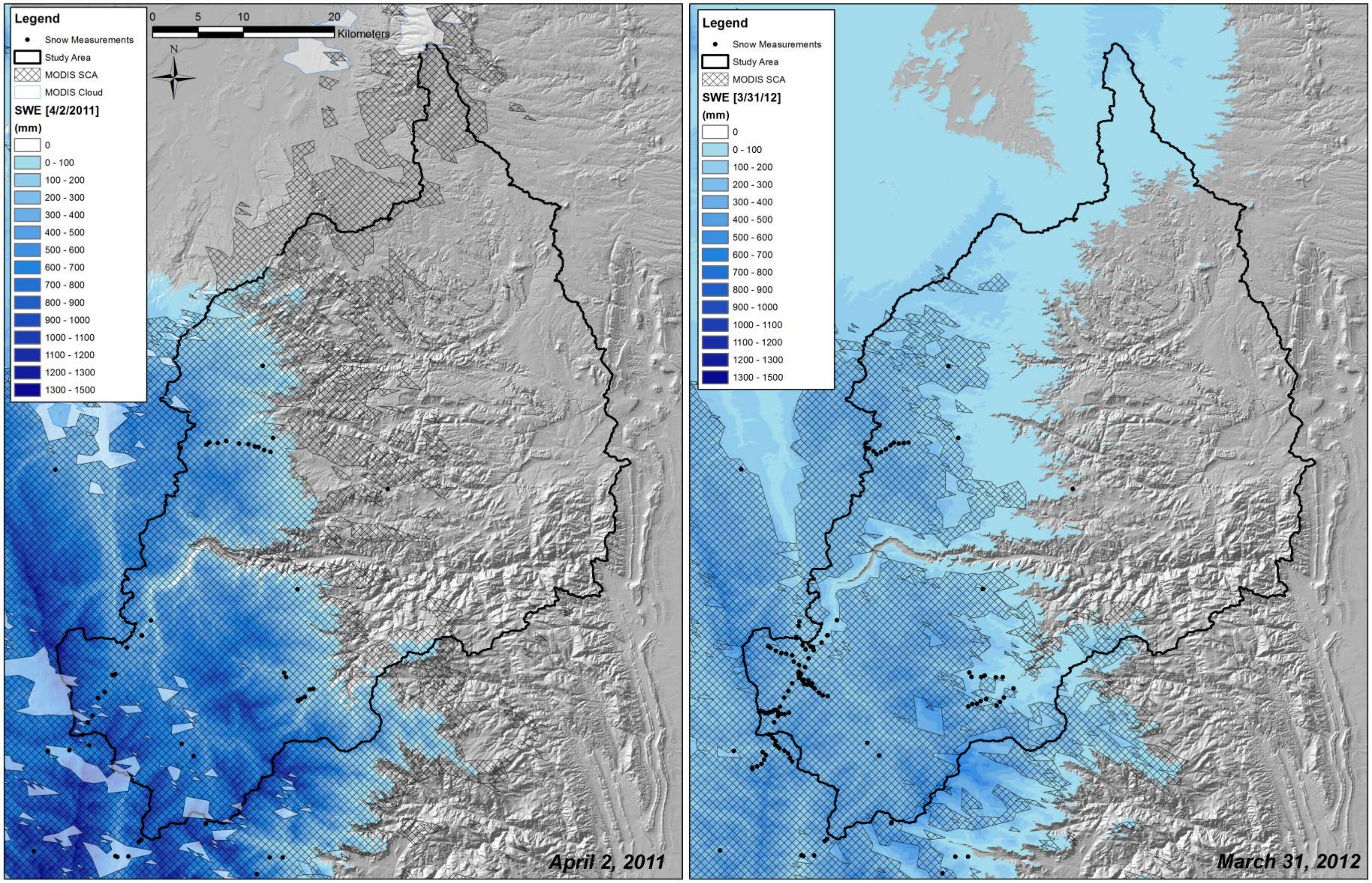

Figure 3.14: Map of model$_{O+F}$ SWE surface overlain by MODIS derived SCA (shown with hatching) within the study area for April 2, 2011 [3.14a] and March 31, 2012 [3.14b] with both field and operational-based measurements shown in black.

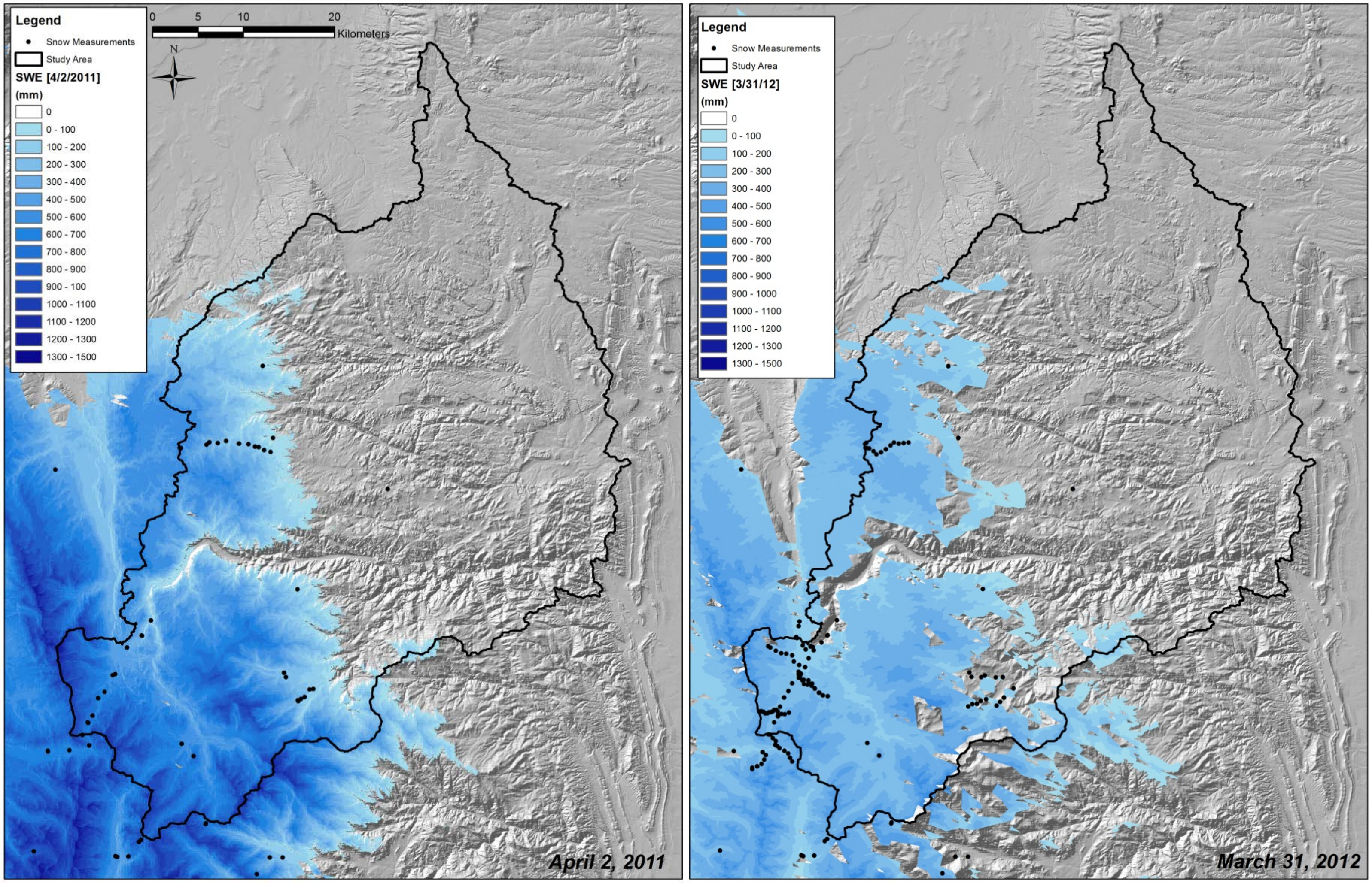

Figure 3.15: Map of model$_{O+F}$ SWE surface clipped by MODIS derived SCA within the study area for April 2, 2011 [3.15a] and March 31, 2012 [3.15b] with both field-based and operational measurements shown in black.

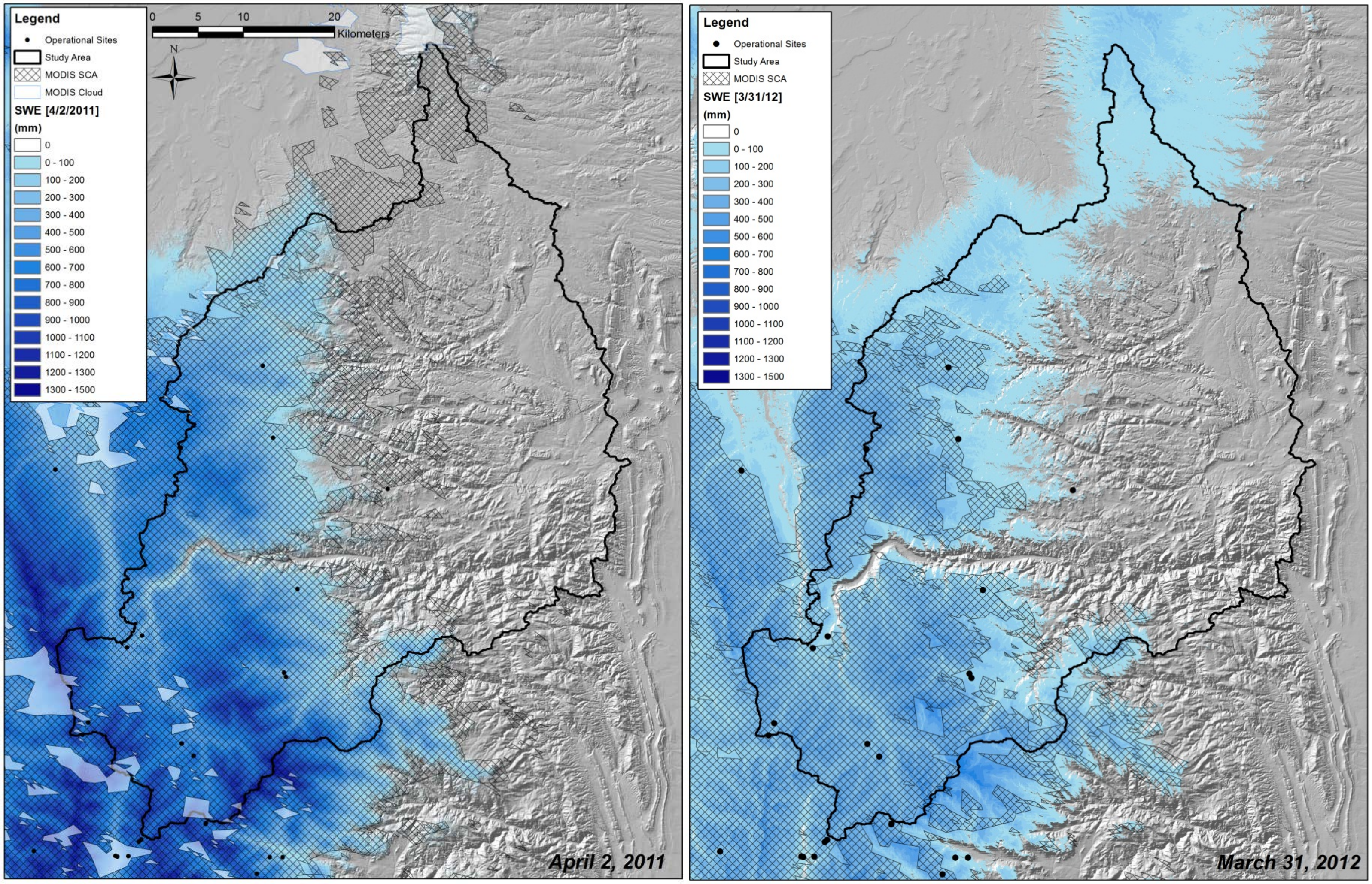

Figure 3.16: Map of model$_O$ SWE surface overlain by MODIS derived SCA (shown with hatching) within the study area for April 2, 2011 [3.16a] and March 31, 2012 [3.16b] with operational-based measurements shown in black.

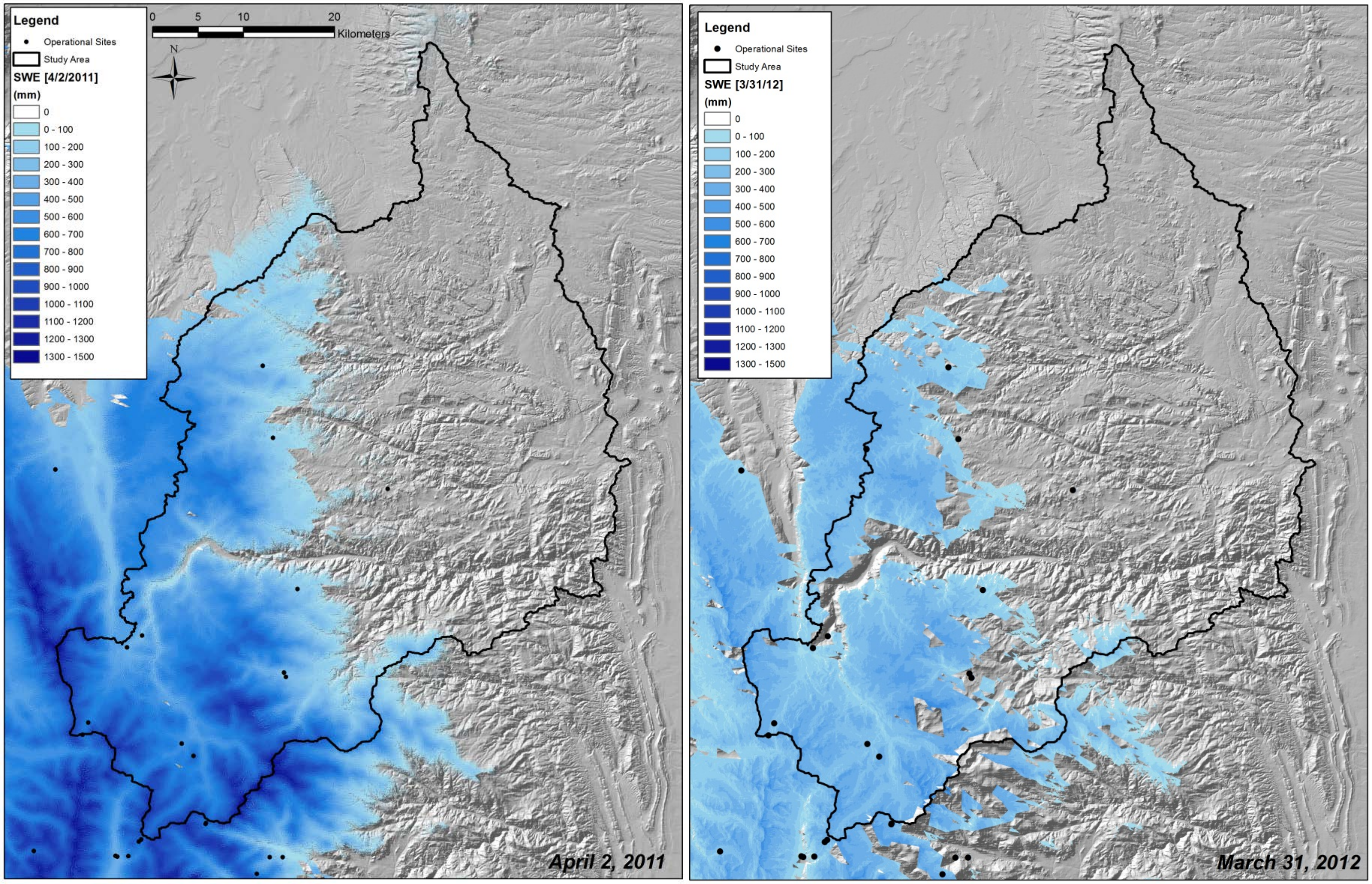

Figure 3.17: Map of model$_O$ SWE surface clipped by MODIS derived SCA within the study area for April 2, 2011 [3.17a] and March 31, 2012 [3.17b] with operational-based measurements shown in black.

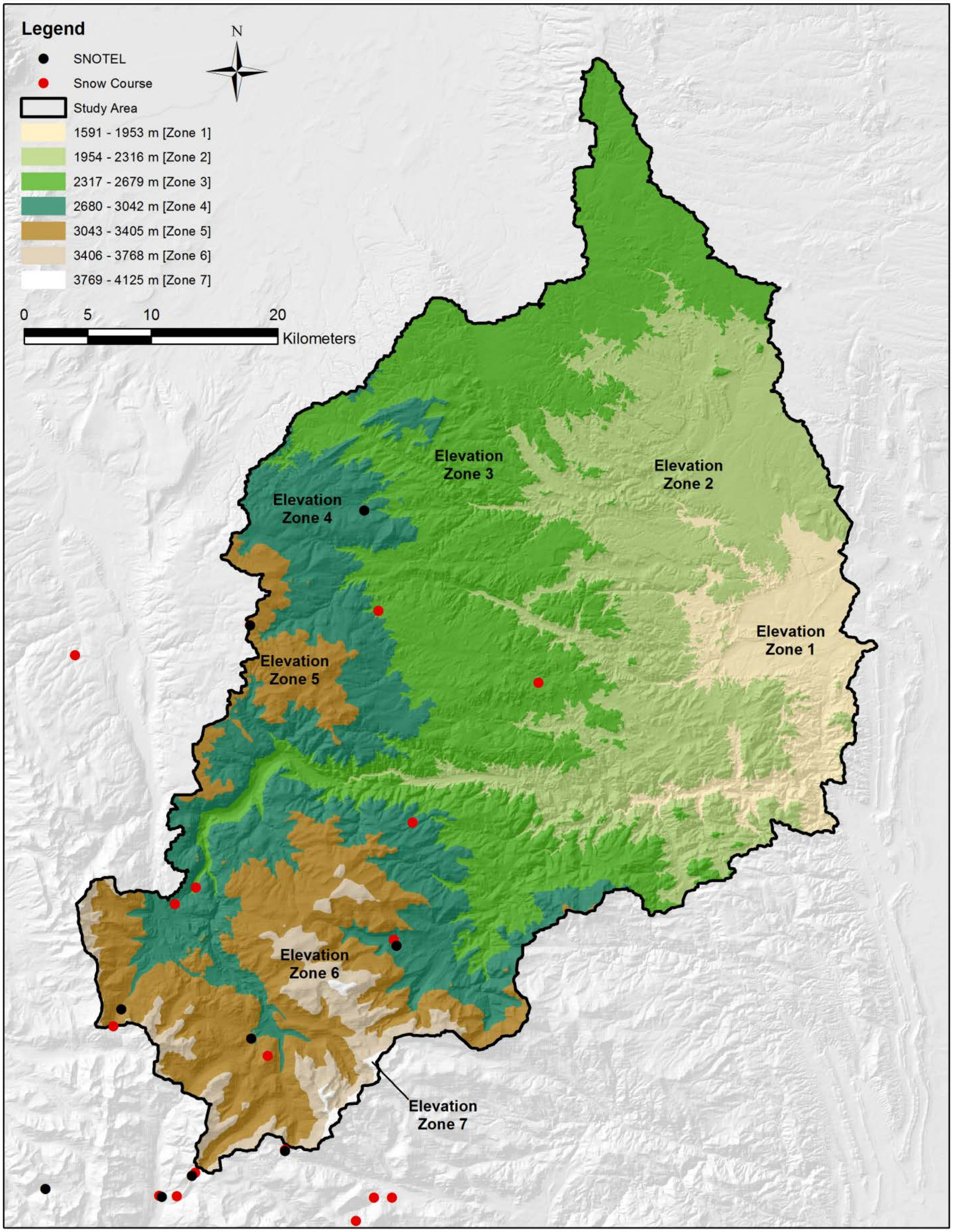

Figure 3.18: Map of the seven elevation zones within the study area identified by Richer [2009].

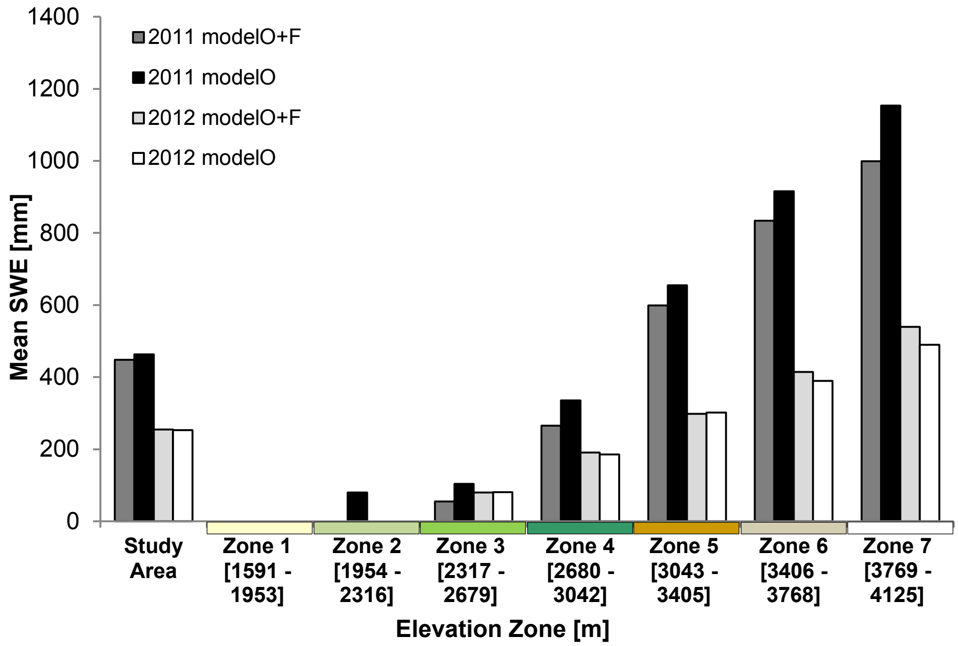

Figure 3.19: Average SWE across the study area and within each elevation zone from model$_{O+F}$ and model$_{O}$ interpolations for WY 2011 and WY 2012.

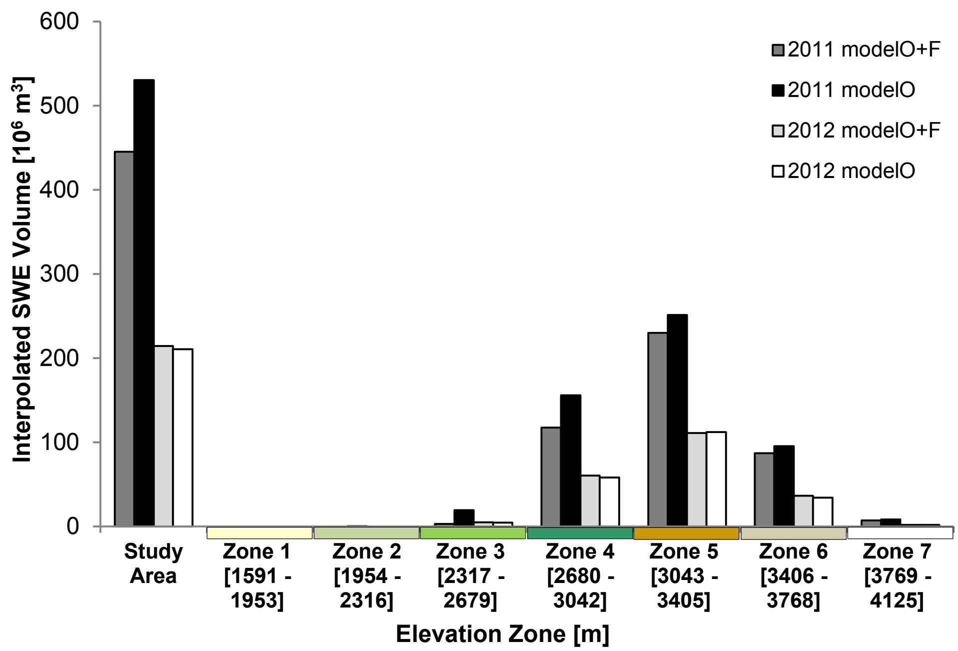

Figure 3.20: Interpolated SWE volume across the study area and within each elevation zone from model$_{O+F}$ and model$_{O}$ interpolations for WY 2011 and WY 2012.

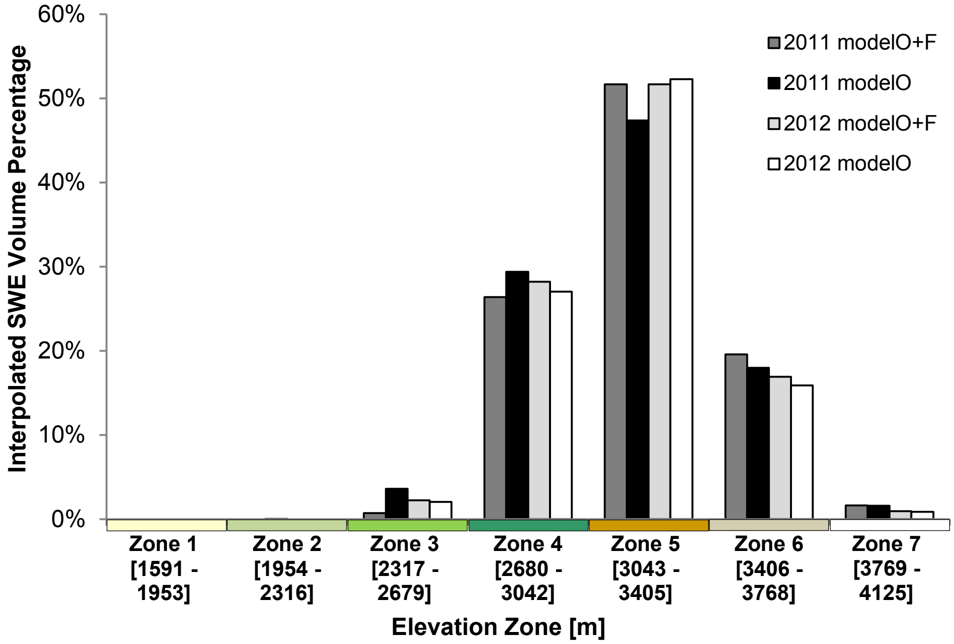

Figure 3.21: Percentage of interpolated SWE volume across the study area within each elevation zone from model_{O+F} and model_O interpolations for WY 2011 and WY 2012.

CHAPTER 4: CONCLUSIONS

This study has used a combination of field and operational-based snow measurements to evaluate snowpack properties across the basin scale. This research was motivated by the need for additional ground-based snowpack observations at a scale that coincides with that of remote sensing observations [Edward Kim, NASA, pers. comm., 2012] and is especially pertinent to water resources forecasting. Additional snowpack measurements at the basin scale can provide valuable verification data for remote sensing and modeling applications and help to improve characterizations of the distribution and patterns of snow water equivalent (SWE); yet field-based measurements are rarely collected at this scale. Studies collecting and analyzing field-based snowpack measurements at the basin scale are therefore an important step in the advancement of our understating of the spatial distribution of snow in mountain environments. The objectives of this thesis were addressed by the following research questions: (1) Can a reliable method of estimating SWE be developed from snow depth for the Cache la Poudre basin? (2) Can the spatial variability of SWE within the Cache la Poudre basin be characterized at the basin scale?

A method for modeling snow density across the Cache la Poudre basin from historical snow course measurements was developed for estimating SWE from snow depth (Chapter 2). The independent variables of snow depth, day of year, elevation, and UTM Easting were used in a multiple linear regression model to estimate snow density. Statistics showed strong performance of SWE calculated from snow depth observations using the snow density model, and model verification suggests the model is transferable to independent data within the bounds of the original dataset. The methods here provide a pathway for estimating SWE from snow depth measurements, which is especially useful when evaluating snowpack properties at the basin scale, where time consuming field-based measurements of SWE are often not feasible.

The spatial variability and observable patterns of SWE within the Cache la Poudre basin were analyzed in Chapter 3 using field and operational-based snowpack measurements. Bivariate relations of SWE and snow depth with physiographic variables show that elevation, latitude, and longitude are most strongly correlated with SWE and snow depth at this scale. Multiple linear regression models were developed for WY 2011 and WY 2012 using both a combined dataset of field-based and operational-based measurements ($model_{O+F}$) and a dataset of operational-based measurements only ($model_{O}$). Model calibration shows that $model_{O}$ outperformed the $model_{O+F}$ for both years, yet, model verification shows a greater error increase for $model_{O}$. SWE was interpolated across the study domain by using each model to calculate SWE on a pixel by pixel basis. The final interpolated SWE surfaces, masked to observed SCA (from an 8-day MODIS product), generally show similar patterns across space despite differing magnitudes between years as well as between input datasets. Within each of the model surfaces, interpolated volume of SWE was greatest within Elevation Zone 5 (3,043 – 3,405 m). Also, despite the differences of interpolated SWE volume observed among the four regression models, the percentage of the total interpolated SWE volume for each model was distributed similarly among elevation zones.

This research provides a further understanding of snowpack distribution and measurement strategies at the basin scale while also providing a field-based snow dataset that can be used within future evaluations of the snowpack at this scale. The snow density model successfully estimates SWE from snow depth measurements by modeling snow density. Using historical operational measurements for development of a regional based snow density model has implications for future field-based basin scale sampling campaigns, suggesting a sampling scheme dominated by snow depth measurements may be successful for evaluating basin-scale SWE variability. The temporal and spatial dataset of field-based snowpack measurements developed in this study is at a scale similar to remote sensing observations as well as modeling applications; these data can be used in those contexts for verification. Additionally, approaches of empirical modeling (e.g., multiple linear regression) for characterizing the distribution of SWE at the basin scale can be compared to remote sensing and modeling output. For instance, the observable patterns of SWE variability within this study, showing to be largely driven by elevation as well as latitude and longitude, could be compared to the patterns of variability observed within a physically based snow evolution model. The comparisons of the statistical relation of the snowpack with terrain based variables and physically based snow evolution modeling can provide insight for basin scale SWE distribution estimations. Therefore, future work will be focused using the spatially distributed snowpack evolution modeling system, SnowModel [Liston and Elder, 2006a] to analyze the spatial patterns of snow accumulation at the basin scale and compare the patterns observed with the field-based methods of this study.

Finally, the continuity of field-based snowpack measurements, as provided within this study, is essential given the assumption of non-stationarity from hydroclimatic change [Milly *et al*., 2008] and indications of more extreme conditions [IPCC, 2007]. This examination of two very different snow years may represent the bounds of extremes and possible the limitations due to non-stationarity. Continued field measurements of the snowpack will aid advancement of remote sensing and modeling applications, but more importantly continue to provide "ground-truth" observations for evaluating the complexities and uncertainties of the changing earth system.

REFERENCES

Akaike, H., 1974. A new look at the statistical model identification. *IEEE Transactions on Automatic Control* **19**(6), 716-723.

Anderton, S. P., S. M. White, and B. Alvera, 2004. Evaluation of spatial variability in snow water equivalent for a high mountain catchment. *Hydrological Processes* **18**(3), 435-453.

Bales, R.C., N.P. Molotch, T.H. Painter, M.D. Dettinger, R. Rice, and J. Dozier, 2006. Mountain hydrology of the western United States. *Water Resources Research* **42**, W08432 [doi:10.1029/2005WR004387].

Bales, R. C., K. A., Dressler, B. Imam, S. R. Fassnacht, and D. Lampkin, 2008. Fractional snow cover in the Colorado and Rio Grande basins, 1995–2002. *Water Resources Research* **44**(1), W01425 [doi:10.1029/2006WR005377].

Balk, B., and K. Elder, 2000. Combining binary decision tree and geostatistical methods to estimate snow distribution in a mountain watershed. *Water Resources Research* **36**(1), 13-26.

Barnett, T.P., J.C. Adam, and D.P. Lettenmaier, 2005. Potential impacts of a warming climate on water availability in snow-dominated regions. *Nature* **438**, 303-309.

Berk, K.N., 1978. Comparing Subset Regression Procedures. *Technometrics* **20**(1), 1-6.

Blöschl, G., 1999. Scaling issues in snow hydrology. *Hydrological Processes* **13**, 2149-2175.

Blöschl, G., R. Kirnbauer, and D. Gutknecht, 1991a. Distributed Snowmelt Simulations in an Alpine Catchment 1. Model Evaluation on the Basis of Snow Cover Patterns. *Water Resources Research*, **27**(12), 3171-3179.

Boon, S., 2012. Snow accumulation following forest disturbance. *Ecohydrology* **5**, 279-285.

Cayan, D.R., 1996. Interannual Climate Variability and Snowpack in the Western United States. *Journal of Climate* **9**, 928-948.

Chang, A.T.C., Kelly, R.E., Josberger, E.G., Armstrong, R.L., Foster, J.L., and Mognard, N.M., 2005. Analysis of ground-measured and passive-microwave-derived snow depth variations in midwinter across the northern Great Plains. *Journal of Hydrometeorology* **6**, 20-33.

Cline, D., S. Yueh, B. Chapman, B. Stankov, A. Gasiewski, D. Masters, K. Elder, R. Kelly, T. Painter, S. Miller, S. Katzberg, and L. Mahrt, 2009. NASA Cold Land Processes Experiment (CLPX 2002/03): Airborne Remote Sensing. *Journal of Hydrometeorology* **10**, 338-346, [doi: 10.1175/2008JHM883.1].

Clow, D.W., 2010. Changes in the Timing of Snowmelt and Streamflow in Colorado: A Response to Recent Warming. *Journal of Climate* **23**, 2293-2306, [doi: 10.1175/2009JCLI2951.1]

Daly, S.F., R. Davis, E. Ochs, and T. Pangburn, 2000. An approach to spatially distributed snow modeling of the Sacramento and San Joaquin basins, California. *Hydrological Processes* **14**, 3257-3271.

Daly, C., R.P. Neilson, and D.L. Phillips, 1994. A statistical-topographic model for mapping climatological precipitation over mountainous terrain. *Journal of Applied Meteorology* **33**, 140-158.

Deems, J.S., S.R. Fassnacht, and K.J. Elder, 2008. Interannual Consistency in Fractal Snow Depth Patterns at Two Colorado Mountain Sites. *Journal of Hydrometeorology* **9**, 977-988, [doi: 10.1175/2008JHM901.1]

Dingman, S.L., 1981. Elevation: A major influence on the hydrology of New Hampshire and Vermont, USA. *Hydrol. Sci. Bull.* **26**, 399-413.

Doesken, N.J., and A. Judson, 1996. *The Snow Booklet: A Guide to the Science, Climatology, and Measurement of Snow in the United States*, Dep. of Atmos. Sci., Colo. State Univ., Fort Collins, CO.

Dressler, K., S. R. Fassnacht, and R. C. Bales, 2006. A Comparison of Snow Telemetry and Snow Course Measurements in the Colorado River Basin. *Journal of Hydrometeorology* **7**, 705-712.

Elder, K., D. Cline, G. Liston, and R. Armstrong, 2009. NASA Cold Land Processes Experiment (CLPX 2002/03): Field Measurements of Snowpack Properties and Soil Moisture. *Journal of Hydrometeorology* **10**, 320-329, [doi: 10.1175/2008JHM877.1].

Elder, K., J. Dozier, and J. Michaelson, 1991. Snow accumulation and distribution in an Alpine watershed. *Water Resources Research* **27**, 1541-1552.

Elder, K., W. Rosenthal, R.E. Davis, 1998. Estimating the spatial distribution of snow water equivalence in a montane watershed. *Hydrological Processes* **12**, 1793-1808.

Erickson, T.A., M.W. Williams, A. Winstral, 2005. Persistence of topographic controls on the spatial distribution of snow in rugged mountain terrain, Colorado, United States. *Water Resources Research* **41**, W04014 [doi:10.1029/2003WR002973].

Erxleben, J., K. Elder, and R. Davis, 2002. Comparison of spatial interpolation methods for estimating snow distribution in the Colorado Rocky Mountains. *Hydrological Processes* **16**, 3627-3649, [doi:10.1002/hyp.1239].

Fassnacht, S.R., K.A. Dressler, and R.C. Bales, 2001. Physiographic parameters as indicators of snowpack state for the Colorado River Basin. *Proceedings of the Eastern Snow Conference* **58**, 45-48.

Fassnacht, S.R., K.A. Dressler, and R.C. Bales, 2003. Snow water equivalent interpolation for the Colorado River Basin from snow telemetry (SNOTEL) data. *Water Resources Research* **39**(8), 1208 [doi:10.1029/2002WR001512].

Fassnacht, S.R., C.M. Heun, J.I. López-Moreno, and J.B.P. Latron, 2010. Variability of Snow Density Measurements in the Rio Esera Valley, Pyrenees Mountains, Spain. *Cuandernos de Investigación Geográfica (Journal of Geographical Research)*, **36**(1), 59-72.

Fassnacht, S.R., M.E. Skordahl, and J.E. Derry, 2008. Variability at Colorado Operational Snow Measurement Sites, Snowcourse Stations at Collocated Snow Telemetry Stations. *Proceedings of the Eastern Snow Conference* **65**, 141-145.

Fassnacht, S.R., K.A. Dressler, D.M. Hulstrand, R.C. Bales, and G. Patterson, 2012. Temporal Inconsistencies in Coarse-Scale Snow Water Equivalent Patterns: Colorado River Basin Snow Telemetry-Topography Regressions. *Pirineos* **167**, 167-186.

Gilbert, R.O., 1987. *Statistical methods for environmental pollution monitoring*. Van Nostrand Reinhold, New York, NY.

Gillespie, M., 2011. *USDA – Natural Resources Conservation Services's Snow Survey and Water Supply Forecasting Program*. Presentation given at Colorado State University, Fort Collins, CO.

Harshburger, B. J., K. S. Humes, V. P. Walden, T. R. Blandford, B. C. Moore, and R. J. Dezzani, 2010. Spatial interpolation of snow water equivalency using surface observations and remotely sensed images of snow-covered area. *Hydrological Processes* **24**, 1285-1295.

Homer, C., J. Dewitz, J. Fry, M. Coan, N. Hossain, C. Larson, N. Herold, A. McKerrow, J.N. VanDriel, and J. Wickham, 2007. Completion of the 2001 National Land Cover Database for the Conterminous United States. *Photogrammetric Engineering and Remote Sensing* **73**(4), 337-341.

Ihaka, R.G. and R. Gentleman, 1996. R: a language for data analysis and graphics. *Journal of Computational and Graphical Statistics* **5**, 299-314.

Intergovernmental Panel on Climate Change (IPCC), 2007. *Climate Change 2007: The Physical Science Basis: Contribution of Working Group I to the Fourth Assessment Report of the IPCC*, edited by S. Solomon *et al*., Cambridge Univ. Press, Cambridge, U.K.

Jonas, T., C. Marty, and J. Magnusson, 2009. Estimating the snow water equivalent from snow depth measurements in the Swiss Alps. *Journal of Hydrology* **378**(1-2), 161-167.

Jost, G., M. Weiler, D. R. Gluns, and Y. Alila, 2007. The influence of forest and topography on snow accumulation and melt at the watershed-scale. *Journal of Hydrology* **347**, 101-115.

Kelly, R., 2009. The AMSR-E snow depth algorithm: description and initial results. *Journal of the Remote Sensing Society of Japan* **29**, 307-317.

Kimerling, A.J., A.R. Buckley, P.C. Muehrcke, and J.E. Muehrcke, 2011. *Map Use: Reading Analysis Interpretation, Seventh Edition*. ESRI Press Academic, Redlands, California.

Kutner, M.H, C.J. Nachtsheim, J. Neter, W. Li, 2005. *Applied Linear Statistical Models, Fifth Edition*. McGraw-Hill/Irwin, New York, NY.

Liston, G.E. and K. Elder, 2006a. A distributed snow-evolution modeling system (SnowModel). *Journal of Hydrometeorology* **7**, 1259-1276.

Liston, G.E. and M. Sturm, 1998. A snow-transport model for complex terrain. *Journal of Glaciology* **44**(148), 498-516.

Logan, L.A., 1973. Basin-wide water equivalent estimation from snowpack depth measurements. *IAHS Publication*, **107**, 864-884.

López-Moreno, J.I. and D. Nogués-Bravo, 2006. Interpolating local snow depth data: an evaluation of methods. *Hydrological Processes* **20**, 2217-2231, [doi: 10.1002/hyp.6199].

López-Moreno, J.I., S.R. Fassnacht, S.Beguería, and J.B.P. Latron, 2011. Variability of snow depth at the plot scale: implications for mean depth estimation and sampling strategies. *The Cryosphere* **5**, 617-629, [doi:10.5194/tc-5-617-2011].

Mallows, C.L., 1973. Come Comments on C_P. *Technometrics* **15**(4), 661-675.

McClung, D. and P. Schaerer, 2006. *The Avalanche Handbook, Third Edition*. The Mountaineers Books, Seattle, WA.

Milly P. *et al*., 2008. Stationarity Is Dead: Whither Water Management? *Science* **319**, 573-574.

Mizukami, N. and S. Perica, 2008. Spatiotemporal characteristics of snowpack density in the mountainous regions of the Western United States. *Journal of Hydrometeorology* **9**(6), 1416–1426, [doi: 10.1175/2008JHM981.1].

Molotch, N.P. and R.C. Bales, 2005. Scaling snow observations from the point to the grid element: Implications for observation network design. *Water Resources Research* **41**, W11421 [doi:10.1029/2005WR004229].

Molotch, N.P., R.C. Bales, M.T. Colee, and J. Dozier, 2003. Optimization of Binary Regression Tree Models for Estimating the Spatial Distribution of Snow Water Equivalent in an Alpine Basin. *Western Snow Conference* **71**, 3-15.

Molotch, N.P., M.T. Colee, R.C. Bales, and J. Dozier, 2005. Estimating the spatial distribution of snow water equivalent in an alpine basin using binary regression tree models: The impact of digital elevation data and independent variable selection. *Hydrological Processes* **19**, 1459-1479, [doi:10.1002/hyp.5586].

Pomeroy, J.W. and D.M. Gray, 1995. *Snow Accumulation, Relocation and Management*. National Hydrology Research Institute Science Report No. 7, p. 144.

Pugh, E.T. and E.E. Small, 2011. The impact of pine beetle infestation on snow accumulation and melt in the headwaters of the Colorado River. *Ecohydrology*, [doi: 10.1002/eco.239].

Richer, E.E. 2009. Snowmelt runoff analysis and modeling for the Upper Cache la Poudre River Basin, Colorado. M.S. Thesis, Colorado State University; 117.

Richer, E.E., S.K. Kampf, S.R. Fassnacht, and C.C. Moore. In review. Spatiotemporal index for analyzing controls on snow climatology: Application in the Colorado Front Range. *Physical Geography*. Submitted for review on August 8, 2012.

Salmi, T., A. Määttä, P. Anttila, T. Ruoho-Airola, and T. Amnell, 2002. Detecting Trends of Annual Values of Atmospheric Pollutants by the Mann-Kendall Test and Sen's Slope Estimates - The Excel Template Application MAKESENS. *Publications on Air Quality* **31**, Finnish Meteorological Institute, Helsinki.

Stewart, I.T., 2009. Changes in snowpack and snowmelt runoff for key mountain regions. *Hydrological Processes* **23**, 78-94.

Strum, M., B. Taras, G.E. Liston, C. Derksen, T. Jonas, and J. Lea, 2010. Estimating Snow Water Equivalent Using Snow Depth Data and Climate Classes. *Journal of Hydrometeorology* **11**, 1380-1394, [doi: 10.1175/2010JHM1202.1]

Viviroli, D., R. Weingartner, and B. Messerli, 2003. Assessing the Hydrological Significance Of the World's Mountains. *Mountain Research and Development* **23**(1), 32-40.

Viviroli, D. et al., 2011. Climate change and mountain water resources: overview and recommendations for research, management and policy. *Hydrology and Earth System Sciences* **15**(2), 471-504, [doi:10.5194/hess-15-471-2011].

Washichak J.N. and D.W. McAndrew, 1967. Snow Measurement Accuracy in High Density Snow Course Network in Colorado. *Proceedings of the Western Snow Conference* **35**, 43-49.

Winstral, A., K. Elder, and R. E. Davis, 2002. Spatial Snow Modeling of Wind-Redistributed Snow Using Terrain-Based Parameters. *Journal of Hydrometeorology* **3**(5), 524-538.

APPENDIX A: SUPPLEMENTAL MAPS

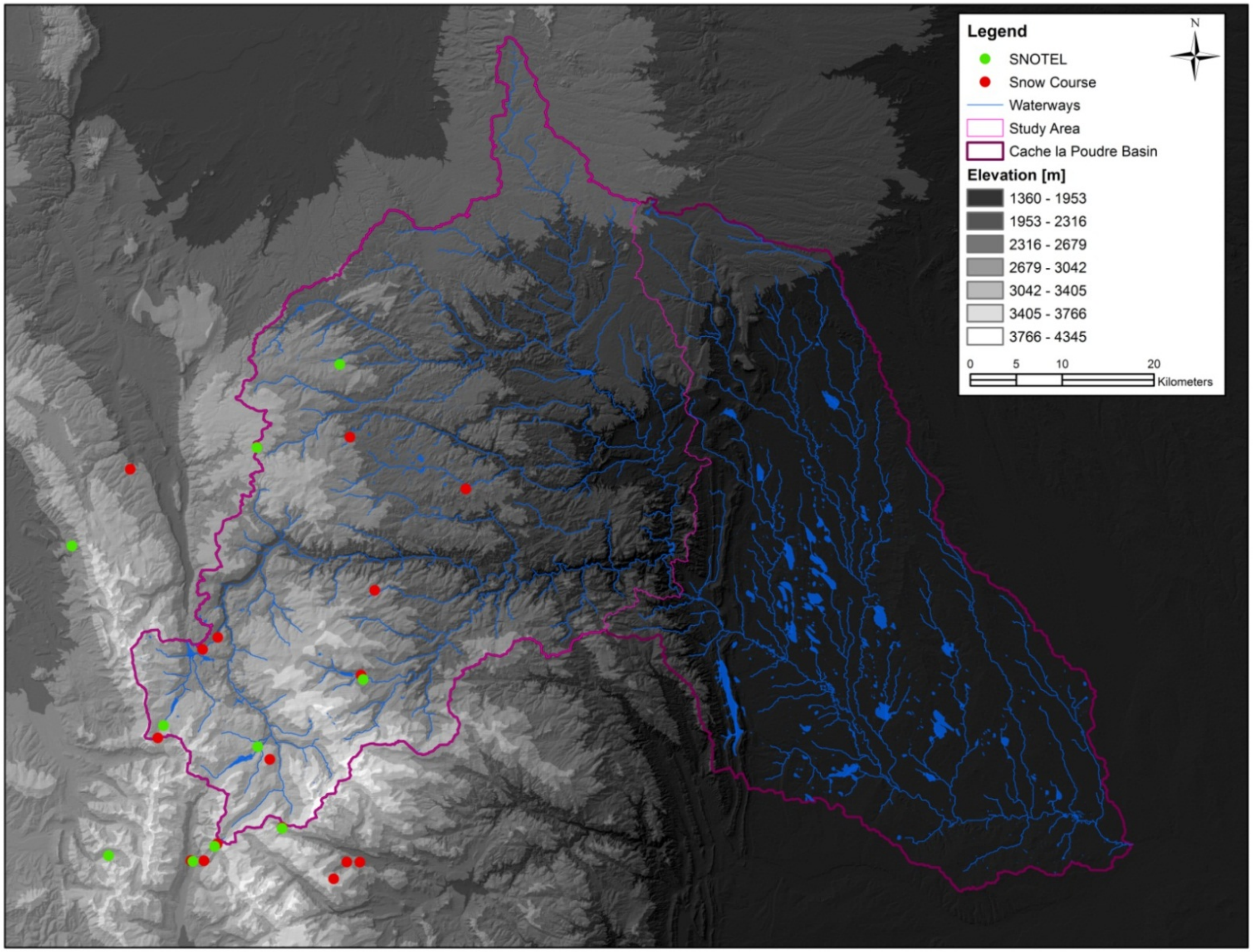

Figure A.1: DEM elevation map of the Cache la Poudre basin including locations of NRCS operational stations <*http://seamless.usgs.gov/*>.

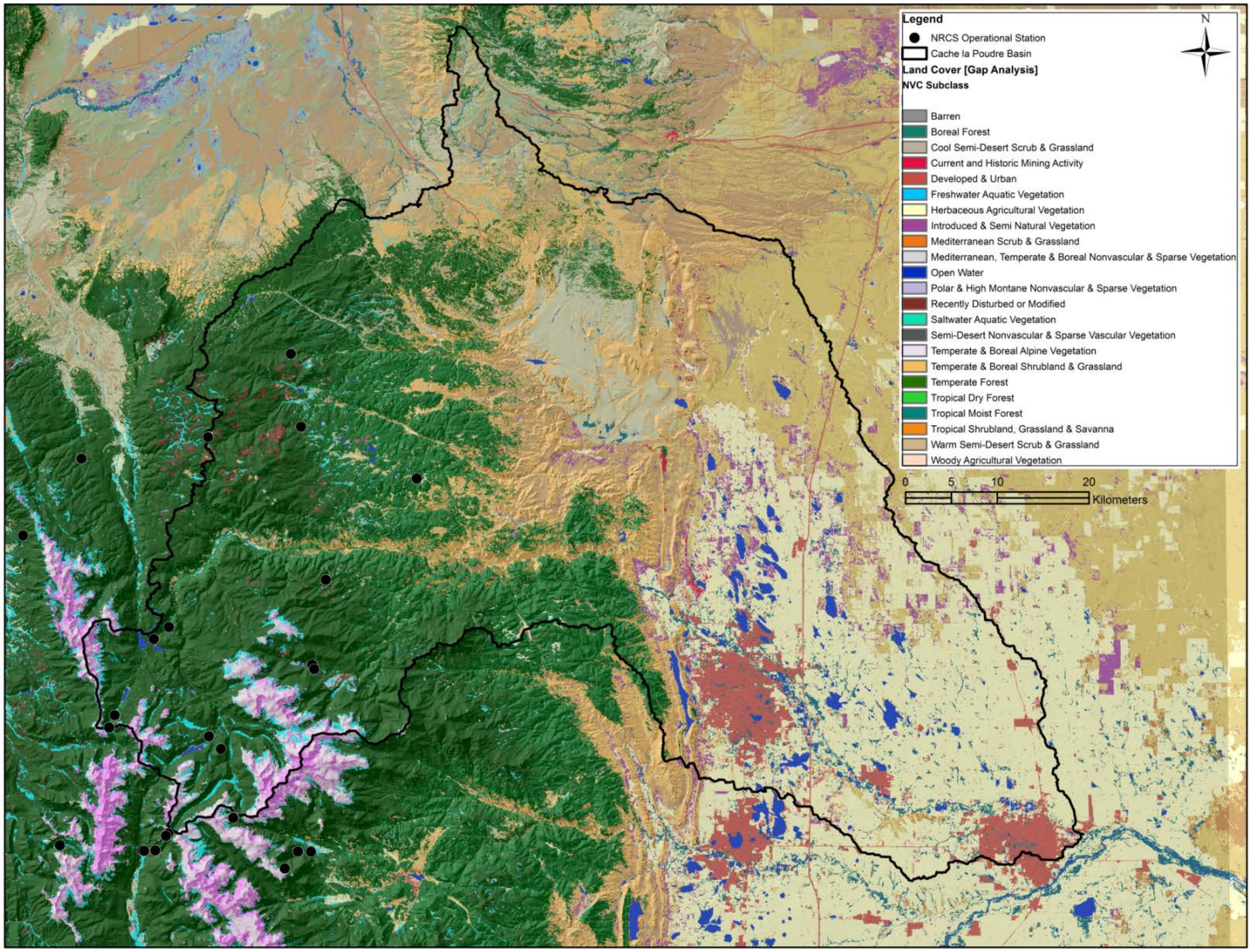

Figure A.2: Land cover map of the Cache la Poudre basin from the USGS Gap Analysis Program including locations of NRCS operational stations <*http://gapanalysis.usgs.gov/*>.

APPENDIX B: FIELD SNOWPACK MEASUREMENTS

Cache la Poudre Basin Study Area, CO
Field-based snowpack data
Date: 2010-11-23

Transect	Site Number	GPS Location			d_s Measurements (cm) - 1m interval											Mean d_s (cm)	Mean SWE Measurement			CC	CT	TM	Notes
		Easting	Northing	Elevation (m)	1	2	3	4	5	6	7	8	9	10	11		d_s (cm)	ρ_s (kgm^{-3})	SWE (mm)				
C	1	482311	4501681	1,607	0	---	---	---	---	---	---	---	---	---	---	0.0	---	---	---	---	---	---	no snow
C	2	481072	4501543	1,612	2	---	---	---	---	---	---	---	---	---	---	2.0	---	---	---	---	---	---	
C	3	479970	4504434	1,633	2	---	---	---	---	---	---	---	---	---	---	2.0	---	---	---	---	---	---	
C	4	473796	4504326	1,753	2	---	---	---	---	---	---	---	---	---	---	2.0	---	---	---	---	---	---	
C	5	470577	4504240	1,799	2	---	---	---	---	---	---	---	---	---	---	2.0	---	---	---	---	---	---	
C	6	467105	4503568	1,852	2	---	---	---	---	---	---	---	---	---	---	2.0	---	---	---	---	---	---	
C	7	463458	4504270	1,956	2	---	---	---	---	---	---	---	---	---	---	2.0	---	---	---	---	---	---	
C	8	459281	4503392	2,074	2	---	---	---	---	---	---	---	---	---	---	2.0	---	---	---	---	---	---	
C	9	455537	4505136	2,140	5	---	---	---	---	---	---	---	---	---	---	5.0	---	---	---	---	---	---	
C	10	446565	4505924	2,260	5	---	---	---	---	---	---	---	---	---	---	5.0	---	---	---	---	---	---	
C	11	442532	4505134	2,334	18	16	15	13	17	20	---	---	---	---	---	16.5	---	---	---	---	---	---	
C	12	438675	4506767	2,365	11	9	6	11	11	8	---	---	---	---	---	9.3	---	---	---	---	---	---	
C	13	435754	4505167	2,376	17	17	6	16	19	16	---	---	---	---	---	15.2	---	---	---	---	---	---	
C	14	431720	4502177	2,463	9	8	15	14	13	14	---	---	---	---	---	12.2	---	---	---	---	---	---	
C	15	431772	4498491	2,576	25	23	24	24	25	25	---	---	---	---	---	24.3	---	---	---	---	---	---	
C	16	***	***	2,649	32	33	29	30	37	39	---	---	---	---	---	33.3	---	---	---	---	---	---	
C	17	***	***	2,758	31	28	30	27	29	33	---	---	---	---	---	29.7	---	---	---	---	---	---	
C	18	427826	4492577	2,878	65	47	45	80	90	86	84	---	---	---	---	71.0	---	---	---	---	---	---	
C	19	425958	4489932	3,062	84	91	95	99	100	98	---	---	---	---	---	94.5	---	---	---	---	---	---	
C	20	425330	4488003	3,062	80	104	118	106	96	104	---	---	---	---	---	101.3	---	---	---	---	---	---	
C	21	***	***	3,095	98	97	99	101	101	108	---	---	---	---	---	100.7	---	---	---	---	---	---	
C	22	***	***	3,141	93	100	106	107	102	103	---	---	---	---	---	101.8	---	---	---	---	---	---	
C	23	422791	4484168	2,967	55	47	47	45	37	29	---	---	---	---	---	43.3	---	---	---	---	---	---	
C	24	420409	4484110	2,869	68	66	69	66	66	66	---	---	---	---	---	66.8	---	---	---	---	---	---	
C	25	420410	4484037	2,862	65	65	64	62	57	54	---	---	---	---	---	61.2	---	---	---	---	---	---	
C	26	414448	4485031	2,763	41	39	35	37	40	36	---	---	---	---	---	38.0	---	---	---	---	---	---	
C	27	424989	4484701	3,089	107	112	111	123	102	98	100	83	82	90	88	99.6	---	---	---	---	---	---	
C	28	426688	4490611	3,008	82	82	98	83	87	92	83	84	87	76	63	83.4	---	---	---	---	---	---	
C	29	427550	4492446	2,901	55	48	56	60	54	51	52	36	45	48	57	51.1	---	---	---	---	---	---	

Notes:

--- = no measurement
*** = NRCS coordinates not reported

Transect
C = CO Highway 14

Snow variables
d_s = snow depth
ρ_s = snow density
SWE = snow water equivalent

SWE measurement
can = cylindrical can [diameter = 15.3 cm]
tube = snow sampling tube [diameter = 6.6 cm]
fed = Federal sampler [diameter = 3.77 cm]

CC = Canopy Cover
C = closed
P = partially closed
O = open

CT = Community Type
LP = Lodgepole Pine
SF = Spruce/Fir
AS = Aspen Stand
AL = Alpine
W = Wetland

TM = Tree Mortality
O - open/no canopy
AG - alive with green needles
DR - dead with red needles
DG - dead and gray (no needles)

Cache la Poudre Basin Study Area, CO
Field-based snowpack data
Date: 2010-12-04

Transect	Site Number	GPS Location			d_s Measurements (cm) - 1m interval											Mean d_s (cm)	Mean SWE Measurement			CC	CT	TM	Notes
		Easting	Northing	Elevation (m)	1	2	3	4	5	6	7	8	9	10	11		d_s (cm)	ρ_s (kgm^{-3})	SWE (mm)				
C	1	482311	4501681	1,607	0	0	0	0	0	0	0	0	0	0	0	0.0	---	---	---	---	---	---	no snow
C	2	481072	4501543	1,612	0	0	0	0	0	0	0	0	0	0	0	0.0	---	---	---	---	---	---	no snow
C	3	479933	4504436	1,633	0	0	0	0	0	0	0	0	0	0	0	0.0	---	---	---	---	---	---	no snow
C	4	473679	4504205	1,753	0	0	0	0	0	0	0	0	0	0	0	0.0	---	---	---	---	---	---	no snow
C	5	470577	4504240	1,799	0	0	0	0	0	0	0	0	0	0	0	0.0	---	---	---	---	---	---	no snow
C	6	467105	4503568	1,852	0	0	0	0	0	0	0	0	0	0	0	0.0	---	---	---	---	---	---	no snow
C	7	463455	4504259	1,956	0	0	0	0	0	0	0	0	0	0	0	0.0	---	---	---	---	---	---	no snow
C	8	459281	4503392	2,074	0	0	0	0	0	0	0	0	0	0	0	0.0	---	---	---	---	---	---	no snow
C	9	455533	4505135	2,140	0	0	0	0	0	0	0	0	0	0	0	0.0	---	---	---	---	---	---	no snow
C	10	446544	4505927	2,260	0	0	0	0	0	0	0	0	0	0	0	0.0	---	---	---	---	---	---	no snow
C	11	442526	4505139	2,334	9	6	6	1	10	8	2	10	2	2	1	5.2	---	---	---	---	---	---	
C	12	438683	4506674	2,365	5	4	1	1	1	1	1	1	1	6	20	3.8	---	---	---	---	---	---	
C	13	435785	4505201	2,376	17	18	17	18	9	6	12	14	14	15	8	13.5	---	---	---	---	---	---	
C	14	431720	4502155	2,463	10	10	18	10	20	11	22	25	21	21	8	16.0	---	---	---	---	---	---	
C	15	431772	4498491	2,576	24	24	25	28	32	29	27	29	24	25	25	26.5	---	---	---	---	---	---	
C	16	***	***	2,649	30	26	26	25	38	31	31	36	39	41	43	33.2	---	---	---	---	---	---	
C	17	***	***	2,758	28	27	33	30	24	28	29	34	31	38	38	30.9	---	---	---	---	---	---	
C	18	427820	4485632	2,878	70	71	66	63	61	59	58	56	56	55	58	61.2	---	---	---	---	---	---	
C	19	425970	4490004	3,062	66	60	58	55	69	78	48	37	46	50	58	56.8	---	---	---	---	---	---	
C	20	425330	4488003	3,062	78	85	94	83	94	71	94	60	100	90	97	86.0	---	---	---	---	---	---	
C	21	***	***	3,095	96	95	98	95	97	104	103	106	110	118	121	103.9	---	---	---	---	---	---	
C	22	***	***	3,141	74	81	74	86	104	120	115	126	145	150	93	106.2	---	---	---	---	---	---	
C	23	---	---	---	---	---	---	---	---	---	---	---	---	---	---	---	---	---	---	---	---	---	
C	24	420419	4484080	2,869	51	51	55	50	54	53	55	53	55	54	55	53.3	---	---	---	---	---	---	
C	25	420407	4484057	2,862	65	69	70	65	73	64	57	46	44	37	26	56.0	---	---	---	---	---	---	
C	26	414437	4485025	2,763	39	39	40	36	38	38	39	43	40	44	43	39.9	---	---	---	---	---	---	
C	27	424986	4484674	3,089	65	80	73	82	83	78	88	85	82	72	63	77.4	---	---	---	---	---	---	
C	28	426686	4490632	3,008	80	71	80	86	78	81	78	75	74	83	84	79.1	---	---	---	---	---	---	
C	29	427599	4492483	2,901	60	68	52	55	54	50	45	56	58	61	56	55.9	---	---	---	---	---	---	

Notes:

--- = no measurement
*** = NRCS coordinates not reported

Transect
C = CO Highway 14

Snow variables
d_s = snow depth
ρ_s = snow density
SWE = snow water equivalent

SWE measurement
can = cylindrical can [diameter = 15.3 cm]
tube = snow sampling tube [diameter = 6.6 cm]
fed = Federal sampler [diameter = 3.77 cm]

CC = Canopy Cover
C = closed
P = partially closed
O = open

CT = Community Type
LP = Lodgepole Pine
SF = Spruce/Fir
AS = Aspen Stand
AL = Alpine
W = Wetland

TM = Tree Mortality
O - open/no canopy
AG - alive with green needles
DR - dead with red needles
DG - dead and gray (no needles)

Cache la Poudre Basin Study Area, CO
Field-based snowpack data
Date: 2011-01-12

Transect	Site Number	GPS Location			d_s Measurements (cm) - 1m interval											Mean d_s (cm)	Mean SWE Measurement			CC	CT	TM	Notes
		Easting	Northing	Elevation (m)	1	2	3	4	5	6	7	8	9	10	11		d_s (cm)	ρ_s (kgm^{-3})	SWE (mm)				
C	1	---	---	---	---	---	---	---	---	---	---	---	---	---	---	---	---	---	---	---	---	---	not sampled
C	2	---	---	---	---	---	---	---	---	---	---	---	---	---	---	---	---	---	---	---	---	---	not sampled
C	3	---	---	---	---	---	---	---	---	---	---	---	---	---	---	---	---	---	---	---	---	---	not sampled
C	4	---	---	---	---	---	---	---	---	---	---	---	---	---	---	---	---	---	---	---	---	---	not sampled
C	5	---	---	---	---	---	---	---	---	---	---	---	---	---	---	---	---	---	---	---	---	---	not sampled
C	6	---	---	---	---	---	---	---	---	---	---	---	---	---	---	---	---	---	---	---	---	---	not sampled
C	7	---	---	---	---	---	---	---	---	---	---	---	---	---	---	---	---	---	---	---	---	---	not sampled
C	8	---	---	---	---	---	---	---	---	---	---	---	---	---	---	---	---	---	---	---	---	---	not sampled
C	9	---	---	---	---	---	---	---	---	---	---	---	---	---	---	---	---	---	---	---	---	---	not sampled
C	10	---	---	---	---	---	---	---	---	---	---	---	---	---	---	---	---	---	---	---	---	---	not sampled
C	11	---	---	---	---	---	---	---	---	---	---	---	---	---	---	---	---	---	---	---	---	---	not sampled
C	12	438675	4506775	2,365	8	10	8	7	13	12	11	24	19	17	14	13.0	14.0	174.1	24.4	---	---	---	can
C	13	435753	4505112	2,386	39	38	33	28	30	34	39	39	37	39	36	35.6	---	---	---	---	---	---	
C	14	431726	4502165	2,469	37	29	19	21	20	18	24	19	15	18	25	22.3	32.0	223.7	71.6	---	---	---	can
C	15	431779	4498492	2,583	44	44	42	42	49	52	55	53	55	51	43	48.2	---	---	---	---	---	---	
C	16	***	***	2,652	54	49	50	44	60	47	50	59	61	61	66	54.6	---	---	---	---	---	---	
C	17	***	***	2,756	51	55	58	57	56	59	59	65	70	73	74	61.5	58.0	214.9	124.7	---	---	---	tube
C	18	427826	4492576	2,880	90	94	104	103	110	99	107	99	109	108	102	102.3	---	---	---	---	---	---	
C	19	425965	4489941	3,062	143	137	146	149	140	147	145	141	135	136	113	139.3	147.0	214.0	314.5	---	---	---	tube
C	20	425333	4488004	3,064	86	110	142	156	150	141	139	139	147	133	147	135.5	---	---	---	---	---	---	
C	21	***	***	---	---	---	---	---	---	---	---	---	---	---	---	---	---	---	---	---	---	---	not sampled
C	22	***	***	3,150	167	168	172	173	179	183	185	184	186	189	187	179.4	---	---	---	---	---	---	
C	23	---	---	---	---	---	---	---	---	---	---	---	---	---	---	---	---	---	---	---	---	---	not sampled
C	24	---	---	---	---	---	---	---	---	---	---	---	---	---	---	---	---	---	---	---	---	---	not sampled
C	25	420405	4484043	2,865	84	90	82	83	80	73	81	69	56	56	43	72.5	84.0	284.1	238.7	---	---	---	tube
C	26	---	---	---	---	---	---	---	---	---	---	---	---	---	---	---	---	---	---	---	---	---	not sampled
C	27	424984	4484695	3,102	104	105	118	115	104	100	126	122	118	116	113	112.8	---	---	---	---	---	---	
C	28	---	---	---	---	---	---	---	---	---	---	---	---	---	---	---	---	---	---	---	---	---	not sampled
C	29	427548	4492446	2,899	98	101	96	96	95	88	89	91	95	96	97	94.7	101.0	232.4	234.7	---	---	---	tube

Notes:

--- = no measurement
*** = NRCS coordinates not reported

Transect
C = CO Highway 14

Snow variables
d_s = snow depth
ρ_s = snow density
SWE = snow water equivalent

SWE measurement
can = cylindrical can [diameter = 15.3 cm]
tube = snow sampling tube [diameter = 6.6 cm]
fed = Federal sampler [diameter = 3.77 cm]

CC = Canopy Cover
C = closed
P = partially closed
O = open

CT = Community Type
LP = Lodgepole Pine
SF = Spruce/Fir
AS = Aspen Stand
AL = Alpine
W = Wetland

TM = Tree Mortality
O - open/no canopy
AG - alive with green needles
DR - dead with red needles
DG - dead and gray (no needles)

Cache la Poudre Basin Study Area, CO
Field-based snowpack data
Date: 2011-02-03

Transect	Site Number	GPS Location			d_s Measurements (cm) - 1m interval											Mean d_s (cm)	Mean SWE Measurement			CC	CT	TM	Notes
		Easting	Northing	Elevation (m)	1	2	3	4	5	6	7	8	9	10	11		d_s (cm)	ρ_s (kgm^{-3})	SWE (mm)				
C	1	482315	4501690	1,607	3	3	3	4	4	3	3	4	3	3	2	3.2	---	---	---	---	---	---	
C	2	---	---	---	---	---	---	---	---	---	---	---	---	---	---	---	---	---	---	---	---	---	not sampled
C	3	479982	4504429	1,626	4	6	7	5	5	6	6	4	5	6	4	5.3	---	---	---	---	---	---	
C	4	473763	4504330	1,749	4	3	4	4	3	4	4	5	4	4	3	3.8	1.50	74.3	1.12	---	---	---	can
C	5	---	---	---	---	---	---	---	---	---	---	---	---	---	---	---	---	---	---	---	---	---	not sampled
C	6	467097	4503582	1,851	5	6	4	6	5	4	5	3	4	6	5	4.8	---	---	---	---	---	---	
C	7	---	---	---	---	---	---	---	---	---	---	---	---	---	---	---	---	---	---	---	---	---	not sampled
C	8	459285	4503396	2,074	5	4	5	5	4	3	4	8	5	5	6	4.9	2.75	99.9	2.75	---	---	---	can
C	9	---	---	---	---	---	---	---	---	---	---	---	---	---	---	---	---	---	---	---	---	---	not sampled
C	10	---	---	---	---	---	---	---	---	---	---	---	---	---	---	---	---	---	---	---	---	---	not sampled
C	11	442526	4505137	2,328	22	23	25	10	30	25	24	16	35	24	10	22.2	20.0	185.2	37.0	---	---	---	can
C	12	438678	4506771	2,364	18	10	8	11	10	10	9	9	9	8	9	10.1	16.0	224.0	35.8	---	---	---	can
C	13	435758	4503112	2,382	36	41	45	39	29	33	35	32	40	41	41	37.5	---	---	---	---	---	---	
C	14	431725	4502166	2,472	30	32	25	29	34	37	36	40	31	35	24	32.1	27.0	195.6	52.8	---	---	---	can
C	15	431777	4498486	2,574	74	71	74	69	65	70	66	62	68	73	68	69.1	---	---	---	---	---	---	
C	16	***	***	2,646	77	68	69	63	64	68	73	74	84	82	84	73.3	---	---	---	---	---	---	
C	17	***	***	2,755	72	75	75	77	86	87	91	92	92	92	90	84.5	72.3	238.7	172.6	---	---	---	tube
C	18	427830	4492579	2,889	141	128	127	131	142	143	131	140	142	127	146	136.2	---	---	---	---	---	---	
C	19	425962	4489940	3,064	167	174	182	181	180	184	185	178	179	172	167	177.2	168.0	258.8	434.8	---	---	---	tube
C	20	425332	4488000	3,063	116	142	175	170	154	146	153	144	134	147	147	148.0	---	---	---	---	---	---	
C	21	***	***	---	---	---	---	---	---	---	---	---	---	---	---	---	---	---	---	---	---	---	not sampled
C	22	***	***	3,144	183	189	183	186	186	194	184	187	188	189	190	187.2	---	---	---	---	---	---	
C	23	---	---	---	---	---	---	---	---	---	---	---	---	---	---	---	---	---	---	---	---	---	not sampled
C	24	---	---	---	---	---	---	---	---	---	---	---	---	---	---	---	---	---	---	---	---	---	not sampled
C	25	420407	4484049	2,858	97	106	110	106	103	89	100	94	81	75	68	93.5	114.8	229.3	263.1	---	---	---	tube
C	26	---	---	---	---	---	---	---	---	---	---	---	---	---	---	---	---	---	---	---	---	---	not sampled
C	27	424989	4484695	3,102	134	139	142	130	144	156	143	143	159	156	159	145.9	---	---	---	---	---	---	
C	28	---	---	---	---	---	---	---	---	---	---	---	---	---	---	---	---	---	---	---	---	---	not sampled
C	29	427552	4492445	2,907	111	118	122	117	127	136	130	128	132	130	128	125.4	117.7	243.1	286.1	---	---	---	tube

Notes:

--- = no measurement
*** = NRCS coordinates not reported

Transect
C = CO Highway 14

Snow variables
d_s = snow depth
ρ_s = snow density
SWE = snow water equivalent

SWE measurement
can = cylindrical can [diameter = 15.3 cm]
tube = snow sampling tube [diameter = 6.6 cm]
fed = Federal sampler [diameter = 3.77 cm]

CC = Canopy Cover
C = closed
P = partially closed
O = open

CT = Community Type
LP = Lodgepole Pine
SF = Spruce/Fir
AS = Aspen Stand
AL = Alpine
W = Wetland

TM = Tree Mortality
O - open/no canopy
AG - alive with green needles
DR - dead with red needles
DG - dead and gray (no needles)

Cache la Poudre Basin Study Area, CO
Field-based snowpack data
Date: 2011-03-03

Transect	Site Number	GPS Location			d_s Measurements (cm) - 1m interval											Mean d_s (cm)	Mean SWE Measurement			CC	CT	TM	Notes
		Easting	Northing	Elevation (m)	1	2	3	4	5	6	7	8	9	10	11		d_s (cm)	ρ_s (kgm^{-3})	SWE (mm)				
C	1	482311	4501681	1,607	0	0	0	0	0	0	0	0	0	0	0	0.0	---	---	---	---	---	---	no snow
C	2	481072	4501543	1,612	0	0	0	0	0	0	0	0	0	0	0	0.0	---	---	---	---	---	---	no snow
C	3	479970	4504434	1,633	0	0	0	0	0	0	0	0	0	0	0	0.0	---	---	---	---	---	---	no snow
C	4	473796	4504326	1,753	0	0	0	0	0	0	0	0	0	0	0	0.0	---	---	---	---	---	---	no snow
C	5	470577	4504240	1,799	0	0	0	0	0	0	0	0	0	0	0	0.0	---	---	---	---	---	---	no snow
C	6	467105	4503568	1,852	0	0	0	0	0	0	0	0	0	0	0	0.0	---	---	---	---	---	---	no snow
C	7	463458	4504270	1,956	0	0	0	0	0	0	0	0	0	0	0	0.0	---	---	---	---	---	---	no snow
C	8	459281	4503392	2,074	0	0	0	0	0	0	0	0	0	0	0	0.0	---	---	---	---	---	---	no snow
C	9	455537	4505136	2,140	0	0	0	0	0	0	0	0	0	0	0	0.0	---	---	---	---	---	---	no snow
C	10	446565	4505924	2,260	0	0	0	0	0	0	0	0	0	0	0	0.0	---	---	---	---	---	---	no snow
C	11	442532	4505134	2,334	37	30	33	38	37	0	31	28	39	32	3	28.0	32.0	172.1	55.1	---	---	---	can
C	12	438675	4506767	2,365	6	8	8	15	8	6	6	7	8	12	14	8.9	8.8	269.5	23.6	---	---	---	can
C	13	435754	4505167	2,376	29	31	37	31	34	42	41	44	48	46	42	38.6	---	---	---	---	---	---	
C	14	431720	4502177	2,463	13	19	10	15	14	11	14	14	5	9	11	12.3	14.5	324.5	47.0	---	---	---	can
C	15	431772	4498491	2,576	74	73	71	68	69	63	71	75	83	78	63	71.6	---	---	---	---	---	---	
C	16	***	***	2,649	80	78	74	75	77	79	86	81	90	91	95	82.4	---	---	---	---	---	---	
C	17	***	***	2,758	100	102	104	102	102	100	95	95	100	99	91	99.1	92.0	311.7	286.7	---	---	---	tube
C	18	427826	4492577	2,878	135	133	132	158	156	168	161	177	188	175	169	159.3	---	---	---	---	---	---	
C	19	425958	4489932	3,062	191	185	181	180	184	190	200	198	185	178	188	187.3	---	---	---	---	---	---	
C	20	425330	4488003	3,062	118	121	128	164	179	171	166	178	156	182	161	156.7	---	---	---	---	---	---	
C	21	***	***	3,095	189	193	186	185	188	181	199	207	212	213	221	197.6	---	---	---	---	---	---	
C	22	***	***	3,141	194	192	187	190	185	187	178	180	181	185	184	185.7	---	---	---	---	---	---	
C	23	422791	4484168	2,967	80	80	73	67	68	77	74	70	77	118	110	81.3	---	---	---	---	---	---	
C	24	---	---	---	---	---	---	---	---	---	---	---	---	---	---	---	---	---	---	---	---	---	not sampled
C	25	420410	4484037	2,862	147	147	142	143	135	143	146	157	164	163	160	149.7	146.5	318.0	465.9	---	---	---	tube
C	26	414448	4485031	2,763	92	91	92	96	95	94	101	96	94	93	96	94.5	---	---	---	---	---	---	
C	27	424989	4484701	3,089	159	171	166	167	181	186	177	172	159	159	164	169.2	---	---	---	---	---	---	
C	28	---	---	---	---	---	---	---	---	---	---	---	---	---	---	---	---	---	---	---	---	---	not sampled
C	29	427550	4492446	2,901	171	166	160	158	163	157	155	155	155	147	149	157.8	---	---	---	---	---	---	

Notes:

--- = no measurement
*** = NRCS coordinates not reported

Transect
C = CO Highway 14

Snow variables
d_s = snow depth
ρ_s = snow density
SWE = snow water equivalent

SWE measurement
can = cylindrical can [diameter = 15.3 cm]
tube = snow sampling tube [diameter = 6.6 cm]
fed = Federal sampler [diameter = 3.77 cm]

CC = Canopy Cover
C = closed
P = partially closed
O = open

CT = Community Type
LP = Lodgepole Pine
SF = Spruce/Fir
AS = Aspen Stand
AL = Alpine
W = Wetland

TM = Tree Mortality
O - open/no canopy
AG - alive with green needles
DR - dead with red needles
DG - dead and gray (no needles)

Cache la Poudre Basin Study Area, CO
Field-based snowpack data
Date: 2011-03-31

Transect	Site Number	GPS Location			d_s Measurements (cm) - 1m interval											Mean d_s (cm)	Mean SWE Measurement			CC	CT	TM	Notes
		Easting	Northing	Elevation (m)	1	2	3	4	5	6	7	8	9	10	11		d_s (cm)	ρ_s (kgm^{-3})	SWE (mm)				
D	1	444915	4517071	2,732	18	21	25	24	34	33	28	27	23	19	18	24.5	---	---	---	---	---	---	
D	2	444211	4517282	2,797	67	60	71	67	65	73	77	78	82	71	87	72.5	70.0	322.8	226.0	---	---	---	can
D	3	443624	4517606	2,830	25	35	40	40	43	39	31	23	32	39	41	35.3	---	---	---	---	---	---	
D	4	443222	4517664	2,890	73	58	82	86	79	77	82	63	57	49	60	69.6	81.3	312.5	254.0	---	---	---	fed
D	5	442482	4517931	2,882	44	31	22	21	21	22	26	46	59	66	58	37.8	38.0	247.7	94.1	---	---	---	can
D	6	441450	4517978	2,844	94	87	80	78	78	77	70	65	53	53	51	71.5	---	---	---	---	---	---	
D	7	440045	4518276	2,798	125	110	96	100	116	122	123	143	130	151	168	125.8	108.0	352.9	381.0	---	---	---	fed
D	8	439110	4518052	2,852	108	99	96	97	94	97	99	108	108	109	113	102.5	---	---	---	---	---	---	
D	9	438201	4518135	2,884	66	56	54	74	79	84	85	90	82	84	75	75.4	---	---	---	---	---	---	
D	10	438168	4518108	2,876	77	88	86	81	69	64	57	59	59	70	76	71.5	---	---	---	---	---	---	
D	11	437878	4517864	2,895	87	90	94	103	86	82	80	66	54	66	92	81.8	81.0	233.8	189.4	---	---	---	can

Notes:

--- = no measurement
*** = NRCS coordinates not reported

Transect
D = Deadman Hill [Deadman Road]

Snow variables
d_s = snow depth
ρ_s = snow density
SWE = snow water equivalent

SWE measurement
can = cylindrical can [diameter = 15.3 cm]
tube = snow sampling tube [diameter = 6.6 cm]
fed = Federal sampler [diameter = 3.77 cm]

CC = Canopy Cover
C = closed
P = partially closed
O = open

CT = Community Type
LP = Lodgepole Pine
SF = Spruce/Fir
AS = Aspen Stand
AL = Alpine
W = Wetland

TM = Tree Mortality
O - open/no canopy
AG - alive with green needles
DR - dead with red needles
DG - dead and gray (no needles)

Cache la Poudre Basin Study Area, CO
Field-based snowpack data
Date: 2011-04-02

Transect	Site Number	GPS Location			d_s Measurements (cm) - 1m interval											Mean d_s (cm)	Mean SWE Measurement			CC	CT	TM	Notes
		Easting	Northing	Elevation (m)	1	2	3	4	5	6	7	8	9	10	11		d_s (cm)	ρ_s (kgm^{-3})	SWE (mm)				
C	1	482311	4501681	1,607	0	0	0	0	0	0	0	0	0	0	0	0.0	---	---	---	---	---	---	no snow
C	2	481072	4501543	1,612	0	0	0	0	0	0	0	0	0	0	0	0.0	---	---	---	---	---	---	no snow
C	3	479970	4504434	1,633	0	0	0	0	0	0	0	0	0	0	0	0.0	---	---	---	---	---	---	no snow
C	4	473796	4504326	1,753	0	0	0	0	0	0	0	0	0	0	0	0.0	---	---	---	---	---	---	no snow
C	5	470577	4504240	1,799	0	0	0	0	0	0	0	0	0	0	0	0.0	---	---	---	---	---	---	no snow
C	6	467105	4503568	1,852	0	0	0	0	0	0	0	0	0	0	0	0.0	---	---	---	---	---	---	no snow
C	7	463458	4504270	1,956	0	0	0	0	0	0	0	0	0	0	0	0.0	---	---	---	---	---	---	no snow
C	8	459281	4503392	2,074	0	0	0	0	0	0	0	0	0	0	0	0.0	---	---	---	---	---	---	no snow
C	9	455537	4505136	2,140	0	0	0	0	0	0	0	0	0	0	0	0.0	---	---	---	---	---	---	no snow
C	10	446565	4505924	2,260	0	0	0	0	0	0	0	0	0	0	0	0.0	---	---	---	---	---	---	no snow
C	11	442532	4505134	2,334	0	0	0	0	0	0	0	0	0	0	0	0.0	---	---	---	---	---	---	no snow
C	12	438675	4506767	2,365	0	0	0	0	0	0	0	0	0	0	0	0.0	---	---	---	---	---	---	no snow
C	13	435754	4505167	2,376	0	0	0	0	0	0	0	0	0	0	0	0.0	---	---	---	---	---	---	no snow
C	14	431720	4502177	2,463	0	0	0	0	0	0	0	0	0	0	0	0.0	---	---	---	---	---	---	no snow
C	15	431773	4498491	2,586	60	76	73	75	76	54	53	64	73	78	36	65.3	---	---	---	---	---	---	
C	16	***	***	2,637	68	71	65	63	63	60	62	72	77	81	84	69.6	---	---	---	---	---	---	
C	17	***	***	2,758	104	101	94	99	91	85	84	84	82	87	85	90.5	108.5	290.6	315.3	---	---	---	tube
C	18	427834	4492583	2,895	216	212	215	214	217	214	219	226	224	233	233	220.3	---	---	---	---	---	---	
C	19	425970	4489938	3,068	227	224	225	224	216	219	219	216	218	218	209	219.5	222.9	381.7	850.9	---	---	---	fed
C	20	425329	448802	3,069	190	191	214	207	210	230	225	220	211	210	237	213.2	---	---	---	---	---	---	
C	21	***	***	---	---	---	---	---	---	---	---	---	---	---	---	---	---	---	---	---	---	---	not sampled
C	22	***	***	3,164	241	232	237	235	235	234	239	237	239	247	250	238.7	---	---	---	---	---	---	
C	23	---	---	---	---	---	---	---	---	---	---	---	---	---	---	---	---	---	---	---	---	---	not sampled
C	24	---	---	---	---	---	---	---	---	---	---	---	---	---	---	---	---	---	---	---	---	---	not sampled
C	25	420407	4484030	2,865	172	171	175	186	186	177	185	180	185	165	171	177.5	174.0	357.4	622.3	---	---	---	fed
C	26	---	---	---	---	---	---	---	---	---	---	---	---	---	---	---	---	---	---	---	---	---	not sampled
C	27	424987	4484697	3,102	185	224	220	228	222	218	224	232	230	224	234	221.9	---	---	---	---	---	---	
C	28	426737	4490674	2,999	167	171	179	182	189	180	196	195	201	216	230	191.5	---	---	---	---	---	---	
C	29	427550	4492459	2,904	205	204	195	190	186	180	178	182	178	177	190	187.7	177.3	335.0	593.2	---	---	---	fed

Notes:

--- = no measurement
*** = NRCS coordinates not reported

Transect
C = CO Highway 14

Snow variables
d_s = snow depth
ρ_s = snow density
SWE = snow water equivalent

SWE measurement
can = cylindrical can [diameter = 15.3 cm]
tube = snow sampling tube [diameter = 6.6 cm]
fed = Federal sampler [diameter = 3.77 cm]

CC = Canopy Cover
C = closed
P = partially closed
O = open

CT = Community Type
LP = Lodgepole Pine
SF = Spruce/Fir
AS = Aspen Stand
AL = Alpine
W = Wetland

TM = Tree Mortality
O - open/no canopy
AG - alive with green needles
DR - dead with red needles
DG - dead and gray (no needles)

Cache la Poudre Basin Study Area, CO
Field-based snowpack data
Date: 2011-04-02

Transect	Site Number	GPS Location			d_s Measurements (cm) - 1m interval											Mean d_s (cm)	Mean SWE Measurement			CC	CT	TM	Notes
		Easting	Northing	Elevation (m)	1	2	3	4	5	6	7	8	9	10	11		d_s (cm)	ρ_s (kgm^{-3})	SWE (mm)				
P	1	449626	4490930	2,768	47	48	53	58	64	69	74	82	90	97	105	71.5	---	---	---	---	---	---	
P	2	448683	4490060	2,870	90	76	60	66	48	92	78	79	82	67	54	72.0	45.0	284.9	128.2	---	---	---	can
P	3	448261	4489834	2,891	82	110	106	135	111	101	82	73	64	59	53	88.7	---	---	---	---	---	---	
P	4	447927	4489702	2,910	98	107	115	116	114	111	92	104	97	91	87	102.9	111.0	277.0	307.4	---	---	---	can
P	5	447979	4489588	2,945	105	111	109	105	99	77	64	109	91	105	81	96.0	---	---	---	---	---	---	
P	6	449215	4490887	2,842	38	52	60	67	83	75	68	60	59	56	27	58.6	---	---	---	---	---	---	

Notes:

--- = no measurement
*** = NRCS coordinates not reported

Transect
P = CSU Pingree Park

Snow variables
d_s = snow depth
ρ_s = snow density
SWE = snow water equivalent

SWE measurement
can = cylindrical can [diameter = 15.3 cm]
tube = snow sampling tube [diameter = 6.6 cm]
fed = Federal sampler [diameter = 3.77 cm]

CC = Canopy Cover
C = closed
P = partially closed
O = open

CT = Community Type
LP = Lodgepole Pine
SF = Spruce/Fir
AS = Aspen Stand
AL = Alpine
W = Wetland

TM = Tree Mortality
O - open/no canopy
AG - alive with green needles
DR - dead with red needles
DG - dead and gray (no needles)

Cache la Poudre Basin Study Area, CO
Field-based snowpack data
Date: 2011-04-30

Transect	Site Number	GPS Location			d_s Measurements (cm) - 1m interval											Mean d_s (cm)	Mean SWE Measurement			CC	CT	TM	Notes
		Easting	Northing	Elevation (m)	1	2	3	4	5	6	7	8	9	10	11		d_s (cm)	ρ_s (kgm^{-3})	SWE (mm)				
C	1	482311	4501681	1,607	0	0	0	0	0	0	0	0	0	0	0	0.0	---	---	---	---	---	---	no snow
C	2	481072	4501543	1,612	0	0	0	0	0	0	0	0	0	0	0	0.0	---	---	---	---	---	---	no snow
C	3	479970	4504434	1,633	0	0	0	0	0	0	0	0	0	0	0	0.0	---	---	---	---	---	---	no snow
C	4	473796	4504326	1,753	0	0	0	0	0	0	0	0	0	0	0	0.0	---	---	---	---	---	---	no snow
C	5	470577	4504240	1,799	0	0	0	0	0	0	0	0	0	0	0	0.0	---	---	---	---	---	---	no snow
C	6	467105	4503568	1,852	0	0	0	0	0	0	0	0	0	0	0	0.0	---	---	---	---	---	---	no snow
C	7	463458	4504270	1,956	0	0	0	0	0	0	0	0	0	0	0	0.0	---	---	---	---	---	---	no snow
C	8	459281	4503392	2,074	0	0	0	0	0	0	0	0	0	0	0	0.0	---	---	---	---	---	---	no snow
C	9	455537	4505136	2,140	0	0	0	0	0	0	0	0	0	0	0	0.0	---	---	---	---	---	---	no snow
C	10	446565	4505924	2,260	0	0	0	0	0	0	0	0	0	0	0	0.0	---	---	---	---	---	---	no snow
C	11	442525	4505145	2,343	5	9	11	2	6	4	0	2	0	5	4	4.4	---	---	---	---	---	---	
C	12	438676	4506771	2,358	10	9	9	10	10	9	0	10	8	8	9	8.4	7.0	129.8	9.08	---	---	---	can
C	13	435797	4505182	2,384	9	12	11	11	10	11	12	14	15	13	12	11.8	---	---	---	---	---	---	
C	14	431737	4502157	2,456	10	10	9	13	11	11	11	12	10	14	10	11.0	---	---	---	---	---	---	
C	15	431773	4498491	2,576	80	81	82	75	66	58	70	89	103	109	100	83.0	---	---	---	---	---	---	
C	16	***	***	2,638	95	90	83	85	85	83	86	93	99	104	103	91.5	---	---	---	---	---	---	
C	17	***	***	2,753	133	126	141	141	135	130	125	122	127	121	112	128.5	134.6	301.9	406.4	---	---	---	fed
C	18	427822	4492570	2,882	245	248	217	225	245	220	200	214	224	221	257	228.7	---	---	---	---	---	---	
C	19	425963	4489939	3,061	340	326	329	320	315	323	329	312	300	322	333	322.6	---	---	---	---	---	---	
C	20	425324	4488007	3,067	294	281	268	257	261	280	284	279	287	294	299	280.4	---	---	---	---	---	---	
C	21	***	***	---	---	---	---	---	---	---	---	---	---	---	---	---	---	---	---	---	---	---	not sampled
C	22	***	***	3,159	330	330	326	324	320	321	323	320	320	325	322	323.7	---	---	---	---	---	---	
C	23	---	---	---	---	---	---	---	---	---	---	---	---	---	---	---	---	---	---	---	---	---	not sampled
C	24	---	---	---	---	---	---	---	---	---	---	---	---	---	---	---	---	---	---	---	---	---	not sampled
C	25	420401	4484047	2,868	210	205	210	210	208	204	207	204	206	202	200	206.0	215.9	311.8	673.1	---	---	---	fed
C	26	---	---	---	---	---	---	---	---	---	---	---	---	---	---	---	---	---	---	---	---	---	not sampled
C	27	424980	4484697	3,094	331	340	328	329	320	322	338	325	325	326	320	327.6	---	---	---	---	---	---	
C	28	---	---	---	---	---	---	---	---	---	---	---	---	---	---	---	---	---	---	---	---	---	not sampled
C	29	427550	4492459	2,903	230	222	204	211	216	216	227	218	220	224	226	219.5	210.2	313.9	660.4	---	---	---	fed

Notes:

--- = no measurement
*** = NRCS coordinates not reported

Transect
C = CO Highway 14

Snow variables
d_s = snow depth
ρ_s = snow density
SWE = snow water equivalent

SWE measurement
can = cylindrical can [diameter = 15.3 cm]
tube = snow sampling tube [diameter = 6.6 cm]
fed = Federal sampler [diameter = 3.77 cm]

CC = Canopy Cover
C = closed
P = partially closed
O = open

CT = Community Type
LP = Lodgepole Pine
SF = Spruce/Fir
AS = Aspen Stand
AL = Alpine
W = Wetland

TM = Tree Mortality
O - open/no canopy
AG - alive with green needles
DR - dead with red needles
DG - dead and gray (no needles)

Cache la Poudre Basin Study Area, CO
Field-based snowpack data
Date: 2011-05-31

Transect	Site Number	GPS Location			d_s Measurements (cm) - 1m interval											Mean d_s (cm)	Mean SWE Measurement			CC	CT	TM	Notes
		Easting	Northing	Elevation (m)	1	2	3	4	5	6	7	8	9	10	11		d_s (cm)	ρ_s (kgm^{-3})	SWE (mm)				
C	1	482311	4501681	1,607	0	0	0	0	0	0	0	0	0	0	0	0.0	---	---	---	---	---	---	no snow
C	2	481072	4501543	1,612	0	0	0	0	0	0	0	0	0	0	0	0.0	---	---	---	---	---	---	no snow
C	3	479970	4504434	1,633	0	0	0	0	0	0	0	0	0	0	0	0.0	---	---	---	---	---	---	no snow
C	4	473796	4504326	1,753	0	0	0	0	0	0	0	0	0	0	0	0.0	---	---	---	---	---	---	no snow
C	5	470577	4504240	1,799	0	0	0	0	0	0	0	0	0	0	0	0.0	---	---	---	---	---	---	no snow
C	6	467105	4503568	1,852	0	0	0	0	0	0	0	0	0	0	0	0.0	---	---	---	---	---	---	no snow
C	7	463458	4504270	1,956	0	0	0	0	0	0	0	0	0	0	0	0.0	---	---	---	---	---	---	no snow
C	8	459281	4503392	2,074	0	0	0	0	0	0	0	0	0	0	0	0.0	---	---	---	---	---	---	no snow
C	9	455537	4505136	2,140	0	0	0	0	0	0	0	0	0	0	0	0.0	---	---	---	---	---	---	no snow
C	10	446565	4505924	2,260	0	0	0	0	0	0	0	0	0	0	0	0.0	---	---	---	---	---	---	no snow
C	11	442525	4505145	2,343	0	0	0	0	0	0	0	0	0	0	0	0.0	---	---	---	---	---	---	no snow
C	12	438676	4506771	2,358	0	0	0	0	0	0	0	0	0	0	0	0.0	---	---	---	---	---	---	no snow
C	13	435797	4505182	2,384	0	0	0	0	0	0	0	0	0	0	0	0.0	---	---	---	---	---	---	no snow
C	14	431737	4502157	2,456	0	0	0	0	0	0	0	0	0	0	0	0.0	---	---	---	---	---	---	no snow
C	15	431773	4498491	2,576	0	0	0	0	0	0	0	0	0	0	0	0.0	---	---	---	---	---	---	no snow
C	16	430745	4496817	2,638	0	0	0	0	0	0	0	0	0	0	0	0.0	---	---	---	---	---	---	no snow
C	17	429143	4495496	2,753	0	0	0	0	0	15	20	18	14	12	20	9.0	---	---	---	---	---	---	
C	18	427822	4492570	2,882	131	143	146	161	155	149	159	150	155	159	152	150.9	---	---	---	---	---	---	
C	19	425963	4489939	3,061	245	243	234	245	249	235	230	231	231	234	233	237.3	199.4	468.3	933.5	---	---	---	fed
C	20	425324	4488007	3,067	235	235	210	200	200	205	200	207	210	213	226	212.8	---	---	---	---	---	---	
C	21	---	---	---	---	---	---	---	---	---	---	---	---	---	---	---	---	---	---	---	---	---	not sampled
C	22	424251	4485866	3,159	242	235	233	233	225	230	228	228	232	234	232	232.0	---	---	---	---	---	---	
C	23	---	---	---	---	---	---	---	---	---	---	---	---	---	---	---	---	---	---	---	---	---	not sampled
C	24	---	---	---	---	---	---	---	---	---	---	---	---	---	---	---	---	---	---	---	---	---	not sampled
C	25	420401	4484047	2,868	140	138	140	130	135	132	133	133	134	130	131	134.2	143.5	413.1	592.7	---	---	---	fed
C	26	414448	4485031	2,763	0	0	0	0	0	0	0	0	0	0	0	0.0	---	---	---	---	---	---	no snow
C	27	424980	4484697	3,094	257	245	245	245	244	248	246	237	242	234	235	243.5	---	---	---	---	---	---	
C	28	---	---	---	---	---	---	---	---	---	---	---	---	---	---	---	---	---	---	---	---	---	not sampled
C	29	427550	4492459	2,903	170	162	151	155	140	142	138	153	140	149	155	150.5	162.6	406.3	660.4	---	---	---	fed

Notes:

--- = no measurement
*** = NRCS coordinates not reported

Transect
C = CO Highway 14

Snow variables
d_s = snow depth
ρ_s = snow density
SWE = snow water equivalent

SWE measurement
can = cylindrical can [diameter = 15.3 cm]
tube = snow sampling tube [diameter = 6.6 cm]
fed = Federal sampler [diameter = 3.77 cm]

CC = Canopy Cover
C = closed
P = partially closed
O = open

CT = Community Type
LP = Lodgepole Pine
SF = Spruce/Fir
AS = Aspen Stand
AL = Alpine
W = Wetland

TM = Tree Mortality
O - open/no canopy
AG - alive with green needles
DR - dead with red needles
DG - dead and gray (no needles)

Cache la Poudre Basin Study Area, CO
Field-based snowpack data
Date: 2012-01-02

Transect	Site Number	GPS Location			d_s Measurements (cm) - 1m interval											Mean d_s (cm)	Mean SWE Measurement			CC	CT	TM	Notes
		Easting	Northing	Elevation (m)	1	2	3	4	5	6	7	8	9	10	11		d_s (cm)	ρ_s (kgm^{-3})	SWE (mm)				
C	1	482311	4501681	1,607	0	0	0	0	0	0	0	0	0	0	0	0.0	---	---	---	---	---	---	no snow
C	2	481072	4501543	1,612	0	0	0	0	0	0	0	0	0	0	0	0.0	---	---	---	---	---	---	no snow
C	3	479970	4504434	1,633	0	0	0	0	0	0	0	0	0	0	0	0.0	---	---	---	---	---	---	no snow
C	4	473796	4504326	1,753	0	0	0	0	0	0	0	0	0	0	0	0.0	---	---	---	---	---	---	no snow
C	5	470577	4504240	1,799	0	2	3	5	0	0	0	2	2	1	2	1.5	---	---	---	---	---	---	
C	6	467105	4503568	1,852	0	8	16	16	9	2	14	10	9	8	9	9.2	---	---	---	---	---	---	
C	7	463458	4504270	1,956	0	6	14	15	18	17	20	23	15	10	0	12.5	---	---	---	---	---	---	
C	8	459281	4503392	2,074	13	0	0	2	0	2	3	11	10	12	10	5.7	---	---	---	---	---	---	
C	9	455537	4505136	2,140	0	0	0	0	0	18	27	30	41	51	8	15.9	---	---	---	---	---	---	
C	10	---	---	---	---	---	---	---	---	---	---	---	---	---	---	---	---	---	---	---	---	---	not sampled
C	11	442532	4505134	2,334	19	20	20	24	2	4	30	5	20	5	3	13.8	---	---	---	---	---	---	
C	12	438675	4506767	2,365	1	2	10	18	15	10	2	6	6	7	8	7.7	11.5	183.5	21.1	---	---	---	can
C	13	435754	4505167	2,376	18	21	24	28	26	26	22	16	19	15	14	20.8	---	---	---	---	---	---	
C	14	431720	4502177	2,463	13	15	1	16	16	11	5	8	7	14	15	11.0	15.0	200.5	30.1	---	---	---	can
C	15	431772	4498491	2,576	40	38	40	42	43	42	35	48	45	40	40	41.2	---	---	---	---	---	---	
C	16	***	***	2,649	41	44	35	40	45	41	45	50	50	49	51	44.6	---	---	---	---	---	---	
C	17	***	***	2,758	47	47	44	44	44	40	38	39	27	29	27	38.7	45.0	226.4	101.9	---	---	---	tube
C	18	427826	4492577	2,878	42	45	50	43	58	66	71	70	67	65	60	57.9	---	---	---	---	---	---	
C	19	425958	4489932	3,062	77	70	75	74	79	75	74	72	74	79	75	74.9	76.0	175.2	133.1	---	---	---	tube
C	20	425330	4488003	3,062	69	60	65	75	77	74	55	68	64	62	85	68.5	---	---	---	---	---	---	
C	21	---	---	---	---	---	---	---	---	---	---	---	---	---	---	---	---	---	---	---	---	---	not sampled
C	22	***	***	3,141	74	75	77	76	74	74	71	77	79	77	77	75.5	---	---	---	---	---	---	
C	23	---	---	---	---	---	---	---	---	---	---	---	---	---	---	---	---	---	---	---	---	---	not sampled
C	24	---	---	---	---	---	---	---	---	---	---	---	---	---	---	---	---	---	---	---	---	---	not sampled
C	25	420410	4484037	2,862	26	25	27	30	35	40	39	38	35	44	42	34.6	39.0	94.1	39.0	---	---	---	tube
C	26	---	---	---	---	---	---	---	---	---	---	---	---	---	---	---	---	---	---	---	---	---	not sampled
C	27	424989	4484701	3,089	60	62	65	63	65	65	62	68	70	49	40	60.8	---	---	---	---	---	---	
C	28	---	---	---	---	---	---	---	---	---	---	---	---	---	---	---	---	---	---	---	---	---	not sampled
C	29	427550	4492446	2,901	56	56	56	55	60	49	55	50	50	50	54	53.7	56.0	176.4	98.8	---	---	---	tube

Notes:

--- = no measurement
*** = NRCS coordinates not reported

Transect
C = CO Highway 14

Snow variables
d_s = snow depth
ρ_s = snow density
SWE = snow water equivalent

SWE measurement
can = cylindrical can [diameter = 15.3 cm]
tube = snow sampling tube [diameter = 6.6 cm]
fed = Federal sampler [diameter = 3.77 cm]

CC = Canopy Cover
C = closed
P = partially closed
O = open

CT = Community Type
LP = Lodgepole Pine
SF = Spruce/Fir
AS = Aspen Stand
AL = Alpine
W = Wetland

TM = Tree Mortality
O - open/no canopy
AG - alive with green needles
DR - dead with red needles
DG - dead and gray (no needles)

Cache la Poudre Basin Study Area, CO
Field-based snowpack data
Date: 2012-03-02

Transect	Site Number	GPS Location			d_s Measurements (cm) - 1m interval											Mean d_s (cm)	Mean SWE Measurement			CC	CT	TM	Notes
		Easting	Northing	Elevation (m)	1	2	3	4	5	6	7	8	9	10	11		d_s (cm)	ρ_s (kgm^{-3})	SWE (mm)				
C	1	482311	4501681	1,607	0	0	0	0	0	0	0	0	0	0	0	0.0	---	---	---	---	---	---	no snow
C	2	481072	4501543	1,612	0	0	0	0	0	0	0	0	0	0	0	0.0	---	---	---	---	---	---	no snow
C	3	479970	4504434	1,633	0	0	0	0	0	0	0	0	0	0	0	0.0	---	---	---	---	---	---	no snow
C	4	473796	4504326	1,753	0	0	0	0	0	0	0	0	0	0	0	0.0	---	---	---	---	---	---	no snow
C	5	470577	4504240	1,799	17	18	14	14	18	15	20	20	18	17	20	17.4	---	---	---	---	---	---	
C	6	467105	4503568	1,852	6	10	6	5	5	14	15	10	11	10	6	8.9	---	---	---	---	---	---	
C	7	463458	4504270	1,956	10	5	2	9	10	12	14	14	15	15	14	10.9	---	---	---	---	---	---	
C	8	459281	4503392	2,074	13	11	12	12	14	15	14	10	11	12	12	12.4	---	---	---	---	---	---	
C	9	455537	4505136	2,140	15	16	16	14	14	16	20	20	20	20	15	16.9	---	---	---	---	---	---	
C	10	---	---	---	---	---	---	---	---	---	---	---	---	---	---	---	---	---	---	---	---	---	not sampled
C	11	442532	4505134	2,334	24	30	36	38	30	30	24	16	25	16	10	25.4	---	---	---	---	---	---	
C	12	438675	4506767	2,365	8	5	6	8	9	10	19	14	15	16	16	11.5	16.0	199.7	32.0	---	---	---	can
C	13	435754	4505167	2,376	20	16	21	25	24	20	14	14	5	6	5	15.5	---	---	---	---	---	---	
C	14	431720	4502177	2,463	29	27	10	25	27	25	30	17	21	16	14	21.9	25.0	229.4	57.4	---	---	---	can
C	15	431772	4498491	2,576	65	62	62	51	59	74	59	61	58	88	89	66.2	---	---	---	---	---	---	
C	16	***	***	2,649	30	36	40	40	55	78	79	81	83	89	81	62.9	---	---	---	---	---	---	
C	17	***	***	2,758	68	69	70	60	60	54	64	55	36	41	34	55.5	76.2	233.3	177.8	---	---	---	fed
C	18	427826	4492577	2,878	118	95	105	109	91	94	98	91	99	102	100	100.2	---	---	---	---	---	---	
C	19	425958	4489932	3,062	154	155	155	158	154	154	150	148	146	155	150	152.6	153.7	297.5	457.2	---	---	---	fed
C	20	425330	4488003	3,062	112	112	123	110	115	130	117	140	138	155	170	129.3	---	---	---	---	---	---	
C	21	***	***	---	---	---	---	---	---	---	---	---	---	---	---	---	---	---	---	---	---	---	not sampled
C	22	***	***	3,141	139	144	145	145	147	151	152	152	159	158	161	150.3	---	---	---	---	---	---	
C	23	---	---	---	---	---	---	---	---	---	---	---	---	---	---	---	---	---	---	---	---	---	not sampled
C	24	---	---	---	---	---	---	---	---	---	---	---	---	---	---	---	---	---	---	---	---	---	not sampled
C	25	420410	4484037	2,862	70	76	76	76	75	76	76	80	69	69	57	72.7	---	---	---	---	---	---	
C	26	---	---	---	---	---	---	---	---	---	---	---	---	---	---	---	---	---	---	---	---	---	not sampled
C	27	424989	4484701	3,089	139	133	133	133	139	140	146	132	141	139	140	137.7	---	---	---	---	---	---	
C	28	---	---	---	---	---	---	---	---	---	---	---	---	---	---	---	---	---	---	---	---	---	not sampled
C	29	427550	4492446	2,901	129	125	126	122	121	125	106	110	105	104	100	115.7	121.9	291.7	355.6	---	---	---	fed

Notes:

--- = no measurement
*** = NRCS coordinates not reported

Transect
C = CO Highway 14

Snow variables
d_s = snow depth
ρ_s = snow density
SWE = snow water equivalent

SWE measurement
can = cylindrical can [diameter = 15.3 cm]
tube = snow sampling tube [diameter = 6.6 cm]
fed = Federal sampler [diameter = 3.77 cm]

CC = Canopy Cover
C = closed
P = partially closed
O = open

CT = Community Type
LP = Lodgepole Pine
SF = Spruce/Fir
AS = Aspen Stand
AL = Alpine
W = Wetland

TM = Tree Mortality
O - open/no canopy
AG - alive with green needles
DR - dead with red needles
DG - dead and gray (no needles)

Cache la Poudre Basin Study Area, CO
Field-based snowpack data
Date: 2012-03-29

Transect	Site Number	GPS Location			d_s Measurements (cm) - 1m interval											Mean d_s (cm)	Mean SWE Measurement			CC	CT	TM	Notes
		Easting	Northing	Elevation (m)	1	2	3	4	5	6	7	8	9	10	11		d_s (cm)	ρ_s (kgm^{-3})	SWE (mm)				
C	1	431774	4498466	2,586	11	29	36	49	21	5	22	40	62	66	69	37.3	---	---	---	P	SF	AG	
C	2	***	***	2,653	0	0	0	0	0	18	20	34	40	29	2	13.0	---	---	---	O	AS	O	
C	3	430097	4496003	2,736	63	62	64	76	63	73	60	70	76	67	76	68.2	---	---	---	P	LP	DR	
C	4	429243	4495152	2,752	60	55	50	50	46	50	60	66	55	48	49	53.5	---	---	---	P	LP	AG	
C	5	***	***	2,760	20	33	39	35	34	25	7	2	0	0	0	17.7	---	---	---	O	LP	O	
C	6	428674	4494271	2,810	43	38	39	22	25	19	2	9	24	34	25	25.5	---	---	---	P	LP	DR	
C	7	428277	4493290	2,859	40	41	45	55	65	50	52	49	50	63	58	51.6	---	---	---	P	LP	DG	
C	8	427823	4492583	2,881	62	58	51	44	60	65	55	64	62	48	50	56.3	---	---	---	O	LP	O	
C	9	427560	4492479	2,903	46	45	50	62	64	60	60	55	53	60	54	55.4	55.9	329.5	184.2	P	LP	DG	fed
C	10	426874	4491511	2,962	49	42	46	54	64	66	53	54	79	89	84	61.8	---	---	---	C	SF	AG	
C	11	426457	4490633	3,020	104	80	85	89	56	58	74	58	85	62	73	74.9	---	---	---	P	SF	AG	
C	12	425970	4489937	3,066	99	101	89	86	88	91	96	87	85	85	90	90.6	95.3	360.0	342.9	P	LP	DR	fed
C	13	425530	4488907	3,068	86	72	82	78	74	75	70	62	69	80	75	74.8	---	---	---	P	SF	AG	
C	14	425329	4488013	3,062	49	68	75	84	90	95	102	111	112	120	110	92.4	---	---	---	O	SF	O	
C	15	***	***	3,146	112	114	114	112	116	112	112	115	115	118	128	115.3	---	---	---	O	SF	O	
C	16	424995	4484714	3,097	103	95	90	88	94	95	103	103	93	82	73	92.6	---	---	---	P	SF	AG	
C	17	420409	4484034	2,864	0	0	0	0	0	10	3	23	20	25	24	9.5	---	---	---	O	LP	O	

Notes:

--- = no measurement
*** = NRCS coordinates not reported

Transect
C = CO Highway 14

Snow variables
d_s = snow depth
ρ_s = snow density
SWE = snow water equivalent

SWE measurement
can = cylindrical can [diameter = 15.3 cm]
tube = snow sampling tube [diameter = 6.6 cm]
fed = Federal sampler [diameter = 3.77 cm]

CC = Canopy Cover
C = closed
P = partially closed
O = open

CT = Community Type
LP = Lodgepole Pine
SF = Spruce/Fir
AS = Aspen Stand
AL = Alpine
W = Wetland

TM = Tree Mortality
O - open/no canopy
AG - alive with green needles
DR - dead with red needles
DG - dead and gray (no needles)

Cache la Poudre Basin Study Area, CO
Field-based snowpack data
Date: 2012-03-29

Transect	Site Number	GPS Location			d_s Measurements (cm) - 1m interval											Mean d_s (cm)	Mean SWE Measurement			CC	CT	TM	Notes
		Easting	Northing	Elevation (m)	1	2	3	4	5	6	7	8	9	10	11		d_s (cm)	ρ_s (kgm^{-3})	SWE (mm)				
C3	1	428875	4495563	2,786	42	49	54	57	63	60	50	60	46	41	45	51.5	---	---	---	C	SF	AG	
C3	2	428342	4495235	2,815	31	32	5	15	45	29	25	24	40	40	40	29.6	---	---	---	C	SF	AG	
C3	3	428020	4495702	2,853	52	60	60	74	63	60	65	49	47	44	32	55.1	---	---	---	P	LP	AG	
C3	4	427312	4496600	2,808	66	63	34	70	61	62	51	56	58	62	54	57.9	---	---	---	P	SF	AG	
C3	5	427573	4497838	2,725	53	50	58	52	52	57	55	48	69	56	43	53.9	---	---	---	P	SF	AG	
C3	6	427654	4498331	2,719	40	49	62	51	55	55	50	38	35	35	49	47.2	---	---	---	O	W	AG	

Notes:

--- = no measurement
*** = NRCS coordinates not reported

Transect
C3 = Chambers Lake Road

Snow variables
d_s = snow depth
ρ_s = snow density
SWE = snow water equivalent

SWE measurement
can = cylindrical can [diameter = 15.3 cm]
tube = snow sampling tube [diameter = 6.6 cm]
fed = Federal sampler [diameter = 3.77 cm]

CC = Canopy Cover
C = closed
P = partially closed
O = open

CT = Community Type
LP = Lodgepole Pine
SF = Spruce/Fir
AS = Aspen Stand
AL = Alpine
W = Wetland

TM = Tree Mortality
O - open/no canopy
AG - alive with green needles
DR - dead with red needles
DG - dead and gray (no needles)

Cache la Poudre Basin Study Area, CO
Field-based snowpack data
Date: 2012-03-29

Transect	Site Number	GPS Location			d_s Measurements (cm) - 1m interval											Mean d_s (cm)	Mean SWE Measurement			CC	CT	TM	Notes
		Easting	Northing	Elevation (m)	1	2	3	4	5	6	7	8	9	10	11		d_s (cm)	ρ_s (kgm^{-3})	SWE (mm)				
P2	1	451273	4490939	2,702	16	20	25	30	35	50	60	75	70	46	20	40.6	---	---	---	P	LP	DR	
P2	2	450080	4492179	2,756	45	50	47	58	60	55	46	50	44	50	69	52.2	---	---	---	P	LP	DR	
P2	3	449299	4492155	2,762	14	8	0	0	5	27	30	32	30	24	12	16.5	---	---	---	P	LP	AG	
P2	4	448093	4492359	2,850	46	43	41	45	49	44	50	55	49	52	53	47.9	---	---	---	O	LP	AG	
P2	5	447713	4492192	2,857	47	50	63	64	51	48	30	30	24	32	43	43.8	---	---	---	P	LP	DR	

Notes:

--- = no measurement
*** = NRCS coordinates not reported

Transect
P2 = Pingree Park - Hourglass Reservoir Road

Snow variables
d_s = snow depth
ρ_s = snow density
SWE = snow water equivalent

SWE measurement
can = cylindrical can [diameter = 15.3 cm]
tube = snow sampling tube [diameter = 6.6 cm]
fed = Federal sampler [diameter = 3.77 cm]

CC = Canopy Cover
C = closed
P = partially closed
O = open

CT = Community Type
LP = Lodgepole Pine
SF = Spruce/Fir
AS = Aspen Stand
AL = Alpine
W = Wetland

TM = Tree Mortality
O - open/no canopy
AG - alive with green needles
DR - dead with red needles
DG - dead and gray (no needles)

Cache la Poudre Basin Study Area, CO
Field-based snowpack data
Date: 2012-03-30

Transect	Site Number	GPS Location			d_s Measurements (cm) - 1m interval											Mean d_s (cm)	Mean SWE Measurement			CC	CT	TM	Notes
		Easting	Northing	Elevation (m)	1	2	3	4	5	6	7	8	9	10	11		d_s (cm)	ρ_s (kgm^{-3})	SWE (mm)				
D	1	439698	4518111	2,844	87	84	74	76	60	62	60	45	70	40	42	63.6	---	---	---	P	SF	AG	
D	2	439152	4518043	2,872	51	52	61	34	66	73	63	50	56	50	45	54.6	---	---	---	P	SF	AG	
D	3	438619	4517973	2,874	65	57	50	47	45	41	53	50	41	40	47	48.7	---	---	---	P	SF	AG	
D	4	438094	4518115	2,893	65	66	64	69	56	71	58	50	64	50	55	60.7	---	---	---	P	LP	AG	
D	5	437684	4517768	2,909	45	46	41	40	51	41	45	46	45	55	44	45.4	---	---	---	O	SF	O	
D	6	437196	4517360	2,960	72	70	72	75	68	58	45	50	64	66	69	64.5	---	---	---	P	LP	AG	
D	7	436660	4517048	2,994	94	110	85	60	52	62	58	60	60	41	58	67.3	---	---	---	P	LP	AG	
D	8	436155	4516808	3,001	58	47	65	71	72	60	68	72	72	75	84	67.6	---	---	---	C	LP	DR	
D	9	435826	4517155	3,082	74	82	80	82	73	59	49	30	28	35	25	56.1	---	---	---	P	LP	AG	
D	10	435365	4517465	3,115	79	82	87	105	93	68	69	55	60	75	65	76.2	---	---	---	O	SF	O	
D	11	***	***	3,136	87	96	90	90	94	95	90	94	94	94	100	93.1	---	---	---	O	LP	O	
D	12	435016	4518066	3,187	80	75	78	88	94	105	95	82	78	72	72	83.5	---	---	---	P	LP	AG	

Notes:

--- = no measurement
*** = NRCS coordinates not reported

Transect
D = Deadman Hill [Deadman Road]

Snow variables
d_s = snow depth
ρ_s = snow density
SWE = snow water equivalent

SWE measurement
can = cylindrical can [diameter = 15.3 cm]
tube = snow sampling tube [diameter = 6.6 cm]
fed = Federal sampler [diameter = 3.77 cm]

CC = Canopy Cover
C = closed
P = partially closed
O = open

CT = Community Type
LP = Lodgepole Pine
SF = Spruce/Fir
AS = Aspen Stand
AL = Alpine
W = Wetland

TM = Tree Mortality
O - open/no canopy
AG - alive with green needles
DR - dead with red needles
DG - dead and gray (no needles)

Cache la Poudre Basin Study Area, CO
Field-based snowpack data
Date: 2012-03-31

Transect	Site Number	GPS Location			d_s Measurements (cm) - 1m interval											Mean d_s (cm)	Mean SWE Measurement			CC	CT	TM	Notes
		Easting	Northing	Elevation (m)	1	2	3	4	5	6	7	8	9	10	11		d_s (cm)	ρ_s (kgm^{-3})	SWE (mm)				
C5	1	427577	4492768	2,882	90	96	89	87	85	65	63	16	15	25	61	62.9	---	---	---	P	SF	AG	
C5	2	427647	4493509	2,889	51	48	28	35	38	36	10	6	4	11	50	28.8	---	---	---	P	LP	DR	
C5	3	427048	4493908	2,924	70	64	49	66	74	80	80	55	40	28	16	56.5	---	---	---	P	SF	DG	
C5	4	426867	4494589	2,954	69	59	48	27	36	57	80	94	99	93	82	67.6	---	---	---	P	SF	AG	
C5	5	426221	4494782	2,972	62	51	35	18	0	0	0	0	73	78	12	29.9	---	---	---	P	SF	DG	
C5	6	425650	4494817	3,034	63	21	25	97	110	111	100	121	121	125	130	93.1	---	---	---	P	SF	DG	
C5	7	425055	4495091	3,096	71	91	80	69	47	68	83	70	71	80	84	74.0	---	---	---	P	SF	DG	
C5	8	424444	4495463	3,147	112	107	95	103	94	98	102	95	94	97	94	99.2	---	---	---	P	SF	DG	
C5	9	424222	4495605	3,185	71	93	95	54	43	81	101	95	103	88	89	83.0	---	---	---	P	SF	DG	

Notes:

--- = no measurement
*** = NRCS coordinates not reported

Transect
C5 = Blue Lake

Snow variables
d_s = snow depth
ρ_s = snow density
SWE = snow water equivalent

SWE measurement
can = cylindrical can [diameter = 15.3 cm]
tube = snow sampling tube [diameter = 6.6 cm]
fed = Federal sampler [diameter = 3.77 cm]

CC = Canopy Cover
C = closed
P = partially closed
O = open

CT = Community Type
LP = Lodgepole Pine
SF = Spruce/Fir
AS = Aspen Stand
AL = Alpine
W = Wetland

TM = Tree Mortality
O - open/no canopy
AG - alive with green needles
DR - dead with red needles
DG - dead and gray (no needles)

Cache la Poudre Basin Study Area, CO
Field-based snowpack data
Date: 2012-03-31

Transect	Site Number	GPS Location			d_s Measurements (cm) - 1m interval											Mean d_s (cm)	Mean SWE Measurement			CC	CT	TM	Notes
		Easting	Northing	Elevation (m)	1	2	3	4	5	6	7	8	9	10	11		d_s (cm)	ρ_s (kgm^{-3})	SWE (mm)				
C6	1	427612	4492107	2,929	71	78	78	66	71	74	67	66	58	47	42	65.3	---	---	---	P	LP	DR	
C6	2	428149	4491890	2,964	119	105	108	92	81	77	72	69	71	69	61	84.0	---	---	---	P	LP	AG	
C6	3	428651	4491839	2,974	111	110	99	88	98	101	96	100	93	85	78	96.3	---	---	---	O	SF	AG	
C6	4	429051	4491483	2,966	62	72	64	67	73	71	79	67	60	55	54	65.8	---	---	---	P	SF	AG	
C6	5	429368	4490926	2,978	26	69	97	101	159	148	156	86	99	169	155	115.0	---	---	---	O	SF	AG	
C6	6	429845	4490463	3,010	84	61	60	66	78	77	91	89	90	76	81	77.5	---	---	---	O	LP	AG	
C6	7	430243	4490155	3,036	74	41	42	29	43	46	37	31	51	56	64	46.7	---	---	---	O	SF	AG	
C6	8	430784	4490081	3,058	50	62	83	95	94	92	73	92	104	122	130	90.6	---	---	---	P	SF	AG	

Notes:

--- = no measurement
*** = NRCS coordinates not reported

Transect
C6 = Longdraw Road

Snow variables
d_s = snow depth
ρ_s = snow density
SWE = snow water equivalent

SWE measurement
can = cylindrical can [diameter = 15.3 cm]
tube = snow sampling tube [diameter = 6.6 cm]
fed = Federal sampler [diameter = 3.77 cm]

CC = Canopy Cover
C = closed
P = partially closed
O = open

CT = Community Type
LP = Lodgepole Pine
SF = Spruce/Fir
AS = Aspen Stand
AL = Alpine
W = Wetland

TM = Tree Mortality
O - open/no canopy
AG - alive with green needles
DR - dead with red needles
DG - dead and gray (no needles)

Cache la Poudre Basin Study Area, CO
Field-based snowpack data
Date: 2012-03-31

Transect	Site Number	GPS Location			d_s Measurements (cm) - 1m interval											Mean d_s (cm)	Mean SWE Measurement			CC	CT	TM	Notes
		Easting	Northing	Elevation (m)	1	2	3	4	5	6	7	8	9	10	11		d_s (cm)	ρ_s (kgm^{-3})	SWE (mm)				
C7	1	427851	4492554	2,884	70	60	62	44	46	22	38	52	75	102	114	62.3	---	---	---	P	LP	AG	
C7	2	427735	4492165	2,921	46	126	144	136	115	83	73	70	62	44	73	88.4	---	---	---	P	SF	DG	
C7	3	427994	4491826	2,949	8	40	60	79	73	75	73	70	66	66	57	60.6	---	---	---	P	SF	AG	
C7	4	428178	4491409	2,974	71	63	44	15	0	30	36	26	54	60	48	40.6	---	---	---	P	SF	DG	
C7	5	428556	4491342	3,000	85	80	55	57	54	60	45	59	38	48	35	56.0	---	---	---	P	SF	DG	
C7	6	428873	4491412	2,982	70	78	76	70	62	76	61	62	80	51	54	67.3	---	---	---	P	SF	AG	
C7	7	428988	4491247	2,986	86	80	81	95	80	55	77	78	95	105	96	84.4	---	---	---	P	SF	DG	
C7	8	429362	4490911	2,985	154	180	165	158	183	185	142	103	37	102	78	135.2	---	---	---	O	SF	DG	
C7	9	429788	4490467	3,024	68	75	81	80	73	66	70	68	81	92	101	77.7	---	---	---	P	SF	DG	

Notes:

--- = no measurement
*** = NRCS coordinates not reported

Transect
C7 = Meadows Trail

Snow variables
d_s = snow depth
ρ_s = snow density
SWE = snow water equivalent

SWE measurement
can = cylindrical can [diameter = 15.3 cm]
tube = snow sampling tube [diameter = 6.6 cm]
fed = Federal sampler [diameter = 3.77 cm]

CC = Canopy Cover
C = closed
P = partially closed
O = open

CT = Community Type
LP = Lodgepole Pine
SF = Spruce/Fir
AS = Aspen Stand
AL = Alpine
W = Wetland

TM = Tree Mortality
O - open/no canopy
AG - alive with green needles
DR - dead with red needles
DG - dead and gray (no needles)

Cache la Poudre Basin Study Area, CO
Field-based snowpack data
Date: 2012-03-31

Transect	Site Number	GPS Location			d_s Measurements (cm) - 1m interval											Mean d_s (cm)	Mean SWE Measurement			CC	CT	TM	Notes
		Easting	Northing	Elevation (m)	1	2	3	4	5	6	7	8	9	10	11		d_s (cm)	ρ_s (kgm^{-3})	SWE (mm)				
C8	1	425297	4487866	3,069	105	110	111	115	100	85	79	57	30	15	15	74.7	---	---	---	P	SF	AG	
C8	2	425660	4488129	3,114	20	30	35	30	35	60	50	39	35	20	15	33.5	---	---	---	C	SF	AG	
C8	3	426029	4488096	3,196	160	160	140	144	150	140	142	130	111	131	118	138.7	---	---	---	O	SF	DG	
C8	4	426519	4488256	3,196	90	76	60	60	48	30	20	11	5	1	0	36.5	---	---	---	C	SF	AG	

Notes:

--- = no measurement
*** = NRCS coordinates not reported

Transect
C8 = Zimmerman Lake

Snow variables
d_s = snow depth
ρ_s = snow density
SWE = snow water equivalent

SWE measurement
can = cylindrical can [diameter = 15.3 cm]
tube = snow sampling tube [diameter = 6.6 cm]
fed = Federal sampler [diameter = 3.77 cm]

CC = Canopy Cover
C = closed
P = partially closed
O = open

CT = Community Type
LP = Lodgepole Pine
SF = Spruce/Fir
AS = Aspen Stand
AL = Alpine
W = Wetland

TM = Tree Mortality
O - open/no canopy
AG - alive with green needles
DR - dead with red needles
DG - dead and gray (no needles)

Cache la Poudre Basin Study Area, CO
Field-based snowpack data
Date: 2012-03-31

Transect	Site Number	GPS Location			d_s Measurements (cm) - 1m interval											Mean d_s (cm)	Mean SWE Measurement			CC	CT	TM	Notes
		Easting	Northing	Elevation (m)	1	2	3	4	5	6	7	8	9	10	11		d_s (cm)	ρ_s (kgm^{-3})	SWE (mm)				
C9	1	425270	4488413	3,081	92	97	95	100	103	105	110	114	107	109	115	104.3	92.3	344.7	318.3	O	SF	O	tube
C9	2	425097	4488552	3,109	110	102	112	107	105	108	108	110	118	121	120	111.0	---	---	---	O	SF	O	
C9	3	424886	4488554	3,158	72	77	75	78	74	80	75	77	80	80	81	77.2	86.7	306.5	265.6	P	SF	AG	tube
C9	4	424737	4488424	3,194	79	89	84	79	83	91	86	76	88	91	75	83.7	---	---	---	P	SF	DR	
C9	5	424534	4488335	3,227	91	81	78	78	75	82	83	85	77	71	67	78.9	86.3	304.7	263.1	P	SF	DR	tube
C9	6	424319	4488300	3,251	85	88	92	88	91	91	100	110	108	102	99	95.8	---	---	---	P	SF	DR	
C9	7	424120	4488223	3,273	113	102	94	83	96	106	121	117	115	112	108	106.1	114.7	324.7	372.3	O	SF	O	tube
C9	8	423903	4488190	3,306	152	150	150	141	145	152	157	167	180	150	132	152.4	---	---	---	O	SF	O	
C9	9	423687	4488364	3,323	62	97	90	61	66	67	69	85	110	100	42	77.2	84.0	285.8	240.0	O	SF	O	tube
C9	10	423485	4488408	3,340	130	145	145	152	153	162	167	175	180	183	193	162.3	---	---	---	O	AL	O	
C9	11	423377	4488420	3,347	90	93	92	89	83	90	85	90	87	92	94	89.5	91.0	380.6	346.4	O	AL	O	tube
C9	12	423234	4488384	3,362	0	0	0	0	0	0	0	0	0	0	0	0.0	---	---	---	O	AL	O	no snow

Notes:

--- = no measurement
*** = NRCS coordinates not reported

Transect
C9 = Montgomery Pass

Snow variables
d_s = snow depth
ρ_s = snow density
SWE = snow water equivalent

SWE measurement
can = cylindrical can [diameter = 15.3 cm]
tube = snow sampling tube [diameter = 6.6 cm]
fed = Federal sampler [diameter = 3.77 cm]

CC = Canopy Cover
C = closed
P = partially closed
O = open

CT = Community Type
LP = Lodgepole Pine
SF = Spruce/Fir
AS = Aspen Stand
AL = Alpine
W = Wetland

TM = Tree Mortality
O - open/no canopy
AG - alive with green needles
DR - dead with red needles
DG - dead and gray (no needles)

Cache la Poudre Basin Study Area, CO
Field-based snowpack data
Date: 2012-03-31

Transect	Site Number	GPS Location			d_s Measurements (cm) - 1m interval											Mean d_s (cm)	Mean SWE Measurement			CC	CT	TM	Notes
		Easting	Northing	Elevation (m)	1	2	3	4	5	6	7	8	9	10	11		d_s (cm)	ρ_s (kgm^{-3})	SWE (mm)				
C10	1	424432	4485842	3,147	70	89	62	92	75	70	74	72	68	60	50	71.1	---	---	---	P	LP	DG	
C10	2	424727	4485450	3,144	80	110	135	128	105	105	103	110	110	98	75	105.4	---	---	---	P	LP	DG	
C10	3	425047	4485119	3,145	105	129	131	140	144	164	152	129	121	96	68	125.4	---	---	---	P	LP	DG	
C10	4	425185	4484600	3,148	60	83	63	50	35	30	45	60	85	92	83	62.4	---	---	---	P	LP	DG	
C10	5	425461	4484339	3,166	43	63	62	80	73	84	78	78	71	68	54	68.5	---	---	---	P	LP	DR	
C10	6	426009	4484060	3,158	0	0	0	0	1	51	52	30	32	36	59	23.7	---	---	---	P	SF	DR	
C10	7	426407	4483744	3,156	166	83	142	143	131	98	116	98	94	101	102	115.8	---	---	---	O	SF	O	
C10	8	426609	4483295	3,179	87	68	76	85	101	123	114	108	115	98	110	98.6	---	---	---	C	SF	AG	
C10	9	426860	4482852	3,170	0	0	0	0	0	0	0	0	0	0	0	0.0	---	---	---	O	SF	O	no snow

Notes:

--- = no measurement
*** = NRCS coordinates not reported

Transect
C10 = Michagan Ditch

Snow variables
d_s = snow depth
ρ_s = snow density
SWE = snow water equivalent

SWE measurement
can = cylindrical can [diameter = 15.3 cm]
tube = snow sampling tube [diameter = 6.6 cm]
fed = Federal sampler [diameter = 3.77 cm]

CC = Canopy Cover
C = closed
P = partially closed
O = open

CT = Community Type
LP = Lodgepole Pine
SF = Spruce/Fir
AS = Aspen Stand
AL = Alpine
W = Wetland

TM = Tree Mortality
O - open/no canopy
AG - alive with green needles
DR - dead with red needles
DG - dead and gray (no needles)

Cache la Poudre Basin Study Area, CO
Field-based snowpack data
Date: 2012-03-31

Transect	Site Number	GPS Location			d_s Measurements (cm) - 1m interval											Mean d_s (cm)	Mean SWE Measurement			CC	CT	TM	Notes
		Easting	Northing	Elevation (m)	1	2	3	4	5	6	7	8	9	10	11		d_s (cm)	ρ_s (kgm^{-3})	SWE (mm)				
C11	1	423604	4483895	2,983	35	14	15	35	50	44	55	50	60	45	61	42.2	---	---	---	P	SF	AG	
C11	2	423951	4483565	3,033	57	45	53	41	36	45	48	43	50	31	37	44.2	---	---	---	C	SF	AG	
C11	3	423761	4483068	3,114	109	90	63	65	50	34	10	50	44	75	70	60.0	104.8	303.0	317.5	P	SF	AG	fed
C11	4	423476	4482584	3,125	63	61	64	115	105	88	84	79	89	107	106	87.4	---	---	---	O	SF	O	
C11	5	423002	4482320	3,234	74	70	69	69	75	93	95	100	96	99	98	85.3	---	---	---	O	SF	O	
C11	6	422473	4482192	3,409	234	215	210	195	179	160	115	90	73	60	60	144.6	121.3	204.2	247.7	O	AL	O	fed
C11	7	422454	4482087	3,442	0	0	0	0	0	0	0	0	0	0	0	0.0	---	---	---	O	AL	O	no snow
C11	8	422472	4482041	3,458	135	138	129	130	130	148	140	160	167	159	161	145.2	---	---	---	O	AL	O	

Notes:

--- = no measurement
*** = NRCS coordinates not reported

Transect
C11 = Lake Agnes

Snow variables
d_s = snow depth
ρ_s = snow density
SWE = snow water equivalent

SWE measurement
can = cylindrical can [diameter = 15.3 cm]
tube = snow sampling tube [diameter = 6.6 cm]
fed = Federal sampler [diameter = 3.77 cm]

CC = Canopy Cover
C = closed
P = partially closed
O = open

CT = Community Type
LP = Lodgepole Pine
SF = Spruce/Fir
AS = Aspen Stand
AL = Alpine
W = Wetland

TM = Tree Mortality
O - open/no canopy
AG - alive with green needles
DR - dead with red needles
DG - dead and gray (no needles)

Cache la Poudre Basin Study Area, CO
Field-based snowpack data
Date: 2012-04-01

Transect	Site Number	GPS Location			d_s Measurements (cm) - 1m interval											Mean d_s (cm)	Mean SWE Measurement			CC	CT	TM	Notes
		Easting	Northing	Elevation (m)	1	2	3	4	5	6	7	8	9	10	11		d_s (cm)	ρ_s (kgm^{-3})	SWE (mm)				
P4	1	450191	4489919	2,870	11	20	21	24	26	30	29	30	29	30	28	25.3	---	---	---	P	LP	AG	
P4	2	449792	4489442	2,908	30	39	39	52	55	32	48	47	43	41	64	44.5	---	---	---	P	LP	AG	
P4	3	449395	4489047	2,964	45	40	46	38	50	79	50	38	30	24	31	42.8	---	---	---	P	LP	DR	

Notes:

--- = no measurement
*** = NRCS coordinates not reported

Transect
P4 = Pingree Park - Stormy Peaks

Snow variables
d_s = snow depth
ρ_s = snow density
SWE = snow water equivalent

SWE measurement
can = cylindrical can [diameter = 15.3 cm]
tube = snow sampling tube [diameter = 6.6 cm]
fed = Federal sampler [diameter = 3.77 cm]

CC = Canopy Cover
C = closed
P = partially closed
O = open

CT = Community Type
LP = Lodgepole Pine
SF = Spruce/Fir
AS = Aspen Stand
AL = Alpine
W = Wetland

TM = Tree Mortality
O - open/no canopy
AG - alive with green needles
DR - dead with red needles
DG - dead and gray (no needles)

Cache la Poudre Basin Study Area, CO
Field-based snowpack data
Date: 2012-04-01

Transect	Site Number	GPS Location			d_s Measurements (cm) - 1m interval											Mean d_s (cm)	Mean SWE Measurement			CC	CT	TM	Notes
		Easting	Northing	Elevation (m)	1	2	3	4	5	6	7	8	9	10	11		d_s (cm)	ρ_s (kgm^{-3})	SWE (mm)				
P5	1	448232	4489766	2,907	60	55	49	59	50	49	47	41	30	57	45	49.3	---	---	---	P	SF	AG	
P5	2	447648	4489545	2,940	59	63	54	35	10	68	61	60	43	75	85	55.7	---	---	---	P	SF	AG	
P5	3	447235	4489241	2,997	55	73	78	83	95	75	80	59	62	72	73	73.2	---	---	---	P	SF	AG	
P5	4	446713	4489211	3,009	56	77	67	58	60	56	57	46	68	74	78	63.4	70.5	342.3	241.3	P	LP	AG	fed
P5	5	446268	4488962	3,026	74	80	74	73	70	72	55	52	40	60	50	63.6	74.3	333.3	247.7	P	LP	DG	fed

Notes:

--- = no measurement
*** = NRCS coordinates not reported

Transect
P5 = Pingree Park - Emmaline Lake

Snow variables
d_s = snow depth
ρ_s = snow density
SWE = snow water equivalent

SWE measurement
can = cylindrical can [diameter = 15.3 cm]
tube = snow sampling tube [diameter = 6.6 cm]
fed = Federal sampler [diameter = 3.77 cm]

CC = Canopy Cover
C = closed
P = partially closed
O = open

CT = Community Type
LP = Lodgepole Pine
SF = Spruce/Fir
AS = Aspen Stand
AL = Alpine
W = Wetland

TM = Tree Mortality
O - open/no canopy
AG - alive with green needles
DR - dead with red needles
DG - dead and gray (no needles)

Cache la Poudre Basin Study Area, CO
Field-based snowpack data
Date: 2012-04-28

Transect	Site Number	GPS Location			d_s Measurements (cm) - 1m interval											Mean d_s (cm)	Mean SWE Measurement			CC	CT	TM	Notes
		Easting	Northing	Elevation (m)	1	2	3	4	5	6	7	8	9	10	11		d_s (cm)	ρ_s (kgm^{-3})	SWE (mm)				
C	1	482311	4501681	1,607	0	0	0	0	0	0	0	0	0	0	0	0.0	---	---	---	---	---	---	no snow
C	2	481072	4501543	1,612	0	0	0	0	0	0	0	0	0	0	0	0.0	---	---	---	---	---	---	no snow
C	3	479970	4504434	1,633	0	0	0	0	0	0	0	0	0	0	0	0.0	---	---	---	---	---	---	no snow
C	4	473796	4504326	1,753	0	0	0	0	0	0	0	0	0	0	0	0.0	---	---	---	---	---	---	no snow
C	5	470577	4504240	1,799	0	0	0	0	0	0	0	0	0	0	0	0.0	---	---	---	---	---	---	no snow
C	6	467105	4503568	1,852	0	0	0	0	0	0	0	0	0	0	0	0.0	---	---	---	---	---	---	no snow
C	7	463458	4504270	1,956	0	0	0	0	0	0	0	0	0	0	0	0.0	---	---	---	---	---	---	no snow
C	8	459281	4503392	2,074	0	0	0	0	0	0	0	0	0	0	0	0.0	---	---	---	---	---	---	no snow
C	9	455537	4505136	2,140	0	0	0	0	0	0	0	0	0	0	0	0.0	---	---	---	---	---	---	no snow
C	10	446565	4505924	2,260	0	0	0	0	0	0	0	0	0	0	0	0.0	---	---	---	---	---	---	no snow
C	11	442532	4505134	2,334	0	0	0	0	0	0	0	0	0	0	0	0.0	---	---	---	---	---	---	no snow
C	12	438675	4506767	2,365	0	0	0	0	0	0	0	0	0	0	0	0.0	---	---	---	---	---	---	no snow
C	13	435754	4505167	2,376	0	0	0	0	0	0	0	0	0	0	0	0.0	---	---	---	---	---	---	no snow
C	14	431720	4502177	2,463	0	0	0	0	0	0	0	0	0	0	0	0.0	---	---	---	---	---	---	no snow
C	15	431772	4498491	2,576	1	1	1	1	1	1	2	2	2	1	1	1.3	---	---	---	---	---	---	
C	16	***	***	2,649	5	6	7	6	5	6	5	4	5	4	3	5.1	---	---	---	---	---	---	
C	17	***	***	2,758	1	1	1	1	1	1	1	3	2	3	3	1.6	---	---	---	---	---	---	
C	18	427826	4492577	2,878	8	5	5	8	4	3	6	5	7	5	6	5.6	---	---	---	---	---	---	
C	19	425958	4489932	3,062	33	45	35	30	42	50	41	39	38	33	35	38.3	32.5	344.5	112.0	---	---	---	can
C	20	425330	4488003	3,062	49	58	55	56	52	55	47	60	62	71	75	58.2	---	---	---	---	---	---	
C	21	***	***	---	---	---	---	---	---	---	---	---	---	---	---	---	---	---	---	---	---	---	not sampled
C	22	***	***	3,141	67	76	69	77	73	79	84	75	77	80	72	75.4	54.5	313.1	170.7	---	---	---	can
C	23	422791	4484168	2,967	0	0	0	0	0	0	0	0	0	0	0	0.0	---	---	---	---	---	---	no snow
C	24	420409	4484110	2,869	0	0	0	0	0	0	0	0	0	0	0	0.0	---	---	---	---	---	---	no snow
C	25	420410	4484037	2,862	0	0	0	0	0	0	0	0	0	0	0	0.0	---	---	---	---	---	---	no snow
C	26	414448	4485031	2,763	0	0	0	0	0	0	0	0	0	0	0	0.0	---	---	---	---	---	---	no snow
C	27	424989	4484701	3,089	89	91	90	99	93	90	89	78	80	73	74	86.0	---	---	---	---	---	---	
C	28	---	---	---	---	---	---	---	---	---	---	---	---	---	---	---	---	---	---	---	---	---	not sampled
C	29	427550	4492446	2,901	5	5	4	3	3	3	2	4	4	3	5	3.7	---	---	---	---	---	---	

Notes:

--- = no measurement
*** = NRCS coordinates not reported

Transect
C = CO Highway 14

Snow variables
d_s = snow depth
ρ_s = snow density
SWE = snow water equivalent

SWE measurement
can = cylindrical can [diameter = 15.3 cm]
tube = snow sampling tube [diameter = 6.6 cm]
fed = Federal sampler [diameter = 3.77 cm]

CC = Canopy Cover
C = closed
P = partially closed
O = open

CT = Community Type
LP = Lodgepole Pine
SF = Spruce/Fir
AS = Aspen Stand
AL = Alpine
W = Wetland

TM = Tree Mortality
O - open/no canopy
AG - alive with green needles
DR - dead with red needles
DG - dead and gray (no needles)

APPENDIX C: GIS DATASET

Table C.1: Spatial and temporal data obtained and derived for the Cache la Poudre basin study area GIS dataset.

Data	**Source**
NRCS operational station locations	Natural Resource Conservation Service (NRCS) <*http://www.wcc.nrcs.usda.gov/snow/*>
Field-based measurement locations	GPS locations using Garmin GPSMAP 76 GPS receiver capable of positioning accuracy within 3 m
Streams and Water bodies	United States Geological Survey (USGS) National Hydrography Dataset <*http://nhd.usgs.gov/*>
Land Cover	USGS National Gap Analysis Program (GAP) <*http://gapanalysis.usgs.gov/*>
Digital Elevation Model (DEM)	USGS National Elevation Dataset (NED) <*http://seamless.usgs.gov/*>
Basin boundaries	Derived from DEM using the Spatial Analyst tools within ArcGIS 10
Hillshade	Derived from DEM using the Spatial Analyst tools within ArcGIS 10
Slope	Derived from DEM using the Spatial Analyst tools within ArcGIS 10
Northness	Derived from DEM using ArcGIS 10 as the product of the *cosine* of aspect and the *sine* of slope
Eastness	Derived from DEM using ArcGIS 10 as the product of the *sine* of aspect and the *sine* of slope
Solar Radiation	Derived from DEM using the Area Solar Radiation tool in ArcGIS 10 (Nov 15 through Mar 30)
Curvature	Profile curvature derived from DEM using the Spatial Analyst tools within ArcGIS 10
Canopy Density	National Land Cover Database <*http://www.mrlc.gov*>
UTM Northing Grid (Centroid)	Derived from centroid UTM Northing value of DEM pixel using ArcGIS 10
UTM Easting Grid (Centroid)	Derived from centroid UTM Easting value of DEM pixel using ArcGIS 10
MODIS/Terra 8-day Maximum Snow Extent (snow covered area) late March through early April (2011 - 2012)	NASA's Earth Observing System Data and Information System (EOSDIS) <*http://reverb.echo.nasa.gov*>